

DSpace Institution

DSpace Repository

<http://dspace.org>

Hydraulic engineering

Thesis

2020-08

FLOOD INUNDATION MAPPING IN TEMIE RIVER, UPPER BLUE NILE

Belete, Aynalem Cherie

<http://ir.bdu.edu.et/handle/123456789/12829>

Downloaded from DSpace Repository, DSpace Institution's institutional repository



BAHIR DAR UNIVERSITY
BAHIR DAR INSTITUTE OF TECHNOLOGY
SCHOOL OF RESEARCH AND POSTGRADUATE STUDIES
FACULTY OF CIVIL AND WATER RESOURCE ENGINEERING

FLOOD INUNDATION MAPPING IN TEMIE RIVER, UPPER BLUE
NILE

By

Belete Aynalem Cherie

Bahir Dar, Ethiopia
august, 2020

FLOOD INUNDATION MAPPING IN TEMIE RIVER, UPPER BLUE NILE

By

Belete Aynalem Cherie

A Thesis Submitted to the School of Graduate Studies of Bahir Dar University in Partial Fulfilment of the Requirements for the Degree of Master of Science in Hydraulic Engineering.

Advisor: -Dr. Asegdew Gashaw

Bahir Dar Ethiopia

14 August 2020

DECLARATION

I, Belete Aynalem Cherie, hereby declare that this thesis submitted for the partial fulfilment of the requirements for the Master of Science in Hydraulic engineering, in the original work done by me under the supervision of Dr. Asegdew Gashaw. And it has not been published or submitted elsewhere for the requirement of a degree program to the best of my knowledge and belief. Materials or ideas of other Authors used in this thesis have been duly acknowledged.

Student

Name: _____

Signature: _____

Date: _____

Place: Bahir Dar

This thesis has been submitted to for examination with my approval as a university Advisor

Name: _____

Signature: _____

Date: _____

Bahir Dar Institute of Technology
School of Research and Graduate Studies
Faculty of Civil and Water Resource Engineering
THESIS APPROVAL SHEET

Student: Belete Aynalem B.D August 2020
Name Signature Date

The following graduate faculty members certify that this student has successfully presented the necessary written final thesis and oral presentation for partial fulfilment of the thesis requirements for the Degree of Master of Science in Hydraulic Engineering.

Approved by:

Advisor: Assefaw F(Dr) [Signature]
Name Signature Date

External examiner: [Signature]
Name Signature Date

Internal examiner: Fasikaw Atanaw(Ph.D.) [Signature] 10-Aug-2020
Name Signature Date

Chair holder: Assefaw F(Dr) [Signature]
Name Signature Date

Faculty Dean: Temesgen Enku Nigussie (Ph.D.) [Signature] Aug. 14 2020
Name Signature Date



ACKNOWLEDGEMENT

I would like to thank the Almighty GOD and His beloved mother St. Marry for helping to accomplish my study.

I would like to express my appreciation to Dr. Asegdew Gashaw, for his scientific advice for the full accomplishment of my thesis work and his encouragement and moral support throughout the study. Special thanks to ERA in collaboration with Bahir Dar University for the willingness to give the chance to attend my education and financial support. Thanks all of my special friends for their moral support. The support and help I received from Mr. Mindesilew lakew, a Debre-markos university staff member have been beyond expression. I am also greatly indebted to Mr. Fasikaw Fentie and Mr. Workneh; both helped me after data collection.

Finally, I would also like to thank my family for the unconditional love and support they provided me throughout my life and in particular. Last but not least, thanks go to my beloved fiancé, Mintiwab Getaneh for her comments and encouragements, and also, I would like to express my gratitude for all my friends, who have been helping and encouraging me by telephone and e-mail during the study and thesis writing periods.

ABSTRACT

At this time extraordinary floods are common to many parts of our country causing a lot of losses such agricultural land and grazing land for long period of time. Temie watershed is been one among such place that has affected by flash flooding from rainfall in particular of Temie river which is located at the Right side of the river is mountainous and the left side flat terrain. This study is aimed to identify flood causative factors, peak flood estimation, delineate inundation areas that can be affected by unexpected floods. This thesis accomplished adopting application software's like Google earth, Arc viewGIS, HEC-GeoHMS, HEC-HMS, HEC-GeoRAS and HEC-RAS models. The data used for this thesis is DEM, Land use/land cover map, soil map, soil texture to generate the curve number grid and rainfall and discharge type to determine peak flood in certain return period. Topographic data for the expected flooded area has been obtained from actual field survey data and from Google earth and TIN of the Study Area was created. The modelling process was towards performing steady flow calculations in the intent of routing the river outflow downstream of Temie watershed from the upstream up to the downstream boundary which is 13km from the outlet point .probable maximum precipitation was determined by Gumble's extreme value type in different return period 20, 50,100, 500 and 1000 years and the corresponding results are 95.81, 104.5, 111.3, 128.04 and 134.8mm respectively. The flood magnitude is estimated for 20, 50,100,500 and 1000-years return period peak flood discharge using Computer program HEC-HMS Model.The corresponding values are 50.8, 63.5, 70.8, 86.2 and 94m³/s peak discharge is used for further analysis which is inundation mapping. These flood inundated crop lands having area of 346.7, 352.2, 357.8, 363.0 and 371.03hectares respectively. These corresponded to losses of 9309.4, 9457.4, 9606.1, 9745.5 and 9962.2 quintals of crop respectively. Therefore, the affected areas to be free of any agricultural activities, infrastructure development, investment and residence of people in order to avoid the risk of flooding in the area especially closer to the downstream of River.

Key words: Flood Inundation Mapping, Arc-GIS, HEC-HMS, HEC-RAS

Table of Contents

DECLARATION.....	ii
ACKNOWLEDGEMENT	iv
<i>ABSTRACT</i>	v
LIST OF TABLES	x
LIST OF FIGURES.....	xi
ABBREVIATIONS AND ACRONYMS.....	xii
1 INTRODUCTION.....	1
1.1 Background to the Study	1
1.2 Statement of the Problem	3
1.3 Research Questions.....	4
1.4 Objectives of the study	4
1.4.1 General objective.....	4
1.4.2 Specific objective	4
1.5 Scope/ significance of the study.....	4
2 LITERATURE REVIEW.....	6
2.1 Previous Related Works	7
2.1.1 Related works out of Ethiopia.....	7
2.1.2 Related works in Ethiopia	8
2.2 Overview of Software and Models	9
2.2.1 Digital Elevation Model (DEM)	9
2.2.2 Arc-GIS	10
2.2.3 HEC-RAS.....	10
2.3 Flood Magnitude Estimation.....	10
2.3.1 Rational Method	10
2.3.2 SCS and other Unit Hydrograph Methods.....	11
2.3.3 Regional Regression Analysis	11
3 METHODOLOGY.....	13
3.1 Description of the Study Area.....	13
3.1.1 Geographic Location	13
3.1.2 Geology feature of the study area	14
3.1.3 Climate of the study area.....	14

3.1.4	Topographic feature of the catchment	15
3.1.5	Soil type	15
3.1.6	Land use /Land cover of the Catchment	17
3.1.7	Materials used.....	19
3.1.8	Data Collection and Analysis.....	19
3.2	Peak Discharge Estimation.....	20
3.2.1	Selection of Method	20
3.2.2	SCS Unit Hydrograph Methods	20
3.3	Details of Selected Models	23
3.3.1	HEC-GeoHMS	23
3.3.2	HEC-HMS	24
3.4	Delineation and Identification of Flood Risk Area.....	27
3.4.1	HEC-GeoRAS	27
3.4.2	HEC-RAS	29
3.5	Analysis of Rainfall Data	30
3.5.1	Filling Missing Rainfall Data.....	30
3.5.2	Checking the Stability of Variance and Mean.....	33
3.5.3	Checking the Consistency of Rainfall Data.....	34
3.5.4	Average depth of precipitation over an area.....	39
3.5.5	Determination of Probability Distributions	41
3.5.6	Testing the goodness of fitness of probability.....	45
3.6	HEC-GeoHMS Data Processing	48
3.7	Basin Model.....	50
3.7.1	Physical Description of Sub-basin (HEC-GeoHMS).....	50
3.7.2	Rainfall Loss Computation Methods	52
3.7.3	Rainfall excess (Runoff) Computation Methods.....	53
3.7.4	Transformation method.....	54
3.7.5	Modelling Base Flow with HEC-HMS.....	54
3.7.6	Routing Models	55
3.8	Meteorological Model	56
3.9	Control Specifications	57
3.10	Time Series Components	57

3.11	Base Flow	61
3.12	Runoff Data	61
3.13	Simulation Run and Search Method.....	62
3.13.1	HEC-HMS Input Data.....	62
3.14	HEC-HMS Model Calibration and Validation.....	62
3.15	HEC-RAS Model and Input Data.....	65
3.15.1	HEC-HMS Model Output	65
3.15.2	HEC-Geo-RAS and Data Processing.....	65
3.15.3	HEC-RAS Model	66
3.15.4	HEC-RAS Input Data.....	68
4	RESULTS AND DISCUSSION	73
4.1	HEC-HMS Calibration and Validation	73
4.2	HEC-HMS Model Validation Results and Discussion.....	78
4.3	PMF Inflow Hydrograph	79
4.4	Hydraulic Model development.....	80
4.4.1	Pre-RAS (HEC-GeoRAS) processing	80
4.4.2	HEC-RAS Results	81
4.4.3	Detailed output tables for selected cross sections	83
4.4.4	Flood Inundation Mapping.....	85
4.4.5	Flood Risk Result	90
5	CONCLUSION AND RECOMMENDETION.....	91
5.1	Conclusion	91
5.2	Recommendations	92
6	REFERRENCES.....	93
7	APPENDICES	96
	Annex 1: - The values of detection deviate kn	96
	Annex 2: Reduced Mean (y_n) and Reduced Standard Deviation (s_n)	97
	Annex 3: - Probable maximum precipitation in 20 year by normal Distribution.....	98
	Annex 4: -Probable maximum precipitation in 20 year by Log-normal distribution.....	99
	Annex 5: - Probable maximum precipitation in 20 year by Log Pearson Type-III.....	100
	Annex 6 -Probable maximum precipitation in 20 year by Pearson Type III.....	101
	Annex 7: -Probable maximum precipitation in 20 year by Gamble extreme.....	102

Annex 8: -Typical Hydrological Soil Group in Ethiopia	103
Annex 9: - Temie sub-basins the corresponding soil type and land use.....	105
Annex 10- weighted of curve number	108
Annex 11-Summary Computation sheet for Manning's Roughness Coefficient.....	111
Annex 12: - Output Table of HEC-RAS.....	113

LIST OF TABLES

Table 3-1:- Data type and its purpose.....	19
Table 3-2:- outlier value.....	33
Table 3-3:-Rainfall Stations weight.....	40
Table 3-4:- D -Index for different frequency distribution type.....	46
Table 3-5: - Probability Distributionsin different return period	47
Table 3-6: - Basin catchment characteristics derived from HEC HMS.....	51
Table 3-7:-Sub –basin area of Tamie catchment.....	58
Table 3-8:- Temie Land use Land cover.....	60
Table 3-9:- Performance for recommended statistics (Starks & Moriasi, 2009)	65
Table 4-1:- Objective function summary for Calibration	74
Table 4-2:-Optimized parameter values for Calibration	74
Table 4-3:- Calibration and Validation performance of the model.....	77
Table 4-4: - Peak Discharge output of HEC-HMS from Hyetograph	80
Table 4-5:- Detailed output tables of channel simulation for selected cross sections	83
Table 4-6:-Flood magnitude and corresponding inundated area	89
Table 4-7:- Estimated crop land due to Flooding	90

LIST OF FIGURES

Figure 3-1:- Location of the study area.	13
Figure 3-2:-Geology of the study area.....	14
Figure 3-3:-Topographic features of the study area	15
Figure 3-4:- Soil type of the study Area	16
Figure 3-5: - land use/land cover of the study area	18
Figure 3-6:-Hydrologic Estimates Flow chart	22
Figure 3-7:- HEC- HMS Graphical user interface	26
Figure 3-8:- Modelling approach for Flood Inundation Mapping	29
Figure 3-9:- consistency checking of stations within and around study area.	37
Figure 3-10: - Homogeneity tests of Temie watershed rainfall stations.....	38
Figure 3-11:- Temie watershed rainfall stations using Thiessen polygon	40
Figure 3-12:-Maximum Probability Distributions using normal distribution	42
Figure 3-13: - Maximum Probability Distributions using Log-normal frequency distribution.....	43
Figure 3-14:-Maximum Probability Distributions using Log Pearson type III	44
Figure 3-15:- Maximum Probability Distributions using Pearson type III	44
Figure 3-16:- Maximum Probability Distributions using extreme value type -I.....	45
Figure 3-17: - Probability Distributions in different return periods	47
Figure 3-18:- Modelling approach Rainfall Runoff Modelling	48
Figure 3-19:- Terrain Processing using Arc Hydro Tools	49
Figure 3-20:- HEC-HMS Representation Derived From HEC-GeoHMS.....	51
Figure 3-21:-Sub-basin model Representation Derived from HEC-HMS	58
Figure 3-22:- Temie watershed curve number Grid.....	59
Figure 3-23:- Soil types and texture of the study area	61
Figure 3-24:-U. S Geological Survey Manning's Roughness estimated values	70
Figure 3-25: -Upper Temie River channel and floodplain profile of the study area.....	71
Figure 4-1:-Model Calibration of Simulated and Observed flow	76
Figure 4-2:- HEC-HMS Calibration Result.....	77
Figure 4-3:-Model Validation of Simulated and Observed flow	78
Figure 4-4:-HEC-HMS Validation Result.....	79
Figure 4-5: - Pre-processing in the study Area.....	81
Figure 4-6: - x-y-z View of the Flood Plain in HEC-RAS	82
Figure 4-7: - water surface TIN Generated bounding polygon.....	86
Figure 4-8: - flood velocity and depth distribution map	87
Figure 4-9:-Flood Inundation Map for 20 and 1000Years Return Period respectively .	88

ABBREVIATIONS AND ACRONYMS

DMC	Double Mass Curve
DEM	Digital Elevation Model
1D	One Dimensional
2D	Two Dimensional
ERA	Ethiopia Construction Works, Design and Supervision Corporate
FEMA	Federal Emergency Management Agency
GPS	Global Positioning System
HEC	Hydrologic Engineering Center
HEC-HMS	Hydrologic Engineering Center Hydrology Model System
HEC- GeoHMS System	Hydrological Engineering Center-Geographical Hydrology Model System
HEC-GeoRAS System	Hydrologic Engineering Center-Geographical River Analysis System
HEC-RAS	Hydrologic Engineering Center River Analysis System
HSG	Hydrologic Soil Group
IDF	Inflow Design Flood
LULC	Land Use Land Cover
MoWR	Ministry of Water Resources
NRCS	Natural Resources Conservation Service
NWS	National Weather Service
PMF	Probable Maximum Flood
PMP	Probable Maximum Precipitation
SWAT	Soil and Water Assessment Tool
TIN	Triangulated Irregular Network

USACE	United States of Army Corps of Engineering
USBR	United States Bureau of Reclamation
USDA	United States Department of Agriculture
WSP	water surface profile

1 INTRODUCTION

1.1 Background to the Study

Flood Inundation represent one of the main natural disaster, affecting many states over the year, endangering life, environment and natural resource and leading to large economic losses and social and health problems too. It's a natural process and part of the hydrological cycle of rainfall surface and ground water flow and storage. Floods occur whenever the capacity of the natural or man-made drainage system is unable to cope with the volume of water generated by rainfall(Smith& Ward, 1998).Its considerably in size and duration. With prolonged rain falling over wide areas rivers are fed by a network of ditches, streams and tributaries and flows build up to the point where the normal channel is weighed down and water floods onto surrounding areas. In Ethiopia context, the rainy season is concentrated in the four months between June and September when about 80% of the rains are received. Torrential down pours are common in most parts of the country.

Rivers play a major role in the human civilization as they are the major source of fresh water, transportation, and resources. However, sometimes this relationship is often disturbed because change in river discharge which leads to flood or drought. Floods has been considered as one of the most devastating natural hazards/disasters causes huge immediate damage and long term loss on human activity, economic development of a society as well as on the environment(Mojaddadi, Pradhan, Nampak, Ahmad, & Ghazali, 2017; Patel, Mehta, & Yadav, 2018).The boundary of land and water has always played an important role in human activities; settlements are often located at coasts, river banks or deltas. When the boundary consists of rock, erosion is usually negligible, but finer material can make protection necessary. In a natural situation, the boundary moves freely with erosion and sedimentation. Nothing is actually wrong with erosion, unless certain interests are threatened. Erosion is somewhat like weed: as long as it does not harm any crop or other vegetation, no action is needed or even wanted. There should always be a balance between the effort to protect against erosion and the damage that would be occur otherwise(Mojaddadi et al., 2017).Basic hydraulics survey requires hydrologic, topographic data, geologic data and fieldsurvey data.

Photogrammetric survey and determination of the elevation of dams, spillways, levees and floodwalls may be required to support hydraulic modelling of floodplains, flood control channel design, navigation modelling, water quality assessment, and environmental impact and assessment analysis (Hussein Roshun et al., 2012). Prediction of river hydraulic characteristics in contrast to probable flooding for reducing damages is essential (Mardookhpour & Jamasbi, 2017).

(Timbadiya, Patel, & Porey, 2011) describes the discharge, river stage and other hydraulic properties are interrelated and depend upon the characteristics of channel roughness. Estimation of channel roughness parameter is of key importance in the study of open- channel flow particularly in hydraulic modeling. Channel roughness is a highly variable parameter which depends upon number of factors like surface roughness, vegetation, channel irregularities, channel alignment etc.

Ethiopia is a country with great geographic diversity. Much of its land consists of a large plateau at an elevation higher than 2500 m.a.s.l. with high mountains and deep gorges, river valleys, and lowland plains. The rainy season in Ethiopia is concentrated in the four months between mid-June and mid-October when about 80 % of the annual precipitation is received as torrential downpours.

Ethiopia's topographic and climatic characteristics have made the country vulnerable to high floods that resulted in destruction, casualties and damages to economic, livelihoods, infrastructure, services, and health systems (Manjusree, Bharathi, & Rao). With prolonged rain falling over wide areas rivers are fed by a network of ditches, streams and tributaries and flows build up to the point where the normal channel is overwhelmed and water floods onto surrounding areas (Assefa, 2018). Human activities such as unplanned rapid settlement development, uncontrolled construction of buildings in general and major land use changes can influence the spatial and temporal pattern of hazards. There are several factors that contribute to the flooding problem ranging from topography, geomorphology, drainage, poor drainage engineering structures, climate and other local factors can be mentioned. Most floods are caused by storms in which a lot of precipitation falls in a short period of time. Intensity and duration of the rain are the most influencing factors for flood hazards. The approach of developing proper flood mapping system is to know the extent of the flooding of river so as to redirect the flows to the nearest receiving watercourse as efficiently as possible or constructing flood protection

structures to protect areas susceptible to flooding(Zeleke, 2015). Rainfall, if not intercepted by vegetation, falls on the earth and evaporates, infiltrates or lies in depressions. Any remaining surplus flows over the surface to the nearest stream channel and thence via rivers to the sea. Under conditions of high rainfall intensity or during periods of expanded rainfall, the stream channels cannot accept all the surplus runoff, with the resulting flooding doing great harm to human activities, destroying crops and cattle, and bringing famine in their wake(Woube, 1999). The flooding can be caused by, for instance, heavy rain, snow melt, land subsidence, rising of groundwater, dam failures.

In Temie river catchment most of the nearest area's agricultural areas, grassland, forest land and irrigation lands existed. Therefore, the river flow condition should to be undertaken before sever damage occurs. So that by collecting necessary data's and analysing the data's Using Arc GIS version10.1, hydraulic model HEC-RAS 4.1.0latest versions and using SCS methods.

1.2 Statement of the Problem

In all over the world riverine flood that overtopping from the bank affects human lives, destroying their home and livelihood, moreover affecting the country's business, economy and industry. Having this in Temie River basin at different time in the past due to heavy rain the flow capacity of rivers exceeded locally that causes the rising of water level to occur and damages irrigation lands, agricultural areas so that near to the river at summer time irrigation cannot perform due to overtopping and floodplain and also it affects the transportation system of the surrounding areas. Due to the above-mentioned reasons the river bank overtopping causes should to be assessed and mitigation measures should to be recommended.

In the last decade the frequency of flash floods has markedly increased all over Ethiopia. They have caused a number of deaths and a large amount of property damage. The occurrence of such flash floods is recorded mainly in semi-arid areas with the monsoon-like rain distribution typical of Ethiopia and an annual rainfall around 500-700 mm. The whole country is potentially prone to flash flood hazard (DPPA, 2013 Flood Alert). The shortest return intervals (less than 10 years) were found in semi-arid

areas and at rain gauges located near the main rifting escarpments, i.e. where commonly the headwater of the most of the river catchment is located. The highest rainfall intensities may occur in every month, though they are more common in July and August and, subordinately in March and April. The increased frequency of flash floods in a few areas of Ethiopia cannot be accounted for by any significant change in rainfall intensity (Billi, Alemu, & Ciampalini, 2015).

Floods in the Horn of Africa normally follow the June–September rainy season. According to the UN, the 2006 floods, which followed droughts in 2005, affected 1.8 million people and were the worst in the region for 50 years. In August 2006, overflow of the Dechatu River killed more than 300 people in Dire Dawa (a town in south-eastern Ethiopia), displaced thousands more, and caused extensive damage to homes and markets (Mulugeta et al., 2007).

1.3 Research Questions

The research aims to answer the questions of what are the causative factors for this flooding. Which part and how much of the human lives and the cultivable area are vulnerable by the flood hazard and what measures to be taken to alleviate the problem?

1.4 Objectives of the study

1.4.1 General objective

The overall objective of this research is to prepare flood inundation map for study area.

1.4.2 Specific objective

- To evaluate the flood frequency analysis in the specified catchment
- To simulate flood profiles of the Temie River using HEC-RAS model
- To delineate flood prone area
- To conduct flood risk assessment.

1.5 Scope/ significance of the study

The study focused only on flooding of Temie River particularly at-risk areas starting from Chokie Mountain and hotel, buhageltm, kogna Gult at huletEju Enessie Woreda. Across the two banks of the river, there is crop production, settlement and grassland; whenever flooding occurs at this site, the only property at risk is cultivated area,

irrigation area and grassland. Therefore, the analysis of the effects of flooding on crop production was studied. The cost of crop damage due to flooding was not determined because time value of money is highly variable. So, the effect of flooding on crop was estimated based on the change in production. This study contributes to;

- Reduce the risk of direct flood damage to crops and property.
- Control flooding during farming periods by applying mitigation measures.
- To forecast the maximum peak flood through the year.

2 LITERATURE REVIEW

Flood risk is a fact of life for those living in areas subject to flooding. No matter what project or action is proposed, evaluated, adopted, and implemented for life safety, complete containment or total mitigation is never possible. Further, information used to estimate flood risk, formulate and evaluate plans, and consequent results of the analyses, are uncertain. All measured or estimated values in project development are to various degrees inaccurate, reflecting both inherent natural variability in flooding phenomena, (e.g., cyclonical rainfall patterns) and uncertainty in estimating various parameters (e.g., estimation of n-value) relevant to project works and their performance. The risk framework (comprised of risk assessment, risk management, and risk communication) is an explicit means of better understanding both the flooding and associated consequences, and thus should support development of robust strategies for managing flood risk. Implementing the concept of 'superiority' is one such strategy for managing risk. Superiority simply means providing higher levees at all points except where initial overtopping is desired when practicable in a given system. Not all systems may be able to accommodate superiority measures. Superiority is an increment of the levee height that increases the likelihood that when the system approaches capacity, flooding will occur at a specified overtopping section. Designs that include superiority can initiate overtopping in the least hazardous location. Water surface profiles (WSP) and distribution of overtopping volumes and the subsequent consequences need to be examined to understand where superiority should exist and where overtopping reaches should be located. Documenting overtopping consequences in the levelled area is an element of the strategy in flood hazard and emergency action plans including a local flood warning system. Overtopping reaches may only provide relief up to the capacity of the superiority reach and beyond that capacity the system is assumed to have been overwhelmed. The overtopping reach is to provide a known initial exceedence location and to provide some warning/evacuation time before total system exceedence ((USACE., 2017)).

River bank protection works was turned into water resources engineering and became the purpose of more sustainability works against river bank movement. River bank

protection works are made by channelization or by constructing embankment along with the side of the river. Sometimes salinity intrusion to the ground water found in the southern part of Bangladesh. Farmers of that region try to save their cultivation from salinity and think to construct some kind of barrier between saline and fresh ground water. In Bangladesh, the southern part already has facing so many tremendous cyclonic storm surges that created a bad condition over the region and have no suitable protection works against storm surges. Moreover, tidal water level exceeds the previous level and maximum portion of ground become inundated in normal lunar orbit system. So, present worst condition should be met up(Ahmad, 2017).

2.1 Previous Related Works

2.1.1 Related works out of Ethiopia

Different researchers wrote and published many applicable journals and research papers (thesis's) about river hydraulic analysis in different part of the world. In 1-D Hydrodynamic model to evaluate geomorphic effectiveness of floods on lower Tapi river basin(Darshan Mehta et al., 2017). In this study, geometry of lower Tapi River, flood plain of Surat City and past observed flood data have been used to develop 1-D integrated hydrodynamic model of the lower Tapi River, India. After collecting the entire data using 1-D hydrodynamic model to simulate the flood of year 1944, 1945, 1968, 2006, 2007, 2012 and 2013. He assessed that the river network and cross sections for the present study were extracted from the field surveyed contour map of the river Tapi-River. In this, stability of a segment of lower reaches of Tapi-River approximately 9 km length between Weir cum causeway and Kapodra (Uttran Bridge) is evaluated for its carrying capacity and geomorphic effectiveness.

A study on a river embankment section along the left bank of the Baleswar River, just upstream of the Pirojpur town is chosen for design study (Ahmad, 2017). Statistical analyses were performed on the Annual High Tidal Water Level to estimate 1-in-50-year tidal height with storm surges as design water level. The Design Water Level and soil data used to design structural parameters for the river embankment. Finally, he made comparison between the existing and performed designs. The river has meandering with braided condition and possesses silt carrying capacity. The bank

movement occurs frequently. The flood effect has an impact on that region and during monsoon period, salinity become harmless on cultivation.

(P V Timbadiya et al., 2011) tried to discuss on the requirement of multiple channel roughness coefficient Manning's 'n' values along the river has been spelled out through simulation of floods, using HEC-RAS, for years 1998 and 2003, supported with the photographs of river reaches collected during the field visit of the lower Tapi River. He analysed that Channel roughness is a sensitive parameter in development of hydraulic model for flood forecasting and flood inundation mapping. The performance of the calibrated HEC-RAS based model has been accessed by capturing the flood peaks of observed and simulated floods; and computation of root mean squared error (RMSE) for the inter-mediated gauging stations on the lower Tapi River. (Hussein Roshun et al., 2012) Published journal he discussed on the application of computer technology to analysis of the rainfall-runoff process and the hydraulics of natural rivers. In his work Hydraulic analysis was performed to predict flow characteristic and water surface elevations in the Zaremrood River. This hydraulics analysis uses the US Army Corps of Engineers computer program HEC-RAS, HEC-GeoRAS Extension and GIS application. Results showed that integration of HEC-RAS with GIS using HEC-GeoRAS Extension provides an effective environment for both hydraulic analysis and mapping. Traditional methods for Hydraulic analysis and delineating flood plain should be replaced with new technological models.

2.1.2 Related works in Ethiopia

They worked out research in Dire Dawa. The NDVI maps were classified by using a supervised classification (MLC—maximum likelihood classification). Four land use types were identified on the base of Google Earth_ high-definition images of the same period and the analysis of false colour of the same Land sat images: (1) bare soil, (2) scrubland, (3) open wood and (4) cultivated lands/mix scrubland. The result of the classification, after considering the overlaps in spectral signature between the four soil uses, is reported. Flash floods are posing constraints to the economic growth and the development process of a low-income country such as Ethiopia, and, in order to mitigate such hazard, they put a point that are crucial to understand the relative roles of

two main factors: rainfall intensity and land use change. Their study analyses the recent trends of rainfall intensity across Ethiopia and investigates the relative role of rainfall intensity and land use change in enhancing the frequency of flash flooding of the town of Dire Dawa by the Dachau River. Results indicate that the increase in rainfall intensity is a more important factor than land use change in controlling the increased frequency of flash flood in Dire Dawa.(Assefa, 2018) His paper presents a new systemic paradigm for the assessment of flood hazard and flood risk in the riverine flood-prone areas. Special emphasis is given to the urban areas with mild terrain and complicated topography, in which 2-D fully dynamic flood modelling is proposed. Flood generating factors, i.e. slope, elevation, rainfall, drainage density, land use, and soil type were rated and combined to delineate flood hazard zones using a multi-criteria evaluation technique in a GIS environment. The flood hazard map indicates that 2103.34, 35406.63, 59271.09, 162827.96, and 1491.66 km² corresponds with very high, high, moderate, low, and very low flood hazard, respectively.

(Zelege, 2015), on his research work he tried to assesses the potential impact of flood on extreme hydrological events in Bantyeketu River in Addis Ababa. He used ARC-GIS 10 modelling software to delineate catchment for different river system in Akaki catchment and helps to obtain hydrological and physical parameters and spatial information of the Akaki catchment. And he used hydrological model, HEC-HMS to simulate Runoff in Akaki Catchment. The performance of the model was assessed through calibration process and resulted $R^2=0.7$. Optimal calibration parameters were developed for Akaki Catchment and these parameters was used as an input for HEC-HMS for estimation of peak discharge in the study. The peak discharge for Bantyeketu River for the coming ten years, twenty-five years and fifty years was found to be 13.1 m³/s, 14.7 m³/s and 16 m³/s respectively.

2.2 Overview of Software and Models

2.2.1 Digital Elevation Model (DEM)

Digital Elevation Model (DEM) is the digital representation of the land surface elevation with respect to any reference datum and it is used as an input for ARC-GIS software for catchment delineation and estimation of catchment characteristic. A digital

elevation model (DEM) is a digital file consisting of terrain elevations for ground positions at regularly spaced horizontal intervals (USGS, 2001). Its uses range from scientific, commercial, industrial, and operational to military applications. In the academe or a research institution, DEM is used primarily as an input or as a data source itself in studies along the fields of climate impact studies, water & wildlife management, geological & hydrological modelling, geographic information technology, geomorphology & landscape analysis, mapping purposes, & educational programs.

2.2.2 Arc-GIS

Arc-GIS provide contextual tools for mapping and spatial reasoning so you can explore data & share location-based insights. It is an interesting software used to analyse the spatial data and delineate any area and it will use to the study area.

2.2.3 HEC-RAS

HEC-RAS has been developed for the U.S. Army Corps of Engineers (USACE.). It is a computer program that models the hydraulics of water flow through natural rivers and other channels. Prior to the recent update to Version 4.1.0 the program was one-dimensional, meaning that there is no direct modelling of the hydraulic effect of cross section shape changes, bends, and other two- and three-dimensional aspects of flow. Allow user to perform 1-D, steady flow, 1 and 2-D unsteady flow, and sediment bed transport computation as well as water temperature and quality modelling.

2.3 Flood Magnitude Estimation

There are many hydrologic methods are available to estimate the magnitude of peak flood. If possible, the method shall be calibrated to local conditions and tested for accuracy and reliability. The choice of these methods depends on data available and the practical existing situations. Among the many hydrologic methods, some are explained below.

2.3.1 Rational Method

A rational approach is to obtain the yield of a catchment by assuming a suitable runoff coefficient. It estimates the peak runoff at any location in catchment area as a function of the area, runoff coefficient, and rainfall intensity for duration equal to the time of

concentration. It is best suited to urban storm drain systems and rural ditches. It shall be used with concern if the time of concentration exceeds 30 minutes. This method is used for catchment areas less than 50 hectares (0.5km²) and expressed as below.

2.3.2 SCS and other Unit Hydrograph Methods

The U.S. Soil Conservation Service has developed a synthetic unit hydrograph procedure that has been used widely for developing rural and urban hydrographs. The unit hydrograph used by the SCS method is based upon an analysis of a large number of natural unit hydrographs from a broad cross section of geographic locations and hydrologic regions. This method can be used for catchment areas greater than 50 hectares. This technique requires the same basic data as the Rational Method: catchment area, a runoff factor, time of concentration and rainfall. The SCS approach, however, is more sophisticated in that it considers also the time distribution of the rainfall, the initial rainfall losses to interception and depression storage, and an infiltration rate that decreases during the course of a storm. With SCS method, the direct runoff can be calculated for any storm either real or fabricated, by subtracting infiltration and other losses from the rainfall to obtain the precipitation excess.

A relationship between accumulated rainfall and accumulated runoff was derived by SCS from experimental plots for numerous hydrologic and vegetative cover conditions. Data for land treatment measures, such as contouring and terracing, from experimental catchment areas were included. The equation was developed mainly for small catchment areas for which daily rainfall and catchment area data are ordinarily available. It was developed from recorded storm data that included total amount of rainfall in a calendar day but not its distribution with respect to time. The SCS runoff equation is therefore a method of estimating direct runoff from 24-hours or 1-day storm rainfall.

2.3.3 Regional Regression Analysis

The magnitude of Peak flow can be calculated by using regression equations developed for specific geographic regions. In the equations the dependent variable would be the peak flow, and the independent variables may be area, slope, channel geometry, rainfall and other meteorological, physical or site-specific data. This method shall be used for

all routine designs at sites where applicable. Regression Equations are a commonly accepted method for estimating peak flows at un-gauged sites or sites with insufficient data. Also, they have been shown to be accurate, reliable, and easy to use as well as providing consistent findings. Regression equations are one of the preferred methods for estimating peak flows for larger catchment areas. A regional approach to estimating floods at un-gauged sites can be adopted using this regression model to estimate the flood (ERA Drainage Manual, 2001).

Uses of inundation mapping

Flood Inundation maps can have a variety of uses including emergency action plans, mitigation planning, and Emergency response and consequence assessment.

3 METHODOLOGY

3.1 Description of the Study Area

HuletEjuEnessie is located in North West Ethiopia in the East Gojjam Zone of the Amhara Region Abay Basin, at a distance of 348km from Addis Ababa and 138 km from Bahir-Dar on the secondary road that links Dejen with Bahir Dar overlooking the Abay River. Temie River is one tributary of Abay. It starts at chokies, Gojjam area and joins the main Abay at north part of Kiranyiotown.

3.1.1 Geographic Location

The study area is located at $37^{\circ} 51'32''\text{E}$ to $37^{\circ}55'40''\text{E}$ and $10^{\circ}40'0''\text{N}$ to $10^{\circ}60'0''\text{N}$ and an altitudinal range is from 2479m to 4043m above sea level.

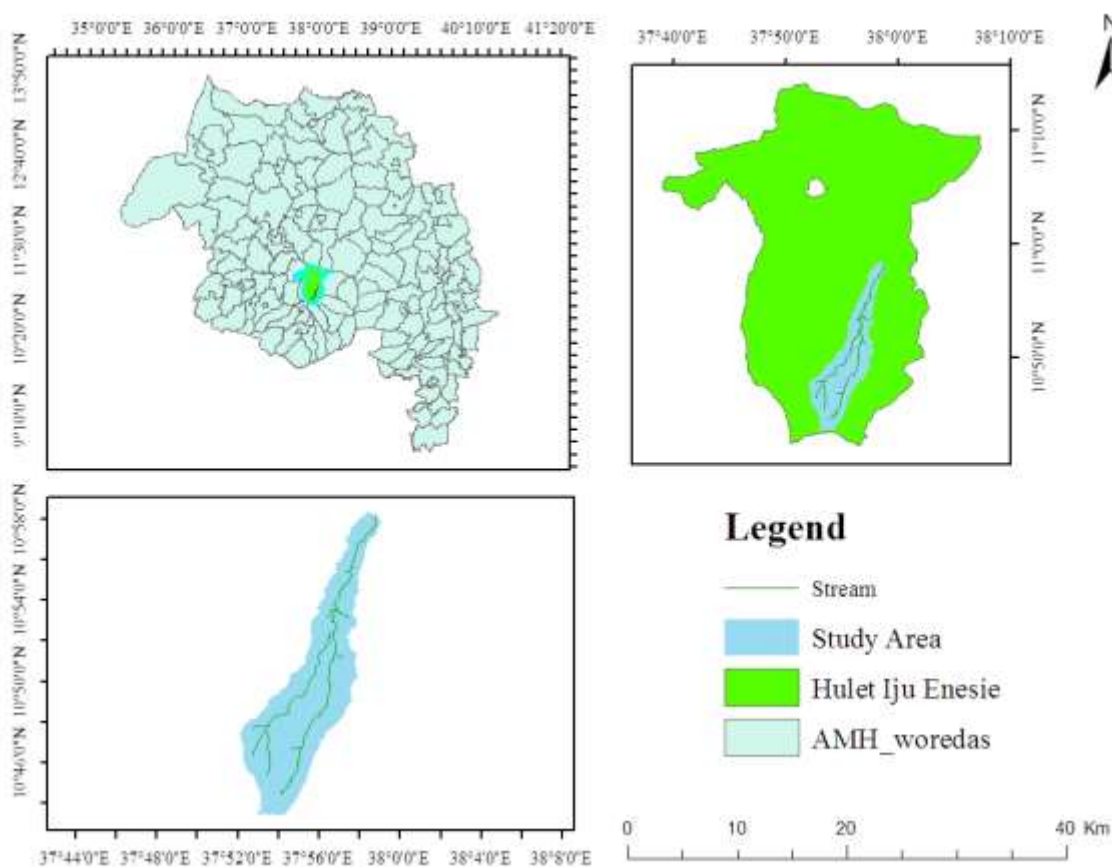


Figure 3-1:- Location of the study area.

3.1.2 Geology feature of the study area

The elevation of the catchment ranges from 2,479m to 4,043m a.s.l. The geological condition of the catchment most upper part code (Q) is clay, silt, Sand, Diatomite, and Beach Sand and the lower part code (NQtb) is alkaline basalt and Trachyte.

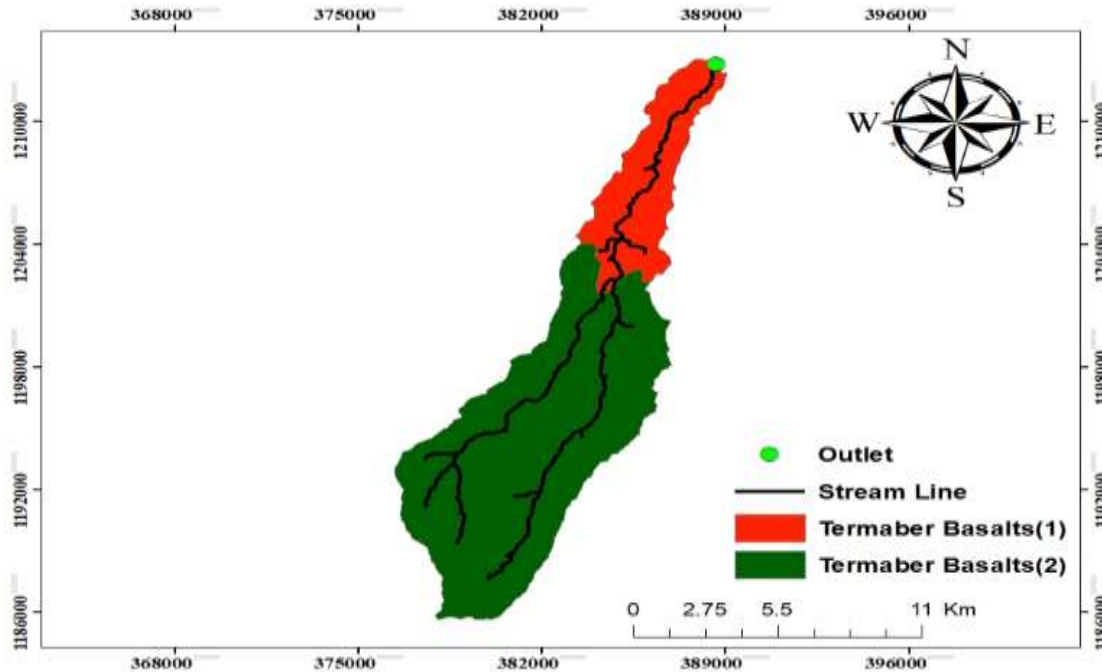


Figure 3-2:-Geology of the study area

3.1.3 Climate of the study area

The sources of moisture in Ethiopia are the Indian and Atlantic Oceans for almost all rain season (Degefu, 1987). Based on the classification of Agro-climate zone on the bases of annual rainfall, temperature, length of growing period and plant types, the year is divided into two seasons: a rainy season mainly is on the months of May to September, and a dry season is from October to March. The amount of rainfall in Ethiopia is affected by the location of the place relative to the source of moisture, the direction of winds and topographical relief. By using Thiessen polygon method the location of the study area falls under Gundowion and Felege Birhan stations. The mean annual rainfall at Gowndion Meteorological station is ranges between 903.7mm and 1526.5mm. The mean annual rainfall at Felege Birhan Meteorological station is ranges between 874mm and 1878mm. The highest rainfall occurs during August and September and river flows peak during this time period.

3.1.4 Topographic feature of the catchment

The study area has apparent topographic variation. All types of slopes are present. According to (Weigel, 1986) the classification dominant slope class is 0 – 2 % flat, 2-10% sloping, 10-15% moderately steep, 15-30% steep slope and > 30% is categorized under very steep slopes as shown in figure below.

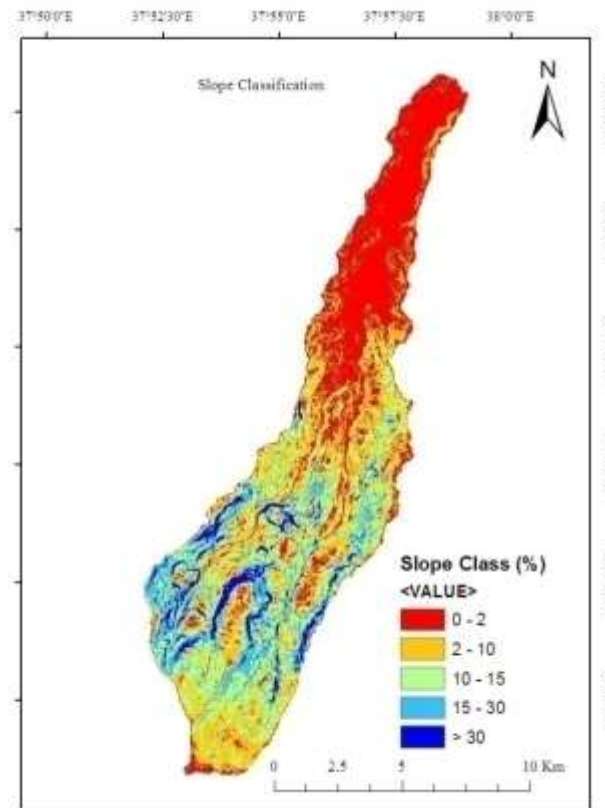


Figure 3-3:-Topographic features of the study area

3.1.5 Soil type

There are different soil types present in the study area which can be classified as Chromic Luvisols, Pellic Vertisols, Eutric Nitisols, Lithosols and Eutric Cambisols as shown below. The dominant part of the floodplain is Pellicvertisols soils and along the Temie River flow the left and right bank of the river is Chromic Luvisols soils.

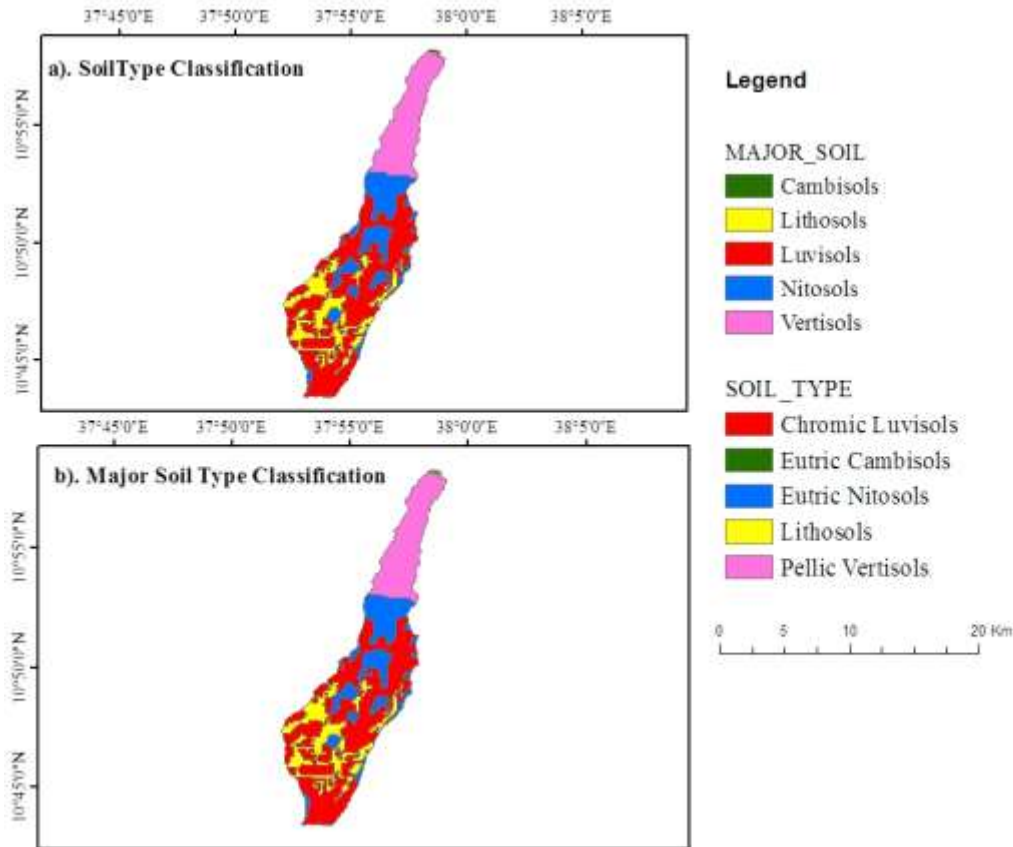


Figure 3-4:- Soil type of the study Area

According to the USDA Natural Resources Conservation Service of National Engineering Handbook the four hydrologic soil groups (HSGs) are described as:

Group A: - Soils in this group have low runoff potential when thoroughly wet. Water is transmitted freely through the soil. Group A soils typically have less than 10 percent clay and more than 90 percent sand or gravel. Some soils having loamy sand, loamy silt textures may be placed in this group if they are well aggregated, of low bulk density, or contain greater than 35 percent rock fragments.

Group B: -Soils in this group have moderately low runoff potential when thoroughly wet. Water transmission through the soil is unimpeded. Group B soils typically have between 10 percent and 20 percent clay and 50 percent to 90 percent sand, loamy sand textures.

Group C: - Soils in this group have moderately high runoff potential when thoroughly wet. Water movement through the soil is somewhat restricted. Group C soils typically

have between 20 percent and 40 percent clay and less than 50 percent sand and have loam, silt loam, sandy clay loam, clay loam, and silt clay loam textures.

Group D: - Soils in this group have high runoff potential when thoroughly wet. Water movement through the soil is restricted or very restricted. Group D soils typically have greater than 40 percent clay, less than 50 percent sand, and have clay textures. All soils with a depth to a water impermeable layer less than 50 centimetres and all soils with a water table within 60 percent centimetres of the surface are in this group.

The most dominant soil type in Temie watershed area is Chromic Luvisols which is group D soil and covers 50% of the total soil type. Therefore; for roughly speaking the catchment generates more runoff into the River.

3.1.6 Land use /Land cover of the Catchment

Land use and land cover change have been among the most vital significant changes taking place around us. Although significant, the magnitude, variety and the spatial variability of the changes taking place has made the quantification and assessment of land use and land cover changes a challenge to scientists. Furthermore, since most of the land use and land cover changes are directly influenced by human activities, they rarely follow standard ecological theories. The Remote Sensing and Geographic Information System have proved to be very important in assessing and analysing land use and land cover changes. Satellite-based Remote Sensing, by virtue of its ability to provide information of land use and land cover at a particular time and location, has revolutionized the study of land use and land cover change. The temporal information on land use and land cover helps identify the areas of change in a region.

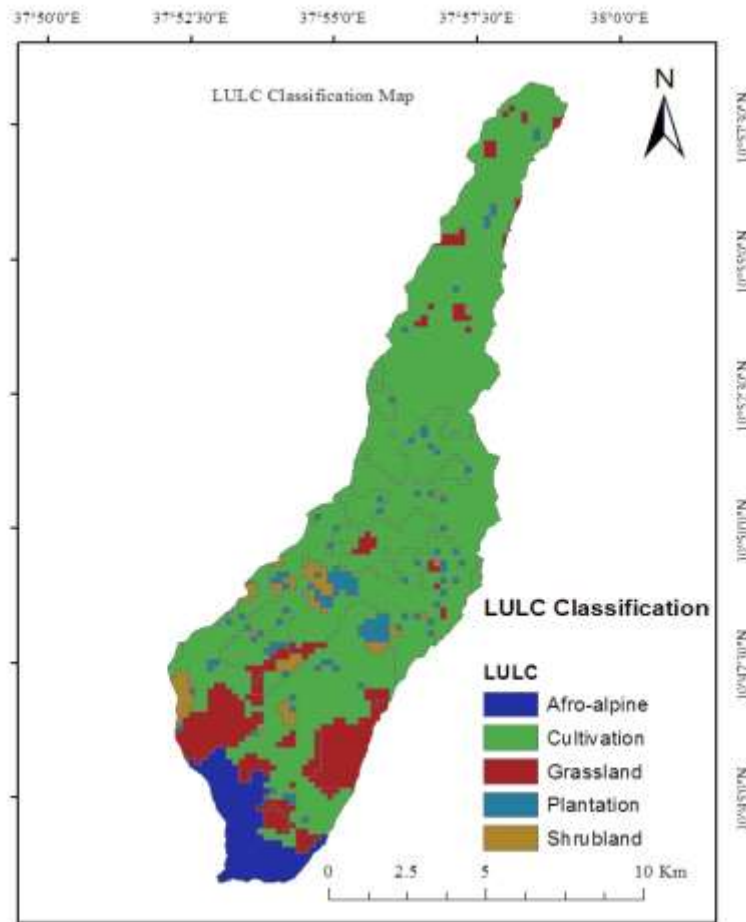


Figure 3-5: - land use/land cover of the study area

The watershed is densely populated and intensively cultivated by smallholders with crop and livestock production was the main farming system. According to the Woreda Agricultural and Rural Development Office report (2018) the main crops are grown in the study area are Teff, maize, wheat, potato and barely. However, crop production is so intensive that there is little room left for pasture to sustain the large number of livestock. Therefore, traditional farming systems are existed in the study area. The land cover of the study area is can be classified as Cropland with grassland.

Generally, this work has two main parts which are site work and homework. The site work part includes examination of the site, taking flood mark records of the site, surveying of the site (collecting elevation data, cross sectional data of the site) using GPS (global positioning system) and collecting the necessity data from different institutions. The homework task includes the other part of the work which is analyzing

precipitation and discharge data using suitable procedures and running with suitable Models. These steps are generally stated as:

- Data collection and analysis,
- Peak discharge estimation,
- Calibration and validation of model
- Flood vulnerable area delineation

3.1.7 Materials used

The materials used for this research work include the following,

- ArcGIS10.1, Arc hydro and HEC-GeoHMS tools
- HEC-HMS4.2.1 hydrological model
- HEC-RAS 4.2.0 and HEC-GeoRAS compatible for ArcGIS10.1 (pre and post processing).

3.1.8 Data Collection and Analysis

The Primary data from field visit and secondary data from different organizations are collected.

Table 3-1:- Data type and its purpose

Types of Data	Purpose	Source
Temie River Basin 30M DEM Resolution	Generating Catchment data using HEC-Geo HMS	Geo-spatial Download
Maximum Daily Rainfall for The Stations	To compute Hydrograph using HEC-HMS	Meteorology Agency
ERA Intensity-Frequency Duration Curve for The Region	To compute Hydrograph using HEC-HMS	ERA Drainage manual
Soil Type and Land-Use for Temie Catchment	For Curve Number Computation	Download

3.2 Peak Discharge Estimation

3.2.1 Selection of Method

Many hydrologic methods are available to estimate peak flood. The method is calibrated to local conditions and tested for accuracy and reliability. The choice of these methods depends on data available and the practical existing situations.

Flash floods develop in hilly and mountainous terrains where the slope of the river is rather steep. The rapid development of the flood is due to the extremely short concentration time of the drainage catchment. This means that precipitation falling on a point in the catchment farthest from the river takes only a short time to reach the river channel and become part of stream flow. Thus, the amount of stream flow rapidly increases and, consequently, the rise in water level. When the flow capacity of the stream is exceeded, the channel overflows and the result is a flash flood.

Flash flood is a surface flow of short duration with a relatively high peak discharge. It is not depending on time and space typical example of unsteady non-uniform flow. This flash flood is common feature in the East Gojjam region during the rainy season. SCS unit hydrograph method is used for catchment areas greater than 50 hectares (0.5km²). Temie catchment area is much greater than 0.5km² which is 118km².

3.2.2 SCS Unit Hydrograph Methods

The U.S. Soil Conservation Service has developed a synthetic unit hydrograph procedure that has been used widely for developing rural and urban hydrographs. The unit hydrograph used by the SCS method is based upon an analysis of a large number of natural unit hydrographs from a broad cross section of geographic locations and hydrologic regions. This method can be used for catchment areas greater than 50 hectares.

This technique requires the same basic data as the Rational Method: catchment area, a runoff factor, time of concentration and rainfall. The SCS approach, however, is more sophisticated in that it considers also the time distribution of the rainfall, the initial rainfall losses to interception and depression storage, and an infiltration rate that decreases during the course of a storm. With SCS method, the direct runoff can be

calculated for any storm either real or fabricated, by subtracting infiltration and other losses from the rainfall to obtain the precipitation excess. The SCS runoff equation is therefore a method of estimating direct runoff from 24-hours or 1-day storm rainfall.

$$\text{The equation is: } Pe = \frac{(P-Ia)^2}{P-Ia+S} \text{ Eq.3-1}$$

Analysis of results from many small experimental watersheds, the SCS developed an empirical relationship of Ia and S: $Ia = 0.2S$,

$$\text{Therefore, the cumulative excess at time t is: } Pe = \frac{(P-0.2S)^2}{P+0.8S}$$

The maximum retention, S, and watershed characteristics are related through an intermediate

$$\text{Parameter, the curve number (CN) as: - } S = \frac{25400}{CN} - 254 \text{ Eq. 3-2}$$

The rest methods of peak flood estimation are given above in literature as an introduction. Hence, the preferred methodology for this study is suitable Computer Programs HEC-GeoHMS and HEC-HMS used to facilitate the SCS hydrologic calculations as well described.

For this methodology, the following steps are followed:

- I. Downloading 30m resolution DEM for study area
- II. HEC-GeoHMS processed as it is a geospatial hydrology toolkit
- III. Using HEC-HMS for modelling and simulating the hydrologic process

The ERA drainage Design hydrologic analysis procedure flowchart shows the steps for the hydrologic analysis and the designs that will use the hydrologic estimates. With modification for flood and the updated technology since the manual prepared, the procedure is presented below.

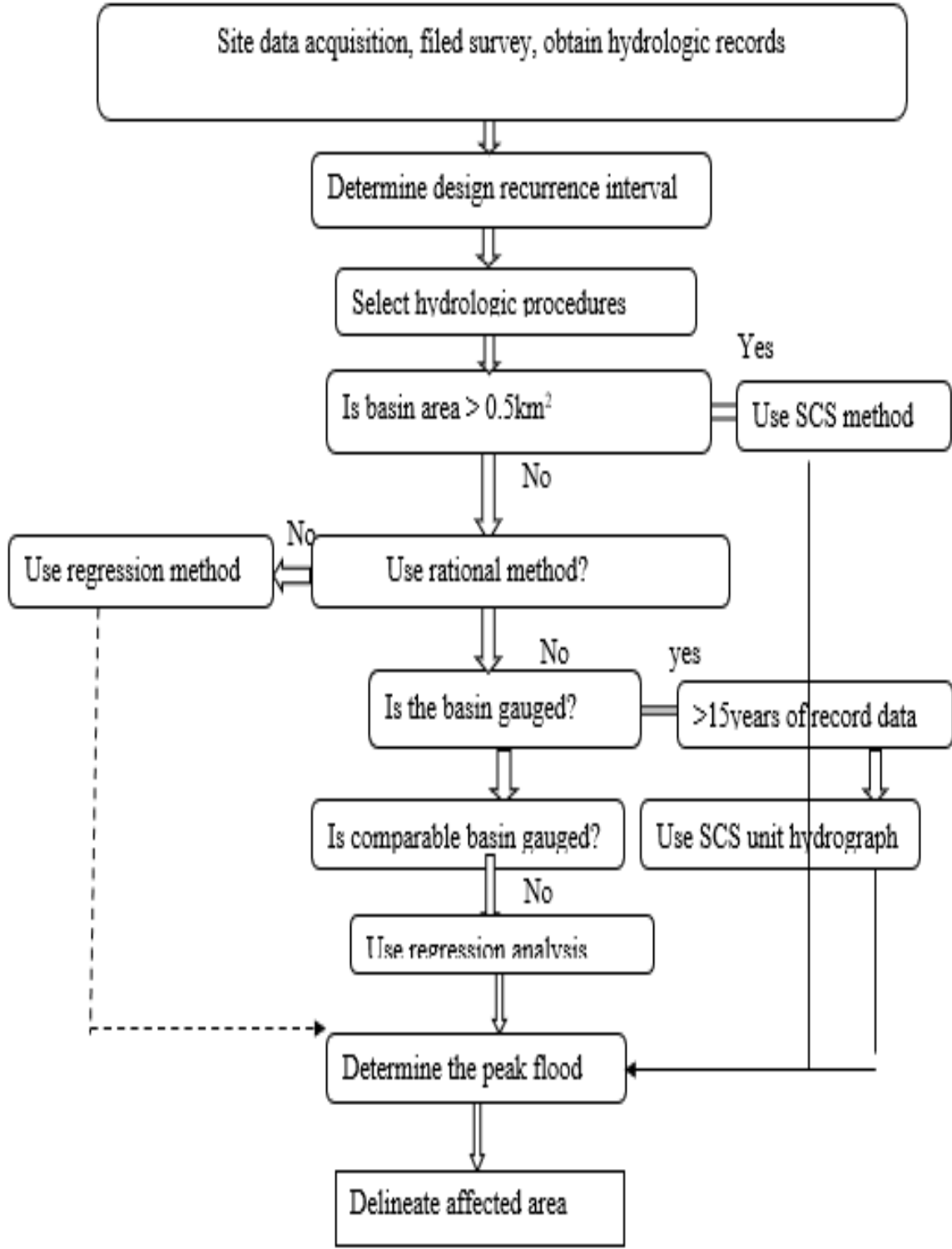


Figure 3-6:-Hydrologic Estimates Flow chart

3.3 Details of Selected Models

3.3.1 HEC-GeoHMS

HEC-GeoHMS is a set of ArcGIS tools specifically designed to process geospatial data and create input files for the Hydrologic Engineering Centre's Hydrologic Modelling System (HEC-HMS). It includes integrated data management and a graphical user interface (GUI). Through the GUI, which consists of menus, tools, and buttons, the user can analyze the terrain information, delineate sub-basins and streams, and prepare hydrologic inputs. HEC-GeoHMS provides the connection for translating GIS spatial information into model files for HEC-HMS. The GIS capability is used for data formatting, processing, and coordinate transformation.

HEC-GeoHMS operates on the DEM to derive sub-basin delineation and to prepare a number of hydrologic inputs. HEC-HMS accepts these hydrologic inputs as a starting point for hydrologic modelling. The following steps describe the major steps in starting a project and taking it through the HEC-GeoHMS process.

- I. Terrain Pre-processing
- II. Hydrologic processing; -Basin Processing, Stream and Watershed CharacteristicsHMS Model Files.
- III. Hydrologic Parameters

Terrain Pre-processing

Using the terrain data as input, terrain pre-processing is a series of steps to drive the drainage network. The steps consist of computing the flow sink, flow direction, flow accumulation, stream definition, and watershed delineation. These steps can be done step by step or in a batch manner. Once these datasets are developed, they are used in the later steps for sub-basin and stream delineation. Tools are available on the basin processing menu that gives the user the capability to delineate and edit basins in accordance with project specifications. The terrain data is processed and analyzed using the eight-pour point approach to determine flow paths. This approach uses the steepest slope to define the direction that water flows from one grid cell to one of its eight neighbours. After terrain pre-processing is completed, the resulting datasets serve as a

spatial database for the study. With the information centralized in the spatial database, pertinent datasets can be extracted for subsequent work to build the hydrologic models. Preliminary watershed and stream delineation provide results that can be verified with published information to detect possible errors in the terrain data.

Hydrologic processing

After the terrain pre-processing is completed and a new project has been created, the basin processing menu can be used to revise the delineations. Customized sub-basin and routing reach delineations. Customized sub-basin and routing reach delineations should include points where information is needed, i.e., stream flow gauge locations flood damage center's, and hydrologic and hydraulic controls.

3.3.2 HEC-HMS

The Hydrologic Engineering Centers Hydrologic Modelling System (HEC-HMS) simulates the precipitation-runoff processes of watershed systems (Schaffenberg, 2013). HMS uses deterministic mathematical modelling to compute various components of the hydrologic cycle. These are evapo-transpiration, precipitation, infiltration, and runoff. HMS is applicable in a wide range of geographic areas for solving the widest possible range of problems including large river basin water supply and flood hydrology, and small urban or natural watershed runoff. Hydrographs produced by HMS are used directly or in conjunction with other software for studies of water availability, urban drainage, flow forecasting, future urbanization impact, reservoir spillway design, flood damage reduction, floodplain regulation, and systems operation. HEC-HMS is a generalized modelling system capable of representing many different watersheds. The program features a completely integrated work environment including a database, data entry utilities, computation engine, and results reporting tools (Schaffenberg, 2013).

The main inputs to the model include: - Watershed stream network and size, Infiltration loss method (Initial and Constant, Deficit and Constant, Exponential, Green-Ampt, Smith Parlange, Soil Moisture Accounting, SCS curve Number), Transform method for transforming excess precipitation into runoff (SCS, Clark or Snyder unit hydrographs, Kinematic wave, ModClark, User specified unit hydrograph), Routing methods

(Muskingum, Kinematic Wave, Lag, Modified Puls, Muskingum Cunge, and Straddle Stagger), and Meteorologic data (precipitation, and time span of the simulation).

The expected outputs from the model include: -FlowHydrographs,Flow Volume, Optimization parameterandFlow Residuals.

HEC-HMS model components

HEC-HMS: - Model Components are used to simulate the hydrologic response in a watershed. This Component includes basin models, Meteorological models, control specifications, and Time series data. A simulation calculates the precipitation-runoff response in the model given the input from the Meteorological model. The control specifications explain the time period and time step of the simulation run. Input data Components such as time series data, paired dataandgridded data are often required as parameter or boundary conditions in basin and Meteorological models (HEC, Hydrologic Engineering Center User's manual, 2015).

Basin Model Components

The basin model represents the physical watershed. The user develops a basin model by adding and connecting hydrologic elements. Hydrologic elements use mathematical models to describe physical processes in the watershed.

Meteorological Model Component

The meteorological model calculates the precipitation input required by a sub-basin element. The meteorological model can utilize both point and gridded precipitation and has the capability to model frozen and liquid precipitation along with evapo-transpiration. The newly added snowmelt method uses a temperature index algorithm to calculate the accumulation and melt of the snow pack. The evapo-transpiration methods include the monthly average method and the new priestly Taylor and gridded priestly Taylor methods. An evapo-transpiration method is only required when simulating the continuous or long-term hydrologic response in a watershed.

User Interface

The user interface consists of a menu bar, tool bar, and four main panes. Starting from the upper left pane in figure 1 and moving Counter-clockwise, these panes will be

referred to as the watershed Explorer, the component Editor, the Message Log, and the Desktop.

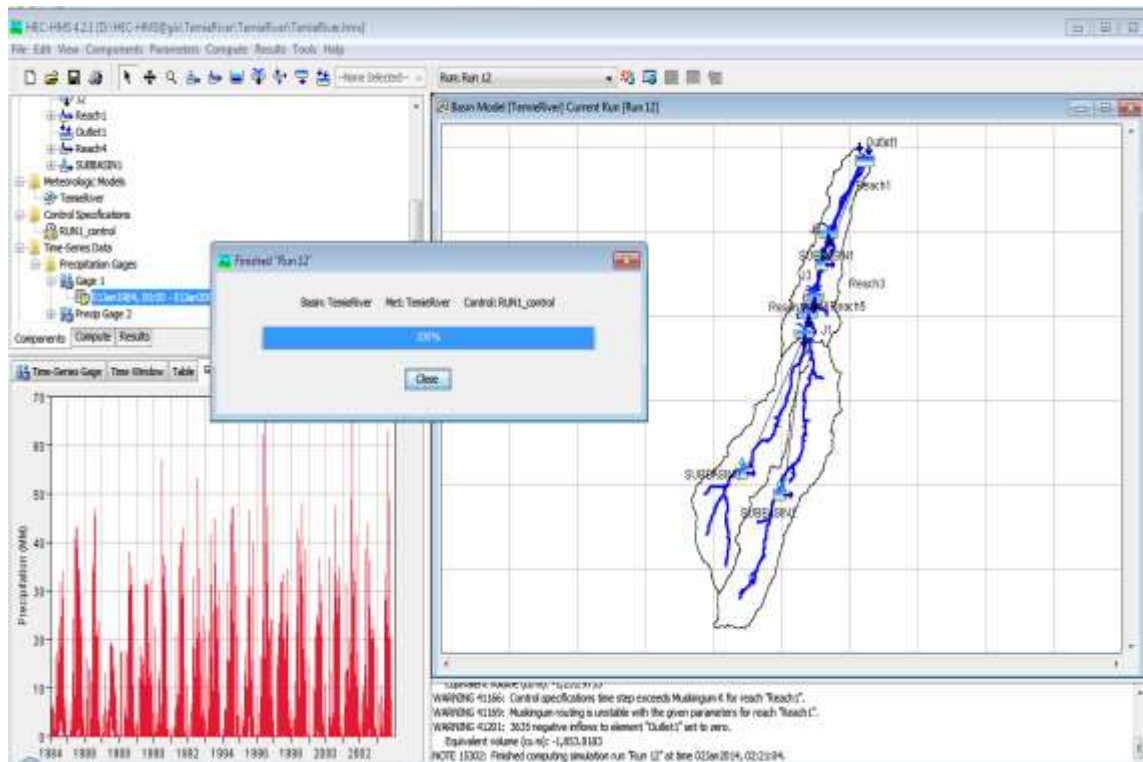


Figure 3-7:- HEC- HMS Graphical user interface

Watershed Explorer

The Watershed Explorer was developed to provide quick access to all components in a HEC-HMS project. For example, the user can easily navigate from a basin model to a precipitation gauge and then to a Meteorological model without using menu options or opening additional windows. The Watershed Explorer is divided into three parts; Components, Compute, and Results. The hierarchal structure of model components, such as basin models, Meteorological models, etc, is available from the “components” tab of the Watershed Explorer. The Watershed Explorer organizes model components into individual folders. When a component is selected, the Watershed Explorer expands to show sub-components.

3.4 Delineation and Identification of Flood Risk Area

The Flood Inundation map shows the area extent to be delineated as buffer zone. Two models HEC-GeoRAS and HEC-RAS are used one after another (i.e. first HEC-GeoRAS then HEC- RAS then back to HEC- GeoRAS) to accomplish the task.

3.4.1 HEC-GeoRAS

HEC-GeoRAS is a set of procedures, tools, and utilities for processing geographic information systems (Woube) data in ArcGIS, using a graphical user interface (GUI). The interface allows preparation of geometric data for import into HEC-RAS and generation of GIS data from Exported HEC-RAS simulation results. HEC-GeoRAS Version 10.1 is used to extract cross sectional station elevation data from a digital terrain model (DTM) represented by a triangulated irregular network (TIN). Downstream reach lengths and bank station locations were determined for each cross section. The geometric data was imported into HEC-RAS Version 4.1.0 using a data exchange format developed by HEC-GeoRAS. The resultant water surface elevations exported from HEC-RAS -simulations were processed by HEC-GeoRAS for floodplain delineation and water depth calculations. Analysis of cross-sectional velocities exported from HEC-RAS was also performed using HEC-GeoRAS. GeoRAS allows the preparation of geometric data for import into HEC-RAS and processes simulation results exported from HEC-RAS with an existing 4m contour interval of stream cross section in TIN format and 30m resolution digital terrain model (DTM) of the river system. The user creates a series of line themes pertinent to developing geometric data for HEC-RAS. The themes created are the Stream Centerline, Flow Path Centrelines (optional), Main Channel Banks (optional), and Cross Section Cut Lines referred to as the RAS Themes. These themes include Land Use (for Manning's n values), Levee Alignment, Ineffective Flow Areas, and Storage Areas, Blocked Obstacles, Bridges/culverts, Inline structures, Lateral structures and storage areas. HEC-GeoRAS 10.1 is an extension for use with ArcGIS (Environmental Systems Research Institute,2000) that provides the user with a set of procedures, tools, and utilities for the preparation of GIS data for import into RAS and generation of GIS data from RAS output.

Procedure followed the flood plain contour interval map is changed to Terrain TIN (a triangulated irregular network) using Arc GIS extension HEC-GeoRAS.

PreRAS (HEC-GeoRAS) Processing

The goal of this section is to develop the spatial data required to generate a HEC-RAS import file with a 3-D stream network and defined 3-D cross sections. The process is divided in three steps which includes: - Preparation of polyline themes defining stream centerline, stream banks, flow path lines and cross-sections, Use of the HEC-GeoRAS preRAS menu functions to extract 3-D spatial data from the TIN to develop 3-D polyline Z themes of the previously defined stream centerline, stream banks, flow path lines and cross-sections and Generation of the HEC-RAS Import File.

Creating RAS Themes

The RAS Themes are the basis for the geometric data extracted in the GIS for hydraulic analysis in HEC-RAS. These Themes include: Stream Centerline, Banks, Flow Paths Centerlines, Cross-Sectional Cut Lines, Land Use, Levee Alignments, Ineffective Flow Areas, and Storage Areas.

Attributing RAS Theme

Once the RAS Themes have been created, the geometric data extraction process began. The Stream Centerline Theme completed and the cross-section attributes (geometric data for each cross section) constructed.

Generating the RAS GIS Import File

To generate the RAS GIS Import File, the 3D stream Centerline and Cross Section Surface Line (3D) shape file created from the RAS Theme. Geometric data from the two 2D (stream Centerline and Cross Section Surface Line) shape files is written to the RAS GIS Export File. The geometric data includes: river, reach, and station identifiers; cross-section cut lines; cross section surface lines; main channel bank stations; downstream reach lengths for the left overbank, main channel; and overbank. HEC-GeoRAS also enables viewing of exported results from RAS. The import file is created from data extracted from data sets (ArcGIS shape files) and from a Digital Terrain Model (DTM) represented by a triangulated irregular network (TIN). Prior to performing hydraulic computations in HEC-RAS, the geometric data must be imported

and completed and flow data must be entered. Once the hydraulic computations are performed, exported water surface and velocity results from HEC-RAS may be imported back to the GIS.

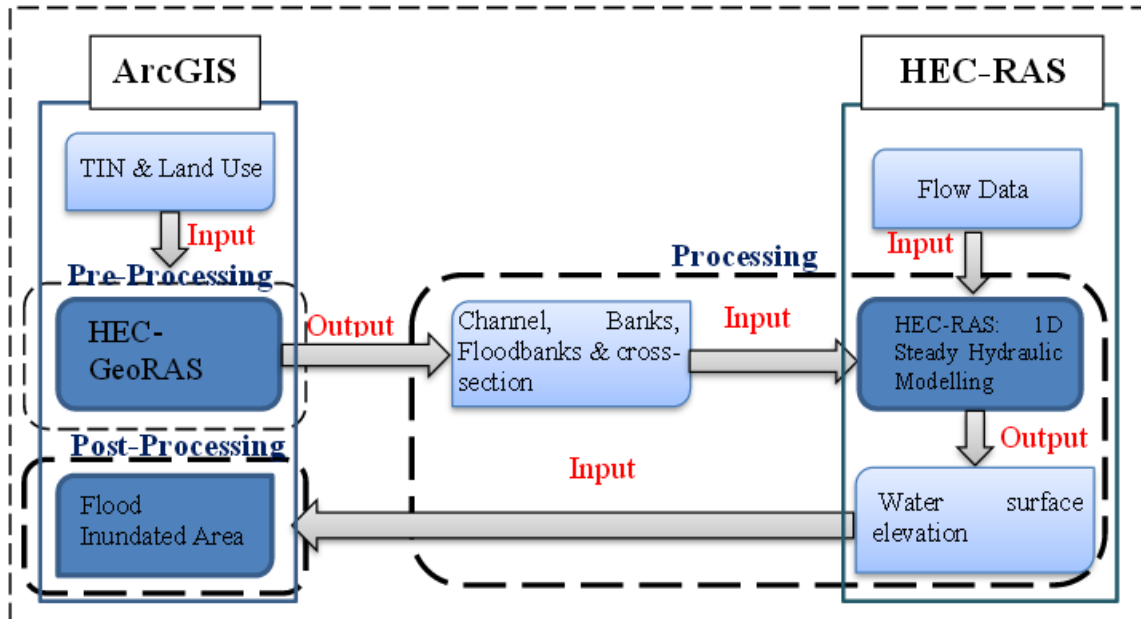


Figure 3-8:- Modelling approach for Flood Inundation Mapping

3.4.2 HEC-RAS

Hydraulic Engineering Center River Analysis System (HEC-RAS) developed by the Hydraulic Engineering center of U.S. Army corps of Engineers. The software allows performing one dimensional steady flow, unsteady, flow calculations, sediment transport/mobile bed computations and water temperature modelling. The system is comprised of a graphical user interface (GUI), separate analysis components, data storage and management capabilities, graphics and reporting facilities. The model is used for determination of water surface profiles for different flow scenarios, is intended for steady flow water surface profile computations and unsteady flow simulation; perform sediment transport simulation and perform water quality simulation. The system is capable of modelling subcritical, supercritical, and mixed-flow regimes for streams consisting of a full network of channels, a dendrite system, or a single river reach. For each HEC-RAS project, there are three required components which are Geometry data, Flow data, and Plan data.

The Geometry data, for instance, consists of a description of the size, shape, and connectivity of stream cross-sections. Likewise, the Flow data contains discharge rates. Finally, Plan data contains information pertinent to the run specifications of the model, including a description of the flow regime.

3.5 Analysis of Rainfall Data

3.5.1 Filling Missing Rainfall Data

Rainfall is that part of atmospheric moisture, which reaches the earth's surface in different forms (Garg, 2005). Hydrologists start working when the precipitation reaches the ground. This connects hydrology with meteorology. Rainfall data plays a central role in developing rainfall –runoff models. Measured precipitation data are important for many problems in hydrologic analysis and design purposes. The main problem in hydrologic analysis is that these data are not fully available as expected. The reason behind for the shortage of these data is either of the malfunctioning of the gauge or may be due to absence of an observer to make the necessary visit to the gauge. These gaps in rainfall record data's can be filled with several approaches. But the result from these data may not be as accurate as the original data. The commonly approaches are:

1. Arithmetic Average Method
2. Normal Ratio Method
3. Regression Method
4. Inverse Distance Weighting Method

Arithmetic Average Method: - The missing record is computed as the simple average of the values at the nearby gauges. Mc Cuen (1998) recommends using this method only when the annual precipitation value at each of the neighboring gauges differs by less than 10% from that of other gauge stations with missing data.

$$p_x = \frac{1}{M} [p_1 + p_2 + p_3 \dots \dots \dots + p_n] \text{Eq. 3-3}$$

Where. P_x is the missing precipitation record, $P_1 P_2 P_3 \dots \dots \dots P_n$ is Precipitation records at the neighbouring stations and M is Number of neighbouring stations

Due to this annual precipitation value at each of the neighbouring gauges differs by less than 10% from that of other gauge stations with missing data, so compatibility of the method is arithmetic average Method is used for filling the missing rainfall data.

Normal Ratio Method: - If the annual precipitations vary considerably by more than 10%, the missing record is estimated by the Normal Ratio Method, by weighing the precipitation at the neighbouring stations by the ratios of normal annual precipitations.

$$p_x = \frac{N_x}{M} \left[\frac{p_1}{N_1} + \frac{p_2}{N_2} + \dots + \frac{p_m}{N_m} \right] \text{Eq. 3-4}$$

Where: N_x is Annual-average precipitation at the gauge with missing values, N_1, N_2, \dots, N_m is Annual average precipitation at neighbouring gauges and $P_1, P_2, P_3, \dots, P_m$ is Precipitation records at the neighbouring stations. Moreover, to calculate percent of difference to decide whether to use station average method or normal ratio method the following equation 3.5 was used.

$$\% \text{ Difference} = \frac{N_x - N_i}{N_x} * 100 \text{Eq.3-5}$$

Where, N_x is the normal annual rainfall amount from the missing data station and N_i is the normal annual rainfall amount from the one of the nearby stations. (Zemadim (PhD), January, 2010).

Regression Method: - multiple linear regression of the form

$$p_x = a_0 + a_1 p_1 + a_2 p_2 + \dots + a_n p_n \text{Eq. 3-6}$$

May be established and the coefficients $a_0, a_1, a_2, \dots, a_n$ can be calculated by least square method. The equation can be used to compute rainfall p_x of the missing station. The use of this method is advantageous over the previous two and can be effectively used when a digital computer is available at a site. A random error component $e_x \times S_{yx}$ may be added to equation above if large amount of missing data is to be estimated whereas the normal random number with zero mean and unit standard deviation. It can be selected from random number tables given in any standard mathematical book. S is the standard error of estimate. The standard error of estimate can be estimated from the equation.

$$S_{yx} = \sqrt{\sum_{i=1}^n (y_i - y_{ei})^2} \text{Eq.3-7}$$

Inverse Distance Method weights: - The annual average value only by their distances “dm” from the gauge with the missing data and so does not require information about

average annual precipitation at the gauges. The Inverse Distance Method weights the annual average values only by their distances, d_m , from the gauge with the missing data and so does not require information about average annual precipitation at the gauges. The missing value is estimated as: -

$$D = \sum_{m=1} d_m^{-b} \text{Eq.3-8}$$

The value of b can be 1 if the weights are inversely proportional to distance or 2, if the weights are proportional to distance squared. If relatively few values are missing at the gauge of interest, it is possible to estimate the missing value by regression method.

Testing of Outliers

Outliers are data points that depart significantly from the trend of the remaining data. The retention or deletion of these outliers can significantly affect the magnitude of statistical parameters computed from the data, especially for small samples. Procedures for treating outliers require judgment involving both mathematical and hydrologic considerations. According to the (Committee, 1981) if the station skew is greater than +0.4, tests for high outliers are considered first; if the station skew is less than - 0.4, tests for low outliers are considered first. Where the station skew is between ± 0.4 , tests for both high and low outliers should be applied before eliminating any outliers from the data set. The following frequency equation can be used to detect outliers;

$$Y_h = y \pm K_n s_y \text{Eq. 3-9}$$

Where: y samples mean, s_y sample standard deviation and the value of the detection deviate K_n obtain using the sample size (n) from Annex 1.(H.McCuen, 1998). The minus sign indicates for low outlier and plus sign indicate for upper outlier.

The K_n values are used in two-sided tests that detect outliers at the 10-percent level of significance in normally distributed data. If the logarithms of the values in a sample are greater than Y_h in the above equation, then they are considered high/low outliers. Flood peaks considered high outliers should be compared with historic flood data and flood information at nearby sites. Historic flood data comprise information on unusually extreme events outside of the systematic record. According to the (Committee, 1981) if information is available that indicates a high outlier is the maximum over an extended

period of time, the outlier is treated as historic flood data and excluded from analysis. If useful historic information is not available to compare to high outliers, then the outliers should be retained as part of the systematic record. Kn value is shown in the annex.

Table 3-2:- outlier value

The value of upper and lower limit				
K_n	2.385			
X_{mean}	3.370	Upper limit	$X_{\text{mean}} + K_n * S$	57.80
S	0.288	Lower limit	$X_{\text{mean}} - K_n * S$	14.62

3.5.2 Checking the Stability of Variance and Mean

Hydrological time series data may exhibit trends referred to as inconsistencies or non-homogeneities. Inconsistencies result from changes in the amount of systematic errors associated with recording of data, such as those arising from changes in instrumentation or observational practices. Non-homogeneity is defined as a change in the statistics of the data set which are caused by natural or man-made changes (e.g. change in land use (deforestation), water use, climatic change, etc.). Split record tests on variances and means are applied to detect the presence of inconsistencies or non-homogeneities. These tests are referred to as the F-test for stability of the variances and t-test for stability of the mean. These two tests can be reinforced by a third test, Spearman's rank correlation test, for indicating absence of trends.

I. Test the Stability of the Variance: the distribution of the variance-ratio of samples from a normal distribution is known as the F, or Fisher distribution that gives an acceptable indication of stability of variance. The test for stability of variance is performed by F-test by using equation 3.10

$$F_t = \frac{\sigma_1^2}{\sigma_2^2} = \frac{s_1^2}{s_2^2} \text{Eq. 3-10}$$

Where, the samples standard deviation s can be calculated using equation 3.11

$$S = \left[\frac{\sum_{i=1}^n (x_i^2) - \frac{(\sum_{i=1}^n x_i)^2}{n}}{n-1} \right]^{0.5} \text{Eq. 3-11}$$

Where X_i is the observation, n is the total number of data in the sample. The variance of the time series is stable, and one can use the sample standard deviation, S , as an estimate of the population standard deviation if the following condition is met.

$F\{v_1, v_2, 2.5\% \} < F_t < F\{v_1, v_2, 97.5\% \}$, Where $v_1 = n_1 - 1$ number of degree of freedom for the numerator, $v_2 = n_2 - 1$ number of degree of freedom for the denominator, and n_1 and n_2 are the number of data in each subset.

II. Test the Stability of the mean: The stability of the mean was checked by the t- test. The t-test consists of calculating and then comparing the means of two or three non-overlapping sub-sets of the time series (the same subsets from the F-test for stability of variance). If the series mean X_1 equal with the series mean of X_2 , the series mean is stable and no need of t- test, but if the series mean (X_1) is less than or greater than that of the series mean (X_2), then, the t-test must be performed using equation 3.12. And the condition $t\{v, 2.5\% \} < t_t < t\{v, 97.5\% \}$ should full fill, so the series mean will be stable.

$$t_t = \frac{\bar{X}_1 - \bar{X}_2}{\left[\frac{(n_1 - 1)s_1^2 + (n_2 - 1)s_2^2}{n_1 + n_2 - 2} \left(\frac{1}{n_1} + \frac{1}{n_2} \right) \right]^{0.5}} \text{Eq.3-12}$$

Where: n is the number of data in the subset, (\bar{x}) the mean of the subset and (S) is variance. (Dahmen & Hall, 1990)).

Here both test for stability of the variance and mean satisfy the conditions, $F\{V_1, V_2, 2.5\% \} < F_t < F\{V_1, V_2, 97.5\% \}$ i.e. $-2.02 < 1.45 < 2.02$. Moreover, the t-test for stability of mean also $t\{v, 2.5\% \} < t_t < t\{v, 97.5\% \}$; $-2.02 < 0.073 < 2.02$. Therefore, the variance as well as the mean of the time series is stable which is, the data is homogeneous, stationery and consistence to use in probability distribution computation.

3.5.3 Checking the Consistency of Rainfall Data

Consistency is to mean when someone behaves or performs in a similar way or when something always happens in a similar way. If the conditions relevant to the recording of rain gauge station have undergone a significant change during the period of record, inconsistency would arise in the rainfall data of that station. Some of the common causes for inconsistency of record includes: - shifting of a rain gauge station to a new

location, the neighbourhood of the station may have undergone a marked change, change in the immediate environment due to damage due to deforestation, obstruction, etc and occurrence of observational error from a certain date both personal and instrumental.

The most common method of checking for inconsistency of a record is the Double-Mass Curve analysis (DMC). The curve is a plot on arithmetic graph paper, of cumulative precipitation collected at a gauge where measurement conditions may have changed significantly against the average of the cumulative precipitation for the same period of record collected at several gauges in the same region. The data is arranged in the reverse order, i.e., the latest record as the first entry and the oldest record as the last entry in the list. A change in proportionality between the measurements at the suspect station and those in the region is reflected in a change in the slope of the trend of the plotted points. If a Double Mass Curve reveals a change in slope that is significant and is due to changed measurement conditions at a particular station, the values of the earlier period of the record should be adjusted to be consistent with latter period records before computation of areal averages. The adjustment is done by applying a correction factor K , on the records before the slope change given by the following relationship.

$$K = \frac{\text{slope for period after slope change}}{\text{slope for period before slope change}}$$

Double mass curve technique compares the accumulated annual or seasonal precipitation at a given station with the concurrent accumulated value of the mean precipitation for a group of surrounding stations. Since the past response is to be related to the present conditions, the data (accumulated precipitation of the station x , i.e. $\sum p_x$ and the cumulative values of the average of the group of the base stations $\sum p_{av}$) are usually assembled in reverse chronological order. Values of $\sum p_x$ are plotted against $\sum p_{av}$ for the concurrent time periods. The precipitation values at station x at and beyond the period of change is corrected using the relation,

$$p_{cx} = p_x \frac{S_c}{S_a} \text{---Eq. 3-13}$$

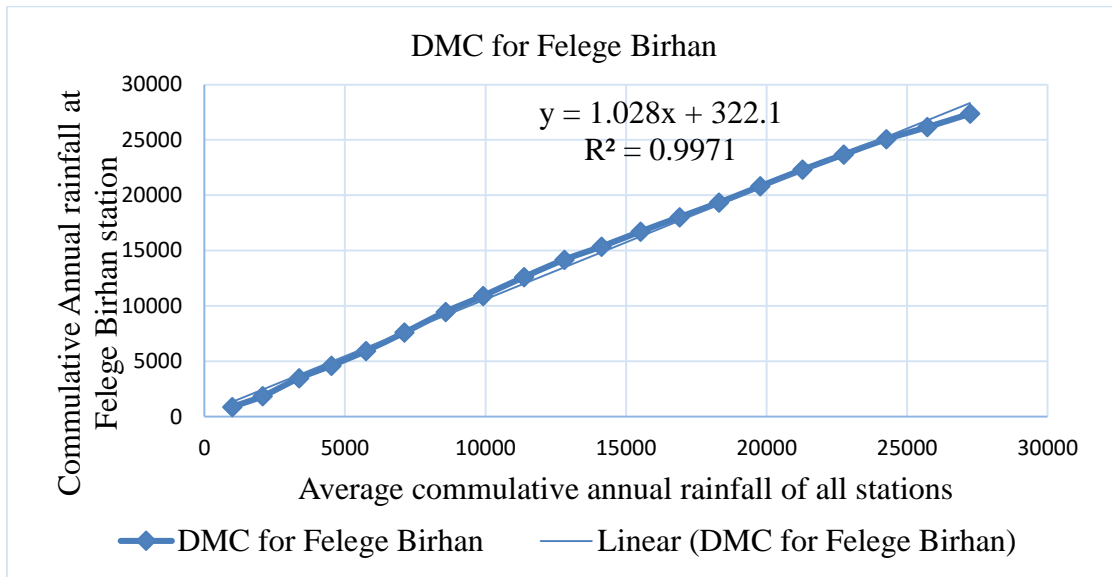
Where, p_{cx} = corrected value of precipitation at station x at any time t .

p_x = Original recorded value of precipitation at station x at time t ,

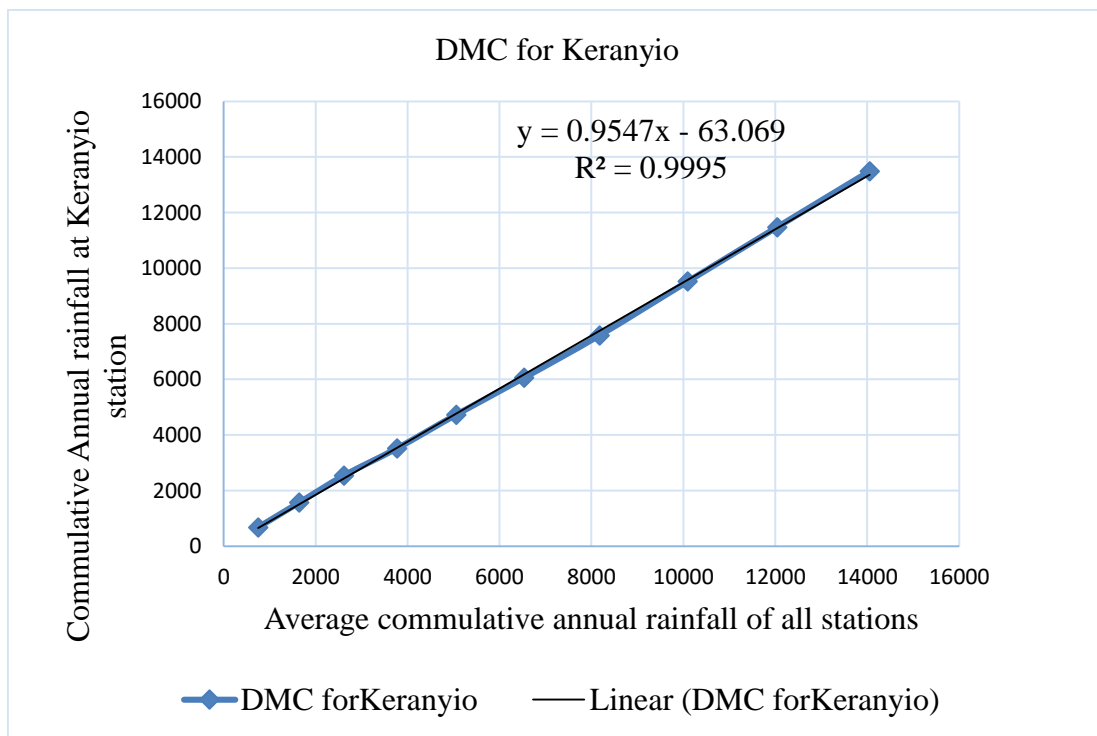
S_c = corrected slope of double mass curve

S_a = original slope of the curve

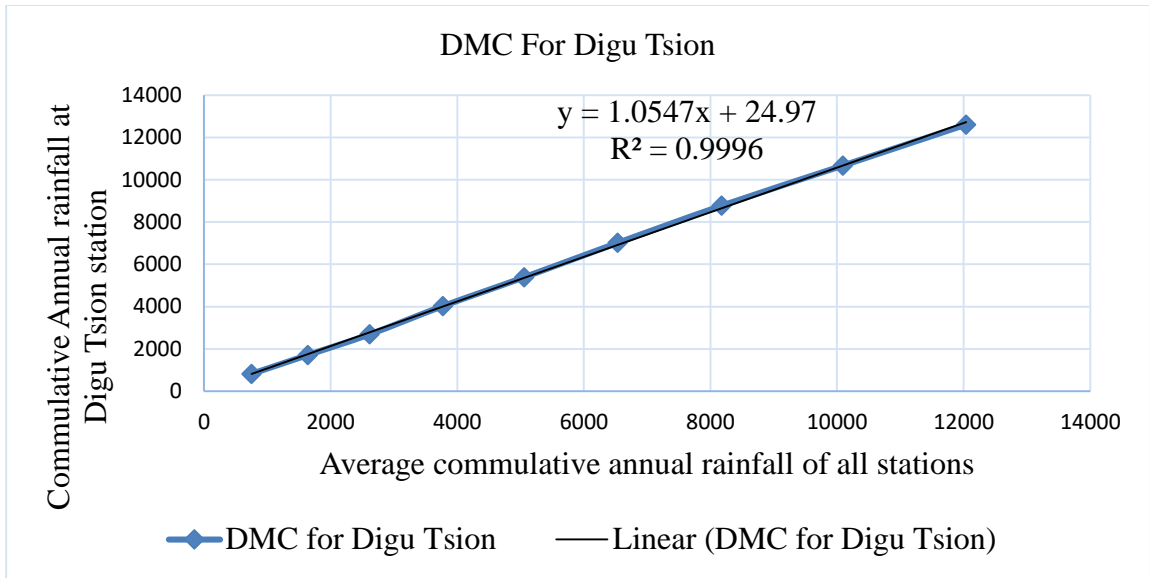
a. Double mass curve of Felege Birhan station



b. Double mass curve of Keraniyo station



c. Double mass curve of DiguTision station



d. Double mass curve of Gundowion station

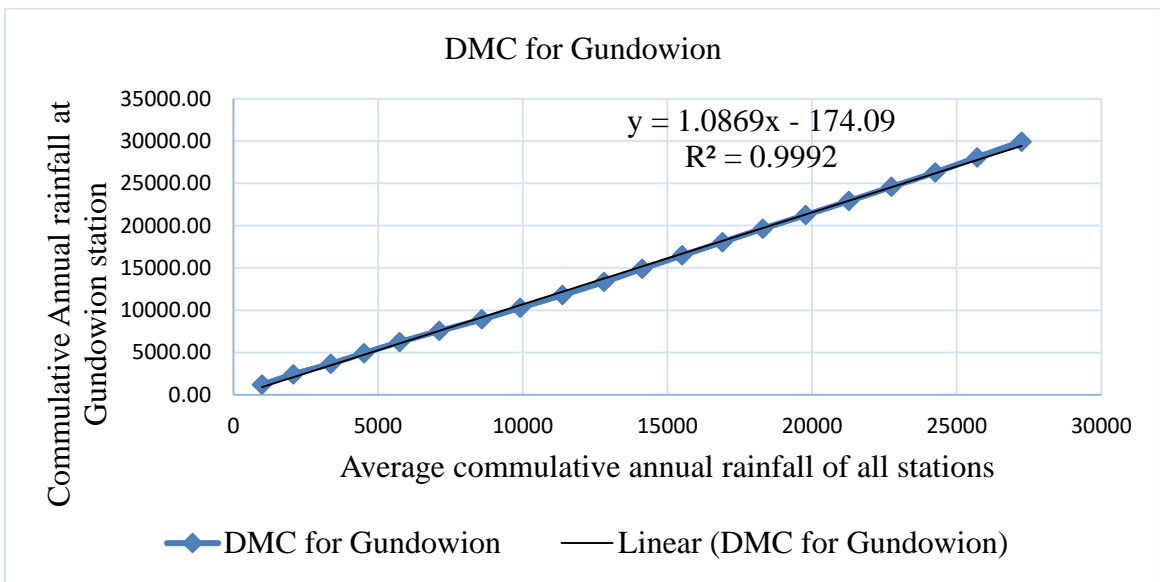


Figure 3-9:- consistency checking of stations within and around study area.

From the above graph we concluded that the data is consistent and the double mass curve of the rainfall is providing information on the duration and magnitude of the storm.

Homogeneity Test

Homogeneity is an important issue to detect the variability of the data. In general, when the data is homogeneous, it means that the measurements of the data are taken

at a time with the same instruments and environments. However, it is a hard task when dealing with rainfall data because it is always caused by changes in measurement techniques, observational procedures, environment characteristics, structures, and location of the stations. In this study, homogeneity test has been applied at two meteorological stations in Temiewatershed area from the period 1984 – 2003.

To check homogeneity of the selected stations in the watershed the non-dimensional rainfall records plotted to compare the stations with each other. The following equation was used.

$$P_i = \frac{P_{i,av}}{P_{av}} * 100 \text{Eq. 3-14}$$

Where: P_i is non - dimensional value of precipitation for the month in station i , $P_{i, av}$ is over year's averaged monthly precipitation for the station i and P_{av} is over year's averaged yearly precipitation of the station i .

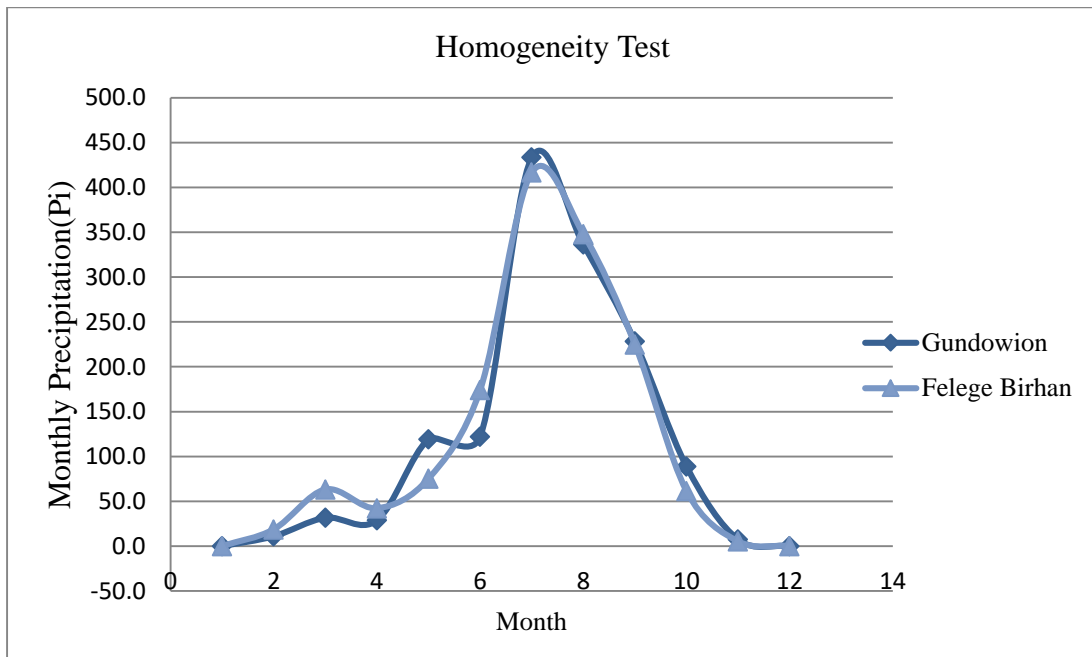


Figure 3-10: - Homogeneity tests of Temie watershed rainfall stations

The above graph shows the two stations within Temie watershed rainfall characteristics are uni-modal. Maximum rainfall has occurred from June up to October for all stations. Therefore; all stations are homogeneous in environment and measurement techniques.

3.5.4 Average depth of precipitation over an area

The average depth of precipitation over a specified area on either the storm basis or seasonal basis or annual basis is often required in several types of hydrologic problems. The depth of rainfall measured by a rain gauge is valid for that rain gauge station and in its immediate vicinity. Over large area like watershed of a stream, there will be several such stations and the average depth of rainfall over the entire area can be estimated by the following method (Te, Maidment, & Mays, 1988). The most common methods are:

- I. Arithmetic mean method
- II. Isohyetal method and
- III. Thiessen polygon method

I. Arithmetic mean method: -It is the simplest method of calculating the average rainfall over the area. The method is suitable for a basin where the gauges are uniformly distributed and the individual gauges catchment do not vary much from the mean. The method assumes that all gauges are weighting equally and is given by:

$$P_{avg} = \frac{1}{n} \sum P_i \quad \text{Eq. 3-15}$$

Where: P_{avg} is aerial rainfall, mm/d, P_i is rainfall record by n number of metrological gauging stations located within the basin, in mm/d. Arithmetic mean does not account for the orographic effects. Therefore; this method doesn't consider gauge stations that are located outside the boundary of the watershed.

II. Isohyetal method; Isohyets are the contours of equal rainfall. This method is the best and most reliable method. It takes account of both the orographic and storm characteristics of the catchments. The main limitation of this method is that it is a subjective approach and needs an experienced analyst to draw contours of equal rainfall depth over the basin.

$$P_{avg} = \frac{A_1 * \left(\frac{P_1 + P_2}{2}\right) + A_2 * \left(\frac{P_1 + P_2}{2}\right) + \dots + A_{n-1} * \left(\frac{P_{n-1} + P_n}{2}\right)}{A_1 + A_2 + \dots + A_n} \quad \text{Eq.3-16}$$

Where: P_{ave} is Aerial rainfall, mm/d; P_1, P_2 is Isohyets, mm/d and A_1, A_2 is Area between the isohyets, km^2 . Even though this method is reportedly better than the other,

it is very difficult to apply the method accurately in the inaccessible and very limited data source.

III. Thiessen polygon method: - Thiessen polygon method takes into account the non-uniform distribution of the rain gauge by assigning a weighting factor for each rain gauge. In this method the entire area is divided into number of triangular areas by joining adjacent rain gauge stations with straight line. If a bisector is draw on each of the lines joining adjacent rain gauge stations, there will be number of polygons and each polygon within itself will have only one rain gauge station.

$$\bar{P} = \frac{1}{A} \sum_{i=1}^n P_i A_i \text{ Eq. 3-17}$$

Where, $A = \sum_{i=1}^n A_i = A_1 + A_2 + A_3 + \dots + A_n$ here, $\frac{A_i}{A}$ is termed the weight factor in i^{th} rain gauge.

Table 3-3:-Rainfall Stations weight

Stations	Area(km ²)	Weight factor
Felege Birhan	56.065	0.4744
Gundowion	62.112	0.5256

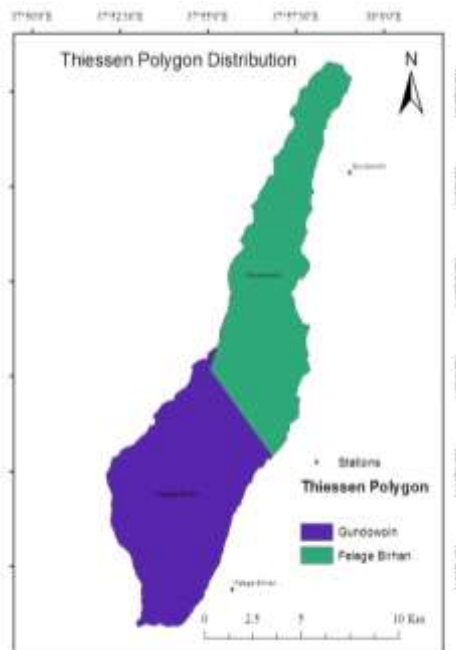


Figure 3-11:- Temie watershed rainfall stations using Thiessen polygon

3.5.5 Determination of Probability Distributions

To calculate probable maximum flood (PMF), first it is necessary to calculate PMP. In PMP is the first task must be determined for modelling and flood inundation mapping. During flood mapping the maximum design flood considered in fixing the maximum Rainfall through a return period is the Probable Maximum Flood (PMF) that may occur within the catchment. For this study, a 20, 50,100,500and 1000-year probable maximum precipitation has been determined using the following most commonly used frequency analysis methods. Moreover, among these methods the one having the smallest D-index will take as Probability Distributions.

- A. Normal Distribution: is used in frequency analysis for fitting empirical distributions to hydrological data, the frequency factor can be expressed by using equation 3.18.

$$X_T = \mu + K_T \delta \quad \text{Eq. 3-18}$$

Where; X_T is the required rainfall for the given return period T; μ : mean value of recorded rain fall event for Successive years,; σ : Standard deviation of the recorded rain fall event for Successive years; K_T : the frequency factor corresponding to an exceedance probability of $P\left(P = \frac{1}{T}\right)$

$K_T = Z$ and can be determined using equation 3.19

Z: the standard normal Variable

$$Z = W - \frac{2.515517 + 0.802853W + 0.01328W^2}{1 + 1.432788W + 0.189269W^2 + 0.001308W^3} \quad \text{Eq. 3-19}$$

$$W = \left(\ln\left(\frac{1}{p^2}\right)\right)^{\frac{1}{2}} \quad \text{Eq. 3-20}$$

Where w: intermediate variable, T: the return period

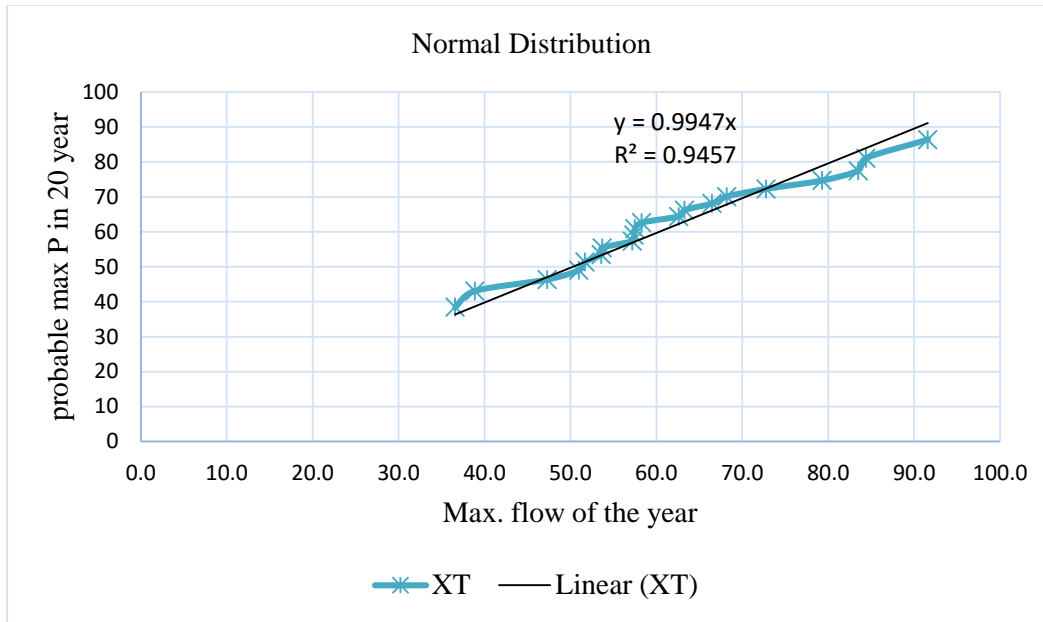


Figure 3-12:-Maximum Probability Distributions using normal distribution

B. Log-normal Frequency Distributions: The same procedure used for fitting the normal distribution also used to fit the lognormal frequency distribution. But first the hydrologic data must first be transformed to logarithms, $y = \log x$, and this transformation creates a new random variable y , the mean μ and standard deviation σ of the logarithms are computed and used as the parameters of the population. Finally, the required precipitation can be estimated using Equation 3.21.(H.McCuen, 1998).

$$Y_T = \mu + K_T \delta \quad \text{Eq. 3-21}$$

Where, $K_T = Z$ and can be calculated using equation 3.22.

$$Z = W - \frac{2.515517 + 0.802853W + 0.01328W^2}{1 + 1.432788W + 0.189269W^2 + 0.001308W^3} \quad \text{Eq. 3-22}$$

$$W = \left(\ln\left(\frac{1}{p^2}\right)\right)^{1/2} \quad \text{Eq. 3-23}$$

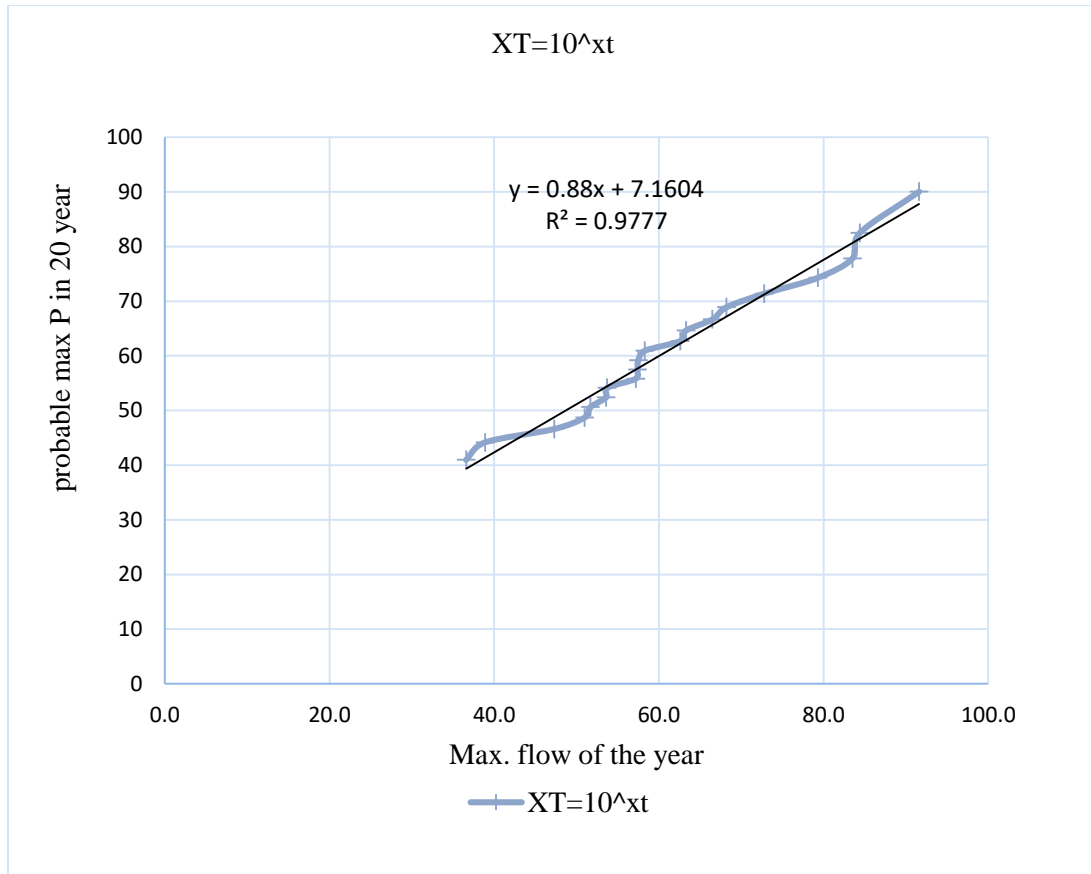


Figure 3-13: - Maximum Probability Distributions using Log-normal frequency distribution

C. Log Pearson Type III: In this distribution the first step is to take the logarithms of the hydrologic data in base 10 i.e $y = \log x$. Also, in log Pearson type-III the mean μ , standard deviation σ and coefficient of skewness C_s are calculated for the logarithms of the data y . And here the frequency factor depends on the return period T and Coefficient of skewness CS i.e. when $C_s=0$, the frequency factor is equal to the standard normal variable z and can be calculated using the above equation 3.22 and 3.23, but when $CS \neq 0$, K_T can be calculated using equation 3.25. Finally using equation 3.24 the required precipitation can be calculated.

$$Y_T = \mu + K_T \delta \quad \text{Eq 3-24}$$

$$K_T = z + (Z^2 - 1)K + \frac{1}{3}(Z^3 - 6Z)K^2 - (Z^2 - 1)K^3 + ZK^4 + \frac{1}{3}(K^5) \quad \text{Eq. 3-25}$$

Where, the coefficient $K = CS/6$ (Chow, 1959).

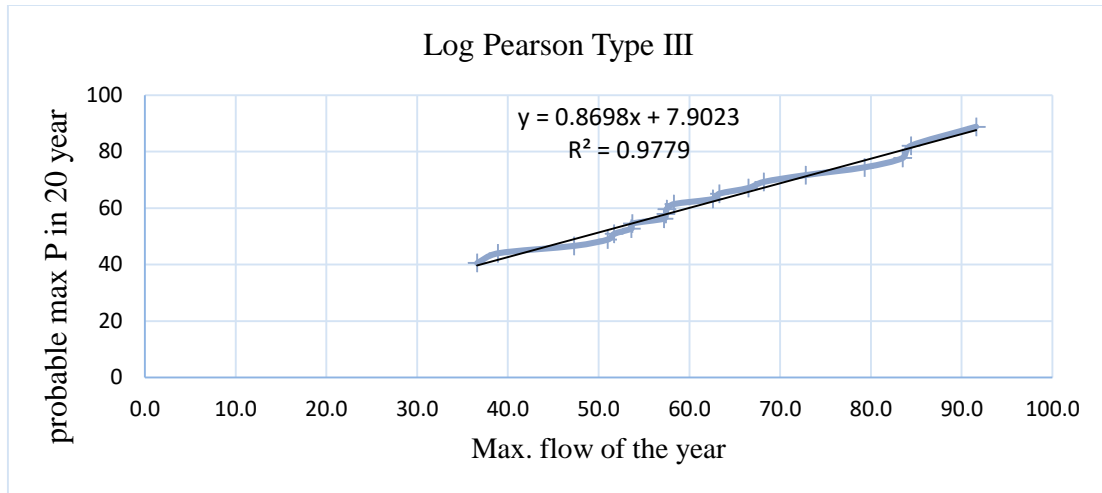


Figure 3-14:-Maximum Probability Distributions using Log Pearson type III

D. Pearson Type III: Here also the same procedures like that of Log Pearson type III is applied, but first it is necessary to estimate the mean μ and the standard deviation σ for the recorded normal precipitation data without changing in to logarithm. Then the frequency factor K_T calculated using equation 3.26 and, finally using equation 3.25 the required precipitation for the given return period T was estimated.

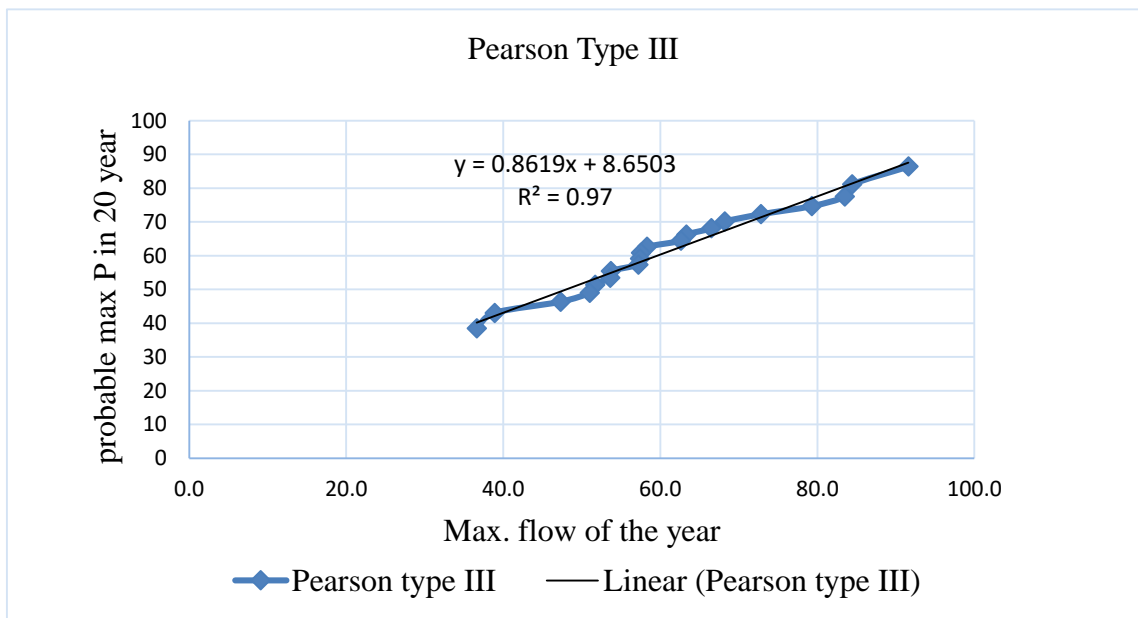


Figure 3-15:- Maximum Probability Distributions using Pearson type III

E. Extreme value type-I (EVI) or Gumbel distribution: one way of estimating EVI as it was introduced by E.J. Gumbel in 1941 based on the principle that the distribution of an extreme event is unlimited and hence the most suitable distribution for fitting the

extreme values is of double exponential type(Luna Moni Das, 2015).Estimating of peak rainfall given by equation 3.26.

$$XT = X + KT\sigma \text{Eq. 3-26}$$

Where X is arithmetic mean of all the peak rainfall in the series, σ is Standard Deviation of all the peak rainfall in the series. The frequency factor, KT of Gumbel is given by equation 3.27.

$$KT = \frac{Y_T - Y_n}{S_n} \text{Eq. 3-27}$$

Where Y_n and σ_n Gumble's Reduced mean and standard deviation respectively which will read from Table as a function of number of data. The maximum value of Y_n is 0.577 when $N \rightarrow \infty$, and the maximum value of S_n is 1.2825 when $N \rightarrow \infty$.

$$YT = -Ln [Ln (\frac{T}{T-1})] \text{Eq-3.29}$$

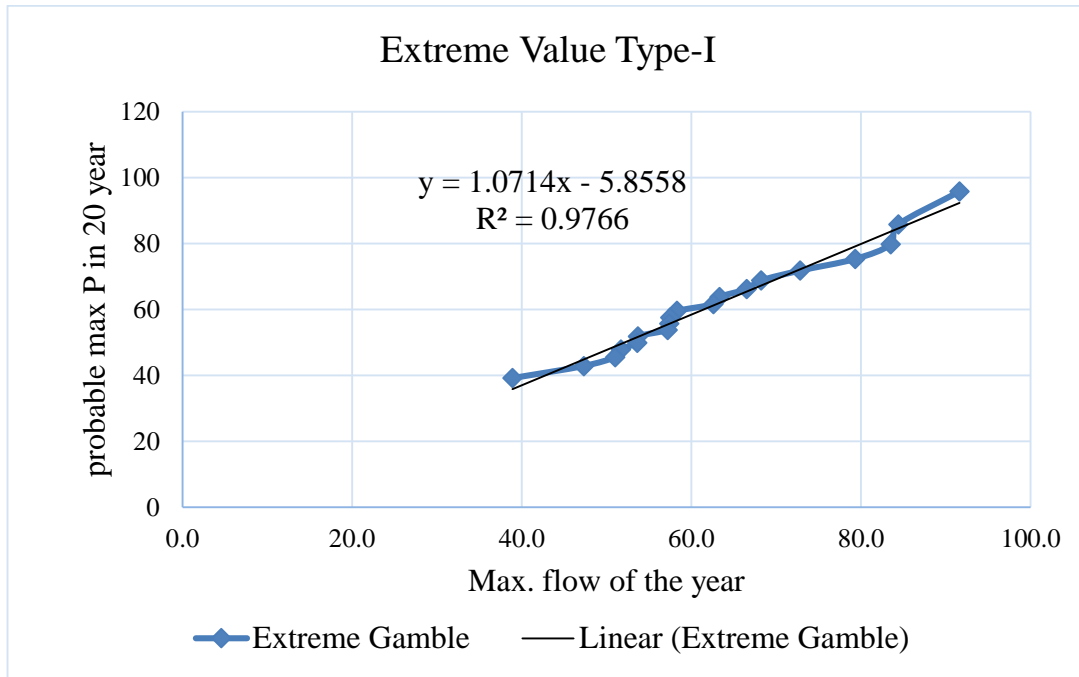


Figure 3-16:- Maximum Probability Distributions using extreme value type -I

3.5.6 Testing the goodness of fitness of probability

D-Index: used to identify the suitable frequency analysis methods to calculate the probable maximum precipitation. Therefore; the selection of a suitable distribution for

rainfall estimation among the above mentioned five frequency analysis methods performed through D-index Test. It is given by equation 3.30.

$$D - \text{Index} = \frac{1}{R} * \sum_{i=1}^6 \text{Abs}(R_i - R_i^*) \text{Eq. 3-30}$$

Where, R is the average value of the series of the recorded rainfall, R_i 's (i=1 up to 6) are the first six highest values in the series of recorded rainfall and R_i^* is the estimated rainfall by probability distribution. The distribution with lowest value of D-Index considered as the best distribution for rainfall estimation. (N.Vivekanandan, August, 2014).

Therefore, based on the above discussed rainfall frequency analysis techniques the Probability Distributions of the study area is presented in Table 3.4. Among the four techniques Extreme value type-I (EVI) or Gumbel distribution has the larger rainfall which is 95.812mm for 20 years return period but the remaining methods have the smallest rainfalls. Moreover, the other computed Probability Distributions presented in the Annex.

Table 3-4:- D -Index for different frequency distribution type

Type of distribution	D -Index	ppt	Remark
Normal	0.269211793	86.4	
Lognormal	0.202632494	90.0	
Log Pearson	0.226139923	88.8	
Pearson type III	0.269211793	86.4	
Gumbel Extreme	0.186298414	95.8	Selected

But, for areas greater than 2500ha this 24-hr Probability Distributions which is point rainfall should be converted into aerial precipitation by using area reduction factor, (Asquith, 1999). Because there is no information of the rainfall hourly distribution when extreme storm events occur, the 24-hr Probability Distributions were hourly distributed by using the following equation:

$$P = M * \sqrt{T} \text{Eq. 3-31}$$

Where P is rainfall depth, T is rainfall duration and M is a constant.

$$kT = Z + (Z^2 - 1) * K + \frac{1}{3}(Z^3 - 6Z) * K^2 - (Z^2 - 1) * K^3 + ZK^4 + \frac{1}{3} * K^5 \text{Eq. 3-32}$$

$$K = \frac{CS}{6} \text{Eq. 3-33}$$

$$W = \left(\ln\left(\frac{1}{p^2}\right)\right)^{0.5} \text{Eq. 3-34}$$

Table 3-5: - Probability Distributions in different return period

Return period	X	YT	Yn	Sn	KT	XT
20	61.8	2.9701	0.5238	1.0628	2.30184	95.8
50	61.8	3.9019	0.5485	1.1607	2.889152	104.5
100	61.8	4.6001	0.56	1.2065	3.348652	111.3
500	61.8	6.2136	0.5724	1.2588	4.481417	128.0
1000	61.8	6.9072	0.5775	1.2826	4.935097	134.8

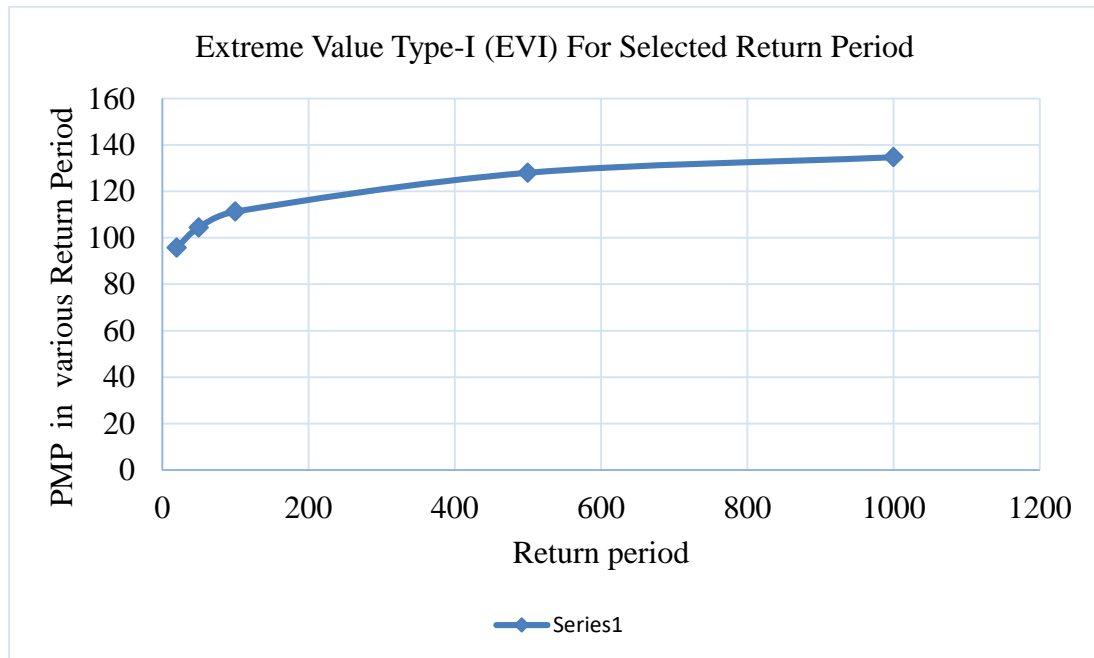


Figure 3-17: - Probability Distributions in different return periods

3.6 HEC-GeoHMS Data Processing

The point of the extensive data pre-processing using Arc-Hydro was to create input files for the HEC-GeoHMS tools. HEC-GeoHMS uses the output files from Arc-Hydro and automatically create sub-basins, longest and centroidal flow paths, basin centroid and other watershed properties. Additionally, parameters such as slope and length are assigned to flow lines and basins. In general, HEC-GeoHMS uses spatial analyst tools to convert geographic information into parameters for each of the basins and flow lines. These parameters are used to create a HEC-HMS model that can be used within the HEC-HMS program. Through the GUI, which consists of menus, tools, and buttons, the user can analyze the terrain information, delineate sub-basins and streams, and prepare hydrologic inputs.

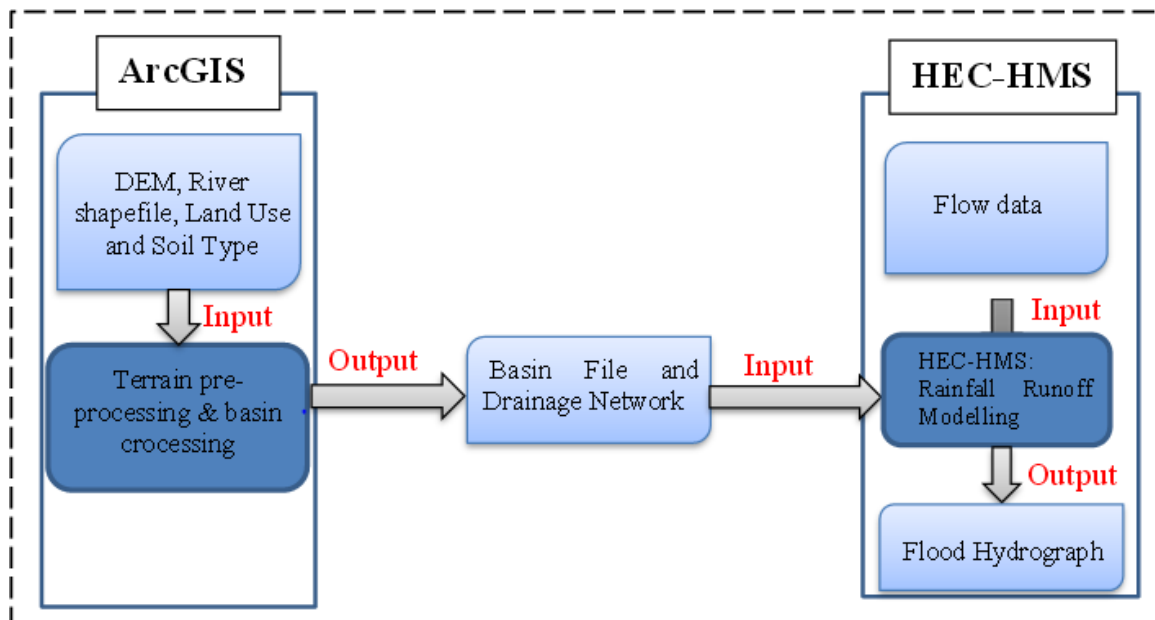


Figure 3-18:- Modelling approach Rainfall Runoff Modelling

The methodology used for carrying out Rainfall Runoff Modelling can be described by categorizing them into three sections, which are as follows:

- i. Creating Basin Model
- ii. Developing Hydrological Parameters
- iii. Hydrological Modeling

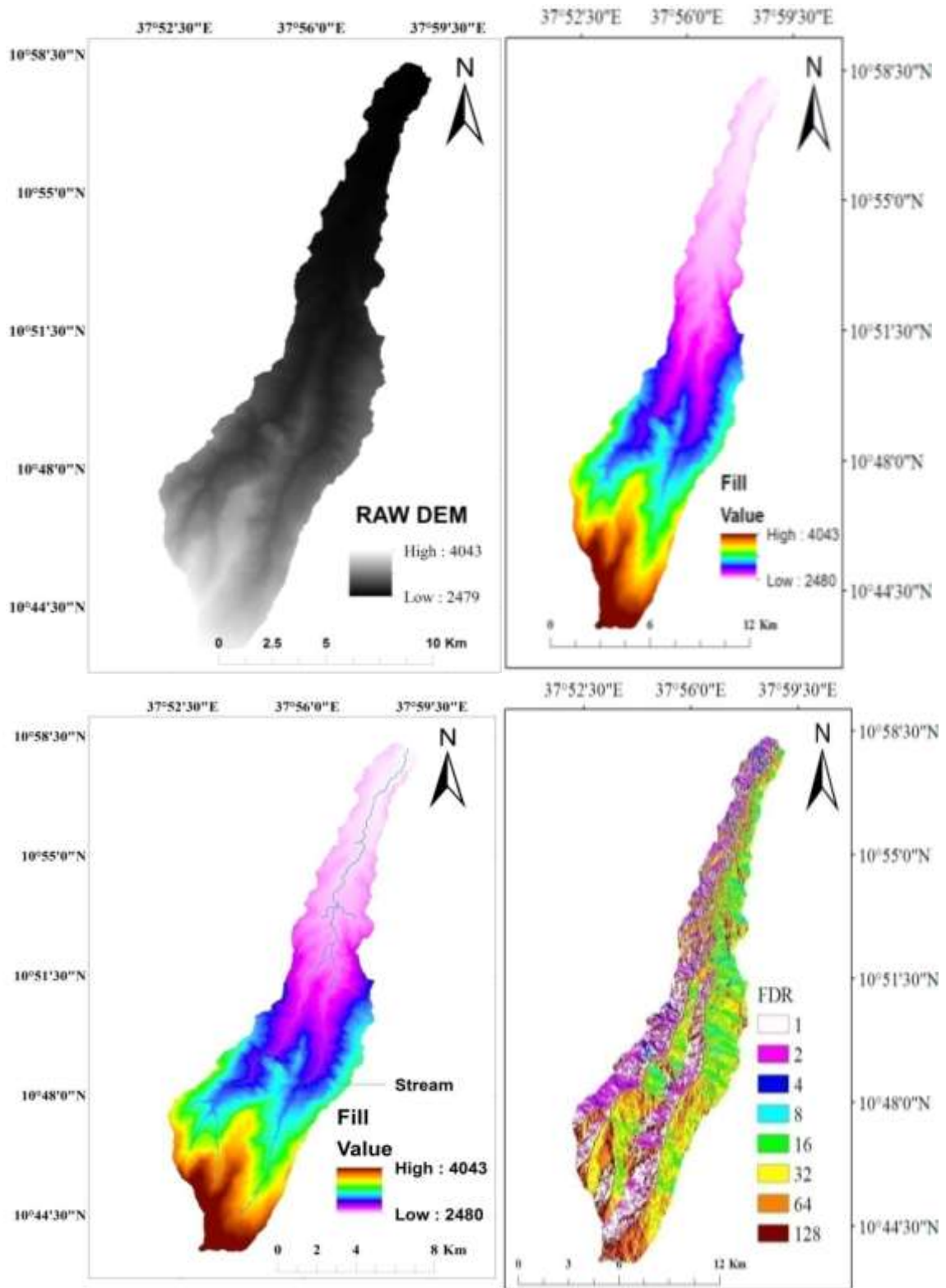


Figure 3-19:- Terrain Processing using Arc Hydro Tools

3.7 Basin Model

Basin model is one of the main components in HEC-HMS project set up. These models contain elements of the basin and their connectivity. The Basin model principally serves to convert atmospheric conditions into stream flow at specific locations in the watershed. HEC-HMS treats the different phases of rainfall-runoff processes with separate mathematical models. All components of the loss models, direct runoff models, base flow and routing models are accessed from the basin model component of HEC-HMS. The basin model is responsible for describing the physical properties of the watershed and the topology of the stream network. This portion describes how watershed information is entered into the program using HEC-GeoHMS and HEC-HMS basin model. It contains the modelling components that describe catchment data, infiltration, surface runoff and channel routing. Outflow is computed from meteorological data by subtracting losses of basin and transforming excess precipitation through the basin. Sub-basins are used to model the catchment. A sub-basin is an element that usually has no inflow and only one outflow.

3.7.1 Physical Description of Sub-basin (HEC-GeoHMS)

Physical Description of Sub-basin (HEC-GeoHMS) Hydrologic elements are used to break the sub-basin into manageable pieces. They are connected together in a dendritic (branched extension or shape of a tree branch) network to form a representation of the stream system. The physical parameter analysis is done using HEC-GeoHMS.

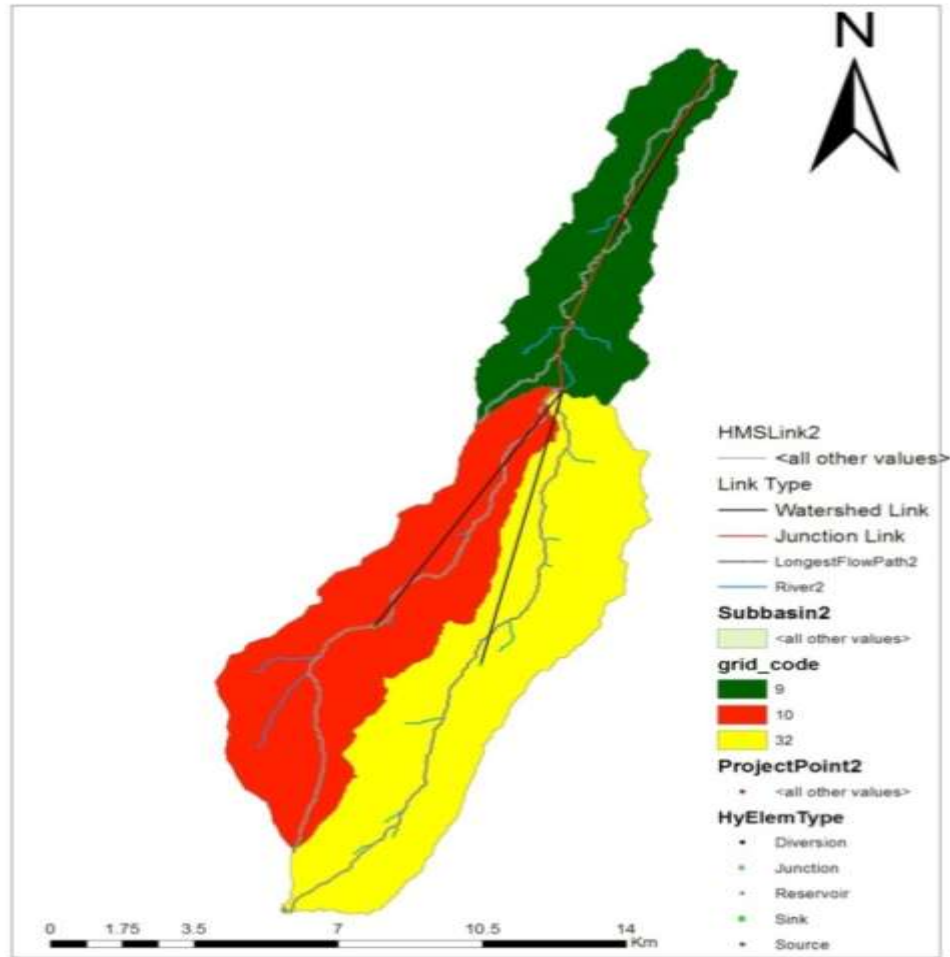


Figure 3-20:- HEC-HMS Representation Derived From HEC-GeoHMS

Table 3-6: - Basin catchment characteristics derived from HEC HMS

Basin Name	Area HMS (km ²)	Shape length(m)	Basin slope	BasinCN
W480	28.3	42755.6	3.3	77.9
W490	40.6	50188.7	21.1	80.0
W710	49.0	57007.5	24.4	77.7

The Curve Number Method

For drainage basins where no runoff has been measured, the Curve Number Method can be used to Estimate the depth of direct runoff from the rainfall depth, given an index describing runoff response characteristics. For a watershed that consists of more than one soil types and land uses, a composite CN is calculated as: -

$$CN_{\text{composite}} = \frac{\sum A_i CN_i}{\sum A_i} \text{Eq. 3-28}$$

Where, CN is the composite CN used for runoff volume computations; CN_i is an index of watersheds subdivisions of uniform land use and soil type; A_i is the CN for subdivision I and I is the drainage area of subdivision.

Initial Abstraction I_a

From analysis of results from many small experimental watersheds, the SCS developed an empirical relationship of I_a and S: The potential maximum retention S has been converted to the Curve Number CN in order to make the operations of interpolating, averaging, and weighting more nearly linear. This relationship is, $CN = \frac{25400}{254+S}$

As the potential maximum retention S can theoretically vary between zero and infinity, the Curve Number CN can range from one hundred to zero. The HEC-HMS program computes incremental Precipitation during a storm by recalculating the infiltration volume at the end of each time interval. Infiltration during each time interval is the difference in volume at the end of two adjacent time intervals.

$$Q = \frac{(p - I_a)^2}{p - I_a + S}; \text{ From the above relation peak runoff can be expressed in the form of; } Q = \frac{(p - 0.2S)^2}{p + 0.8S} \text{ for } p > 0.2S \quad \text{which means } I_a = 0.2S$$

3.7.2 Rainfall Loss Computation Methods

In HEC-HMS model, all land and water in a river basin is categorized either as directly connected impervious surface or pervious surface. From directly connected with to impervious surface all rains can directly change into runoff but rainfall on the pervious surface is subject to losses (USACE, 2001b)

There are seven methods for estimating losses in the HEC-HMS model: initial and constant, deficit and constant, Green and Ampt, SCS curve number, Soil moisture accounting, gridded SCS curve number, and gridded soil moisture accounting. (US Army Corps of Engineers, 2000).

USACE provides general recommendations for choosing HEC-HMS mathematical computation methods. These include: availability of information for calibration and

parameter estimation, appropriateness of the model assumptions, and user preference and experience.

The U.S. Soil Conservation Service has developed a synthetic unit hydrograph procedure that has been used widely for developing rural and urban hydrographs. This method can be used for catchment areas greater than 50 hectares (0.5km²). The SCS runoff equation is therefore a method of estimating direct runoff from 24-hours or 1-day storm rainfall. The maximum retention, S, and watershed characteristics are related through an intermediate parameter, the curve number (CN) as:

$$S = \frac{25400}{CN} - 254$$

3.7.3 Rainfall excess (Runoff) Computation Methods

The HEC-HMS model allows modelling direct runoff with six different methods: Clark unit hydrograph, Snyder unit hydrograph, SCS unit hydrograph, user-defined unit hydrograph, the ModClark quasi-distributed linear transform, and conceptual kinematic wave model. Among the above six methods, (Clark, 1945)Clark unit hydrograph is a frequently used technique for modelling direct runoff resulting from individual storm events (Fleming & Neary, 2004; Nelson, Miller, & Dixon, 1999). Therefore; the Clark unit hydrograph was selected for this study to transform the excess rainfall into surface runoff.

The Clark unit hydrograph method represents two key processes in the transformation of excess rainfall to runoff: translation and attenuation. Translation is based on a synthetic time-area histogram and the time of concentration, T_c. The time area histogram specifies the basin area contributing to flow at the outlet as a function of time. Attenuation is modelled with a linear reservoir (USACE, 2001a). The SCS peak flow method calculates peak flow as a function of drainage basin area, potential watershed storage, and the time of concentration.

Research by the SCS suggests that the UH peak and time of UH peak are related by:

$$U_p = \frac{CA}{T_p} \text{Eq. 3-38}$$

Where, A = watershed area; C = conversion constant (2.08 in SI system).

The time of peak (also known as the time of rise) is related to the duration of the unit of excess precipitation as:

$$T_p = \frac{\Delta t}{2} + t_{lag} \text{Eq. 3-39}$$

Δt is the excess precipitation duration (which is also the computational interval in the run) and t_{lag} is the basin lag, defined as the time difference between the center of mass of rainfall excess and the peak of the UH.

$$t_{lag} = 0.6 * t_c \text{ Eq. 3-40}$$

$$T_c = t_{cbasin} + t_{channel} \text{Eq. 3-41}$$

Where: $t_{channel} = \frac{L}{v}$ and Eq. 3-42

$$t_{cbasin} = (0.885 * L_o^3 / H)^{0.385} \text{Eq. 3-43}$$

Where: t_{cbasin} is time of flow over the basin (hr), $t_{channel}$ is time of flow in the channel(hr), v is velocity of flow in the channel (m/sec) , L is channel length (m) , L_o is the distance from the farthest point to the outlet (m) and H is total fall from the farthest point to the outlet (m)

The required input parameters of the Clark method are:

- Time of concentration, (hr)
- Storage coefficient, S_t , (hr)

3.7.4 Transformation method

A HEC-HMS model of Temie watershed was developed using the SCS curve number method, the Clark Unit Hydrograph transform, Recession base flow method and Muskingum channel routing.

3.7.5 Modelling Base Flow with HEC-HMS

The Base flow models simulate the slow subsurface drainage of water. This base flow is the sustained runoff from precipitation that was stored temporarily in the watershed, plus the delayed subsurface runoff from the current storm. The base flow is added to the direct runoff (obtained with the transformation model) to obtain the total flow, which is routed through the stream reach to the outlet. To model the base flow, HEC-HMS offers

alternative models, which can be combined with other loss, and direct runoff models.

These are: -

- Bounded Recession base flow
- Constant recession base flow
- Linear reservoir base flow
- Recession Base flow

The recession base flow method is designed to approximate the typical behaviour observed in watersheds when channel flow recedes exponentially after an event (US Army Corps of Engineers, 2000). This method is intended primarily for event simulation. However, it does have the ability to automatically reset after each storm event and consequently may be used for continuous simulation. It does not conserve mass within the sub basin.

Due to the above reasons and parameter suitability for calibration and validation, the recession method was selected for this study.

Mathematically it defines the relationship of Q_t the base flow at any time t , to an initial value.

$$Q_t = Q_0 K^t \text{Eq. 3-44}$$

Where: Q_t is the base flow at time t , Q_0 is initial base flow at time zero, and K is an exponential decay constant. This indicates that K is defined as the ratio of base flow at time t to the base flow one day earlier.

The required parameters for recession method are:

- Initial discharge (m^3/sec), R_c ; $R_c \in (0,1)$
- Recession constant
- Threshold type, (m^3/sec or ratio to peak)

3.7.6 Routing Models

Flow routing model is a procedure to determine the time and magnitude of flow (i.e., the flow hydrograph) at a point on watercourse from known or assumed hydrographs at one or more points upstream. In broad sense, flow routing may be considered as an analysis to trace the flow through a hydrologic system of a given input.

Muskingum- routing model is selected due to its preference on the manual uses a simple conservation of mass approach to route flow through the stream reach. However, it does not assume that the water surface is level. By assuming a linear, but non-level, water surface it is possible to account for increased storage during the rising side of a flood wave and decreased storage during the falling side. By adding a travel time for the reach and a weighting between the influence of inflow and outflow, it is possible to approximate attenuation. There are six methods included in the HEC-HMS model to compute river routing: lag kinematic wave, modified Puls, Muskingum, Muskingum – Cunge Standard section, and Muskingum – Cunge 8- point section.

For this thesis, Muskingum routing method was selected. This method uses simple conservation of mass approach to route flow through the stream reach and requires three parameters K, X and number of sub- reaches (n) in the catchment.

$$S = K [XI + (1- X) Q] \text{ Eq 3-45}$$

Where: S is storage (m^3), I is inflow rate (m^3s^{-1}), X is weighting factor between 0 and 0.5, Q is outflow rate (m^3s^{-1}) and K is travel time through the reach (hr.).

The Muskingum K is the travel time through the reach which simulates a delay in stream flow as it moves through the channel. And the Muskingum X is the weighting between inflow and outflow influence. The value of K can be calculated as:

$$K = \frac{L}{V} \text{ Eq. 3-29}$$

Where: L is length of reach (m) and V is mean velocity (ms⁻¹).

The length is the total length of the reach element. The slope is the average slope for the whole reach. These values are measured from the 30m resolution DEM using HEC-GeoHMS. The Manning's n, roughness coefficient, is the average value for the whole reach. This value is estimated from (Te et al., 1988)

3.8 Meteorological Model

Meteorological model is one of the main components in a project. There are seven different precipitation methods. Some precipitation methods require parameter data for each sub-basin. Other methods use the same data for all sub-basins. For this thesis work

Specified hyetograph method is adopted. Meteorologic model can be used with many different basin models. However, results computed by the Meteorologic model will be matched with the sub-basins in the basin models using the name of the sub-basin. If sub-basins in different basin models have the same name, they will both receive the same boundary conditions from the Meteorologic model. Careful naming of sub-basins is necessary so that the correct boundary conditions are computed for each one.

3.9 Control Specifications

The control specifications set the time span of a simulation run. Information in the control specifications includes a starting date and time, ending date and time, and computation time step. For this thesis the starting date, time and ending date, time were 01Jan 1984& 31 Dec2003 respectively and the computational time step was 1Day.

3.10 Time Series Components

These components were used to insert the daily precipitation and flow data to calibrate and validate the model and after calibration and validation, these time series were also used to insert the 24-hr PMP data to forecast the PMF of the study area.

To consider the spatial analysis in the catchment, it is divided into three sub-basins as shown below

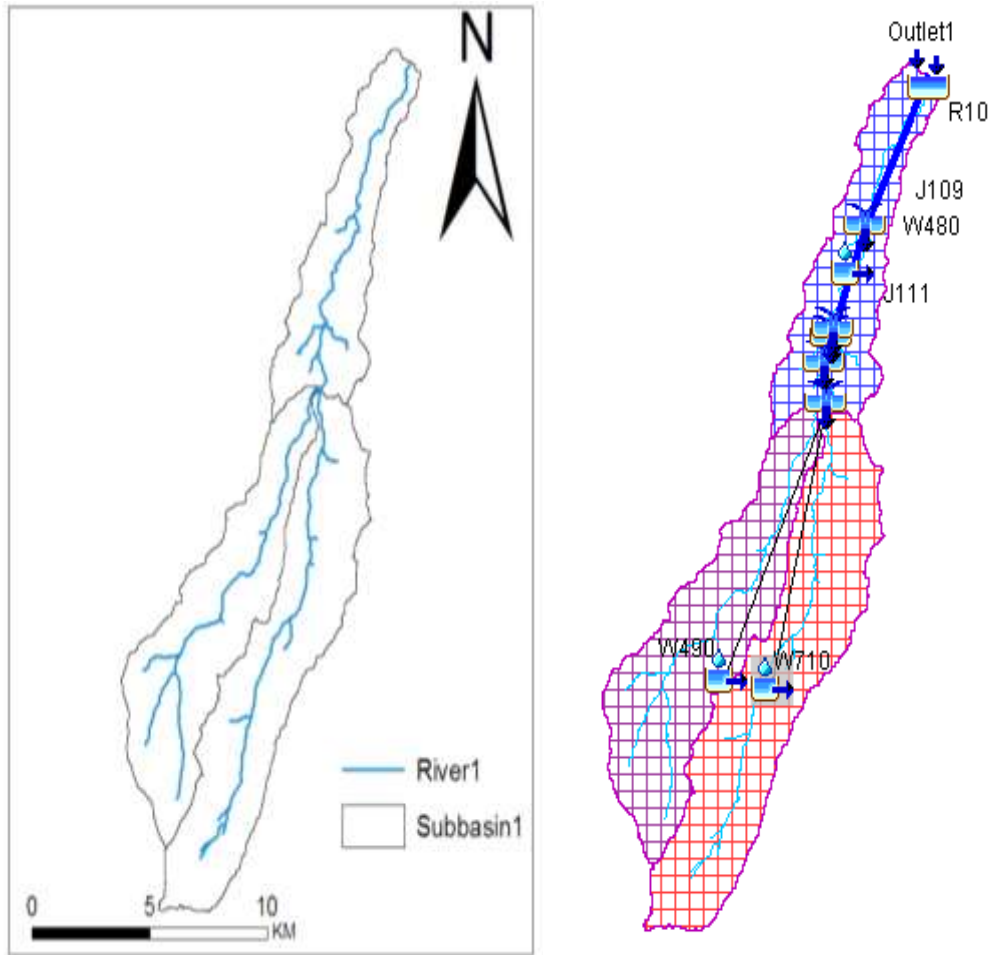


Figure 3-21:-Sub-basin model Representation Derived from HEC-HMS

Loss: -Since it is for calibration purpose, the loss method should be similar to the target area method which is SCS Curve Number Loss method.

Table 3-7:-Sub –basin area of Tamie catchment

Name of sub-basin	Basin Area (km)
Sub-basin1(W480)	28.3
Sub-basin 2(W490)	40.5
Sub –basin3 (W710)	49.0

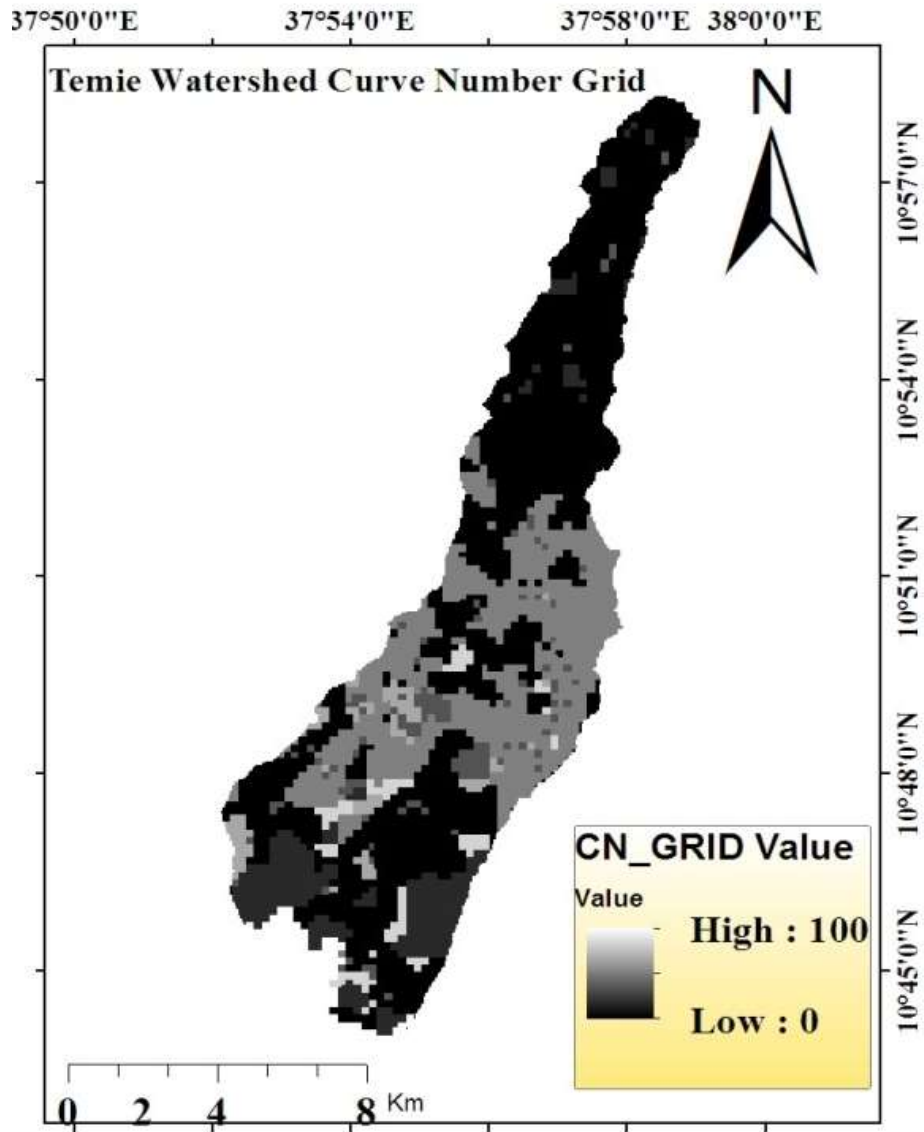


Figure 3-22:- Temie watershed curve number Grid

Table 3-8:- Temie Land use Land cover

Name	Land use	Area (Km²)	Soil type	Area (Km²)
Sub- Basin1 (W480)	Cultivation unstocked	17.0	Pellic Vertisols	10.9
	cultivation lightly stocked	5.7	Lithosols	0.6
	Grass Land	4.3	Eutric Nitosols	2.4
	Forest plant	1.4	Chromic Luvisols Eutric Cambisols	4.8 9.6
Sub- Basin2 (W490)	Cultivation unstocked	24.3	Pellic Vertisols	15.5
	cultivation lightly stocked	8.1	Lithosols	0.9
	Forest plant	4.1	Eutric Nitosols	15.5
	Grass land	2.8	Chromic Luvisols	6.9
	Afro alpine	1.1	Eutric Cambisols	13.8
	Shrub land	1.2		
Sub- Basin3 (W790)	Cultivation unstocked	27.0	Pellic Vertisols	18.8
	cultivation lightly stocked	12.3	Lithosols	1.0
	Forest plant	4.9	Eutric Nitosols	4.2
	Grass land	3.9	Chromic Luvisols	8.3
	Afro alpine	1.3	Eutric Cambisols	16.7
	Shrub land	0.98		

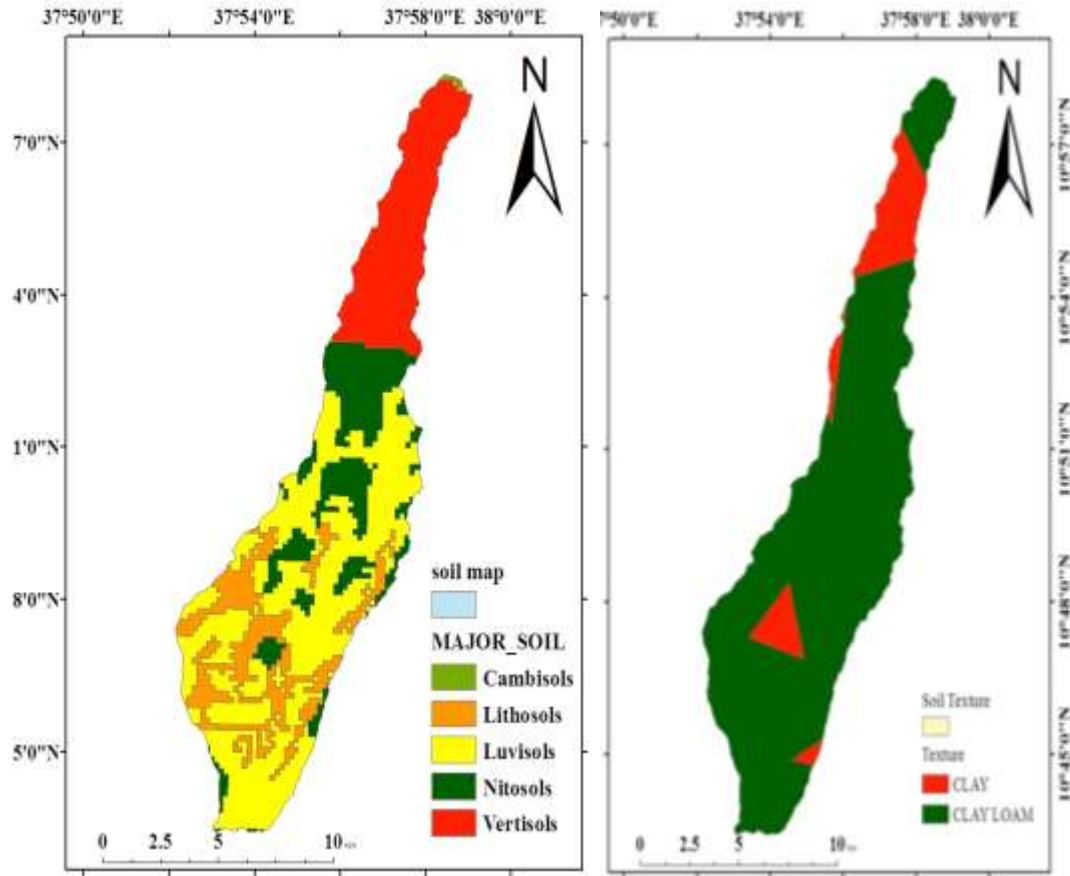


Figure 3-23:- Soil types and texture of the study area

3.11 Base Flow

For the calibration area, recession constant is adopted. Base flow is nicely approximated by a constant flow for each month taking at least 14-day stream flow for each month and for this work the average of the minimum of the respective months are adopted for 20 years of data are used (1984 to 2003). For the calibration, Temie station 14 years (1984 to 1997) daily rainfall data is adopted for Gage weights precipitation modelling.

3.12 Runoff Data

Temie station 14-years (1984 to 1997) daily recorded data are used for the calibration. However, the hydrological data taken from the Ministry of Water Resources does not be similar to the actual condition at site. As per the hydrologist assigned for this catchment, the actual values are less than these values. Since the gauge station is not automatic, there is clearly personal error while recording.

3.13 Simulation Run and Search Method

There are two search methods available for minimizing the objective function and finding optimal parameter values. The univariate gradient method evaluates and adjusts one parameter at a time while holding other parameters constant. The Nelder and Mead method use a downhill simplex to evaluate all parameters simultaneously and determine which parameter to adjust. For this thesis work the univariate gradient Evolution search method was adopted as it resulted in a better result.

3.13.1 HEC-HMS Input Data

The main input data for HEC-HMS are precipitation, observed flow, base flow and different watershed characteristics derived from HEC-GeoHMS process (Scharffenberg & Fleming, 2013). Therefore, the first step should be delineating streams and watersheds, and getting some basic catchment properties. Arc hydro and HEC-GeoHMS which are under GIS environment were used to providing the connection for translating GIS spatial information into model files for HEC-HMS (Gibson, Pak, & Fleming, 2010).

Therefore; for this study the major tasks and procedures that were performed under HEC-GeoHMS include Pre-processing, Project Setup, Basin Processing, Characteristics, Parameters and HMS for the catchment processing and the above Figure 3.25 shows the final HEC-HMS watershed characteristics that were exported from the HEC-GeoHMS output.

3.14 HEC-HMS Model Calibration and Validation

Validation is a process of proving the performance of the model. For this study the validation period was started from 01Jan1998 up to 30Dec2003. The model performance of this HEC-HMS was evaluated using different objective functions. The quantitative measure of the match was described by the objective function that measures the degree of variation between computed and observed hydrographs.

In this study during calibration and validation periods, the goodness of-fit between simulated versus observed hydrograph were evaluated through a number of objective functions. These were Nash and Sutcliffe simulation efficiency (NSE), the coefficient

of determination (R^2), Relative Volumetric Error (RVE), and Peak –weighted root mean square error (PWRMSE).

The Nash and Sutcliffe simulation efficiency is the criteria most widely used for calibration and evaluation of hydrological models with observed data (Gupta, Mantilla, Troutman, Dawdy, & Krajewski, 2010). As stated by (Rientjes, Perera, Haile, Reggiani, & Muthuwatta, 2011), NSE measure that indicates overall fit. Its value ranges between $-\infty$ and 1.0 (1 inclusive) and NSE equal to 1 shows perfect. As (Santhi et al., 2001) states the NSE values range between 0.5 and 1.0 are generally viewed as an acceptable level of model performance, although the values less than or equal to zero shows the mean observed value is a better predictor than the simulated value, which indicates unacceptable performance. A model is said to be perform a very good when values are between 0.8 and 0.9 (Rientjes, Perera, Haile, Reggiani, & Muthuwatta, 2011).

Objective Function

The quantitative measure of the match is described by the objective function that measures the degree of variation between computed and observed hydrographs. There are different objective functions are available in optimization manager and five of them are described below.

- Peak –weighted root mean square error (PWRMSE). This function gives a more weight to large errors than small errors and it gives a greater overall weight to errors near the peak discharge.
- Sum of squared residuals (SSR). The SSR measure gives a greater weight to large errors and lesser weight to small errors and uses the squared differences as the measure of fit.
- Sum of absolute residuals (SAR). The SAR function gives equal weight to both small and large errors.
- Percent error in peak flow (PEPF). The PEPF measure considers only the magnitude of computed peak flow and does not account for total volume or timing of peak.
- Percent error in volume (PEV). The PEV function only considers the computed volume and doesn't account for the magnitude or timing of the peak flow

detailed reference on the formulas and descriptions can be referenced to the HEC-HMS user's manual (USACE,2016). In this thesis, the peak-weighted root mean square was used to get the finally optimized values.

Peak –weighted root mean square error (PWRMSE): -The RMSE is the standard deviation between the measured and calculated head water and is represented with the following equation: Root Mean Square Error (RMSE) in flood modelling indicates the accuracy of flood extent as flood water propagates. This measures the discrepancy between the modelled and observed values on an individual basis and indicates the overall predictive accuracy weight is given to larger discrepancies. With this measure, smaller values indicate better model performance.

$$RMS = \frac{1}{n} \left[\sum_i^n (h_{measured} - h_{observed})_i^2 \right]^{0.5} \text{Eq.3-47}$$

Coefficient of Efficiency (Nash Sutcliffe Efficiency): -In this case it represents the efficiency of the model in scale, which goes from minus 1 to 1(best fit). As proposed by (Nash & Sutcliffe, 1970) An efficiency of lower than zero indicates that the mean value of the observed time series would have been a better predictor than the model. The disadvantage of this efficiency criterion is an over estimation of the model performance during peak flows and an underestimation during low flow conditions.

$$E_N = 1 - \frac{\sum_{i=1}^n (q_{oi} - q_{si})^2}{\sum_{i=1}^n (q_{oi} - q_{oa})^2} \text{Eq. 3-48}$$

Where, q_{oi} is observed value at the i^{th} time interval, q_{oa} is average value of observed discharge, q_{si} is simulated value at the i^{th} time interval, E_N is coefficient of Efficiency and n is number of samples.

Relative volumetric error: - The RVE is a measure that indicates a mass balance error (Rientjes, Perera, Haile, Reggiani, & Muthuwatta, 2011). The value of RVE zero means it performs the best, i.e. there is no difference between simulated and observed runoff. The model performance is very good for RVE between -5% to 5%, while RVE between -10% to -5% and 5% to 10% indicate satisfactory performance.

$$RVE = \frac{\sum_{i=1}^n (Q_{sim,i} - Q_{obs,i})}{\sum_{i=1}^n (Q_{obs,i})} * 100 \text{Eq. 3-49}$$

Coefficient of determination: - This used to estimate how well the scattering of the measured data is predicted by the model. Its value ranges between 0 and 1, with the

zero being no correlation at all and value one correctly correlate measured data to the model. In all the formula, the variables are:

$$R^2 = \frac{[\sum_{i=1}^n (q_{si} - q_{sa})(q_{oi} - q_{oa})]^2}{\sum_{i=1}^n (q_{si} - q_{sa})^2 \sum_{i=1}^n (q_{oi} - q_{oa})^2} \text{Eq. 3-50}$$

Where, q_{oi} is observed value at the i^{th} time interval, R is Coefficient of determination q_{oi} is average value of observed discharge, q_{si} is simulated value at the i^{th} time interval, q_{sa} is average value of simulated discharge and n is number of samples.

Table 3-9:- Performance for recommended statistics (Starks & Moriasi, 2009)

Performing rate	Statistic Parameters			
	R^2	NSE	RVE (%)	PWRMSE (%)
Very good	$R^2 \geq 0.7$	$NSE > 0.75$	$RVE \leq \pm 10$	$PWRMSE \leq \pm 10$
Good	$0.6 < R^2 \leq 0.7$	$0.65 < NSE \leq 0.75$	$\pm 10 \leq RVE \leq \pm 15$	$\pm 10 \leq PWRMSE \leq \pm 15$
Satisfactory	$0.5 < R^2 \leq 0.6$	$0.5 < NSE \leq 0.65$	$\pm 15 \leq RVE \leq \pm 25$	$\pm 15 \leq PWRMSE \leq \pm 25$
Unsatisfactory	$0 \leq R^2 \leq 0.5$	$NSE \leq 0.5$	$RVE \geq \pm 25$	$PWRMSE \geq \pm 25$

3.15 HEC-RAS Model and Input Data

3.15.1 HEC-HMS Model Output

After calibration and validation of the HEC-HMS model were accomplished, PMF was calculated using PMP. The obtained PMF from this model was used as upstream boundary conditions for HEC-RAS model in both sunny day and hydrologic PMF conditions.

3.15.2 HEC-Geo-RAS and Data Processing

HEC-Geo-RAS is a set of Arc-GIS tools specifically designed to process geospatial data use with HEC-RAS. The extension allows users to create an HEC-RAS import file containing geometric data from an existing DEM (Davis, 2005).

Essential data required to work with HEC-GeoRAS are terrain data and land use information. The geometry file for HEC-RAS contains information on cross-sections, hydraulic structures, river banks and other physical attributes of river channels.

The pre-processing using HEC-Geo-RAS involved creating these attributes in GIS, and then exporting them to the HEC-RAS geometry file. In HEC-Geo-RAS, each attribute is stored in a separate feature class called as RAS Layer. After creating RAS layers, these are added to the map document with pre-assigned features. The Stream Centerline layer was used to identify the connectivity of the river system. It was created in the downstream direction and was used to assign river stations to the cross sections, bridges, and other structures to order computational nodes in the HEC-RAS model. The Cross-Sectional Cut Lines layer was the principal data constructed using HEC-Geo-RAS. Cut lines were digitized across the floodplain area to capture the profile of the land surface. Cross sections should be digitized perpendicular to the path of flow in the channel and overbank areas to be consistent with one-dimensional flow characteristics.

3.15.3 HEC-RAS Model

HEC-RAS is an integrated system of software designed for interactive use in multi-tasking, multi-user network environment. The system is comprised of a graphical user interface (GUI), separate hydraulic analysis components, data storage and management capabilities, graphics and reporting facilities. HEC-RAS model has performed the following analysis which is Steady flow water surface profile computation, unsteady flow simulation, Moveable boundary sediment transport computations and Water quality analysis.

A key element is that all four components use a common geometric data representation and common geometric and hydraulic computations routines. HEC-RAS have the ability to present hydraulic properties computed during a flow simulation (Tate, Maidment, Olivera, & Anderson, 2002).

In the previous versions of HEC-RAS, it was possible to simulate the flow as one-dimensional flow only. In February 2016, RAS model with ability to perform 2D hydrodynamic unsteady flow routing using St. Venant equation or Diffusion wave

equation was introduced (Kumar, Lal, Sherring, & Issac, 2017). HEC-RAS can be considered hydraulic effects of bridges, culverts, weirs, and other structures in the river and floodplain on water surface calculations (ENGINEERS–USACE, 2016).

In new version of HEC-RAS model both 1D and 2D model are used for modelling of different studies. While the 1-D models require cross sectional data of flow channels with sufficient extension on both left and right directions, the 2-D models use topographical data in the form of a continuous surface represented by finite element mesh. Due to this the result obtained by 1D and 2D modelling is different due to different reasons. There are some areas where 2D modelling can produce better results than 1D modelling and also situations in which 1D result better than 2D model results (Brunner, 2016).

In this thesis, one dimensional (1-D) steady flow has been performed for Temie River and the result has been used to generate flood inundation area. 1-D steady flow analysis is useful for calculating water surface profile. In this analysis the flow is assumed to be gradually varying along its length. It can calculate the water surface profile for subcritical, supercritical and mixed flow condition. Governing equation for calculation of water surface profile is energy equation which is written as follows:

$$Z_2 + Y_2 + \frac{\partial_2 v_2^2}{2g} = Z_1 + Y_1 + \frac{\partial_1 v_1^2}{2g} + h_e \text{ Eq.3.51}$$

Where, Z_1 and Z_2 is elevation of bottom of the channel at cross section 1 and 2, Y_1 and Y_2 is depth of water at cross section 1 and 2, V_1 and V_2 , ∂_1 and ∂_2 is velocity weighting factors, g is acceleration due to gravity and h_e is energy head loss.

Water surface profile between any two-cross section is calculated by solving the energy equation 3.51 in an iterative way. This process is called as standard step method. The calculation proceeds upstream if the flow is sub critical and downstream if the flow is super critical (French, 1987). For the computation of water surface, each cross-section river is divided into left over bank, main channel and the right over bank and the energy calculated for all three sections. The final energy of the channel is the mean of the energy calculated for all three sections (Brunner, 2016). The head loss in the equation 3.52 comprises of the loss due to friction and contraction / expansion. The friction loss is given by Manning equation which is given below:

$$h_f = LS_f \text{ Eq. 3.52}$$

Where, S_f is representative friction slope (slope of energy grade line) $= \frac{Q}{K}$, Q IS flow in the channel length, K is conveyance factor $= \frac{1.486}{n} AR^{2/3}$, n manning, A is area of the channel, R is hydraulics radius which is calculated as area per wetted perimeter and L is distance weighted reach length;

$$L = \frac{L_{lob}Q_{lob} + L_{ch}Q_{ch} + L_{rob}Q_{rob}}{Q_{lob} + Q_{ch} + Q_{rob}}$$

L_{lob} , L_{ch} , L_{rob} = cross- section reach length in left over bank, main channel and right over bank respectively.

Q_{lob} , Q_{ch} , Q_{rob} = average mean flow between sections for left overbank, main channel and right overbank respectively.

The contraction/ expansion loss is calculated as;

$$h_{ce} = C \left| \frac{\alpha_2 v_2^2}{2g} - \frac{\alpha_1 v_1^2}{2g} \right| \text{ Eq.3.53}$$

Where C = coefficient of contraction/expansion

Combining friction loss and loss due to contraction /expansion, the total energy loss equation is given below:

$$h_e = LS_f + C \left| \frac{\alpha_2 v_2^2}{2g} - \frac{\alpha_1 v_1^2}{2g} \right| \text{ Eq.3.54}$$

The velocity weighing factor α is calculated as;

$$\alpha = \frac{Q_1 V_1^2 + Q_2 V_2^2}{(Q_1 + Q_2) V^2},$$

Where; V = mean velocity of the reach length (Brunner, 2016)

3.15.4 HEC-RAS Input Data

For this thesis, most HEC-RAS input data were processed out of the model and some were processed inside the model. The following are input data for HEC-RAS model:

Geometric data: these data are used to define the shape of the stream and related their physical characteristics. For this study river cross section data were digitized in Arc-GIS 10.1 with compatible HEC-GeoRAS software and have been imported into HEC-RAS.

Manning Roughness: - Estimation of Manning's roughness coefficient (or Manning's n) is very important to simulate open channel flows. As an empirical parameter, the roughness coefficient actually includes the components of surface friction resistance, wave resistance and resistance due to flow unsteadiness (Pudasaini, Wang, & Hutter, 2005). Direct determination of the roughness coefficient is almost impossible in studying natural river flows, including unsteady channel network flows. The roughness coefficient (n in natural channels is difficult to determine in field. Various factors affecting the values of roughness coefficients were presented by (Chow, 1959). Surface roughness, Vegetation, Channel irregularities, Channel alignment, Scour and deposition, Obstructions, Size and shape of the channel, Stage and discharge, Seasonal changes, temperature and Suspended material & bed load etc.

For this study the Author was unable to access any official Manning roughness values for the modelling reaches, therefore had to use arbitrarily but, judicially chosen Manning roughness values based on (Chow, 1959). HEC-RAS User's Manual suggested to use a compiled "n" values for stream and floodplains found in open channel hydraulics.

A number of methods exist for estimating the roughness coefficient. The first method is using books that provide series of pictures of stream channel with a recommended Manning's value for each picture. As shown in Figure 3.26, for any natural channel by comparing these pictures with actual field observed river properties a value of Manning's roughness most similar one can be obtained.

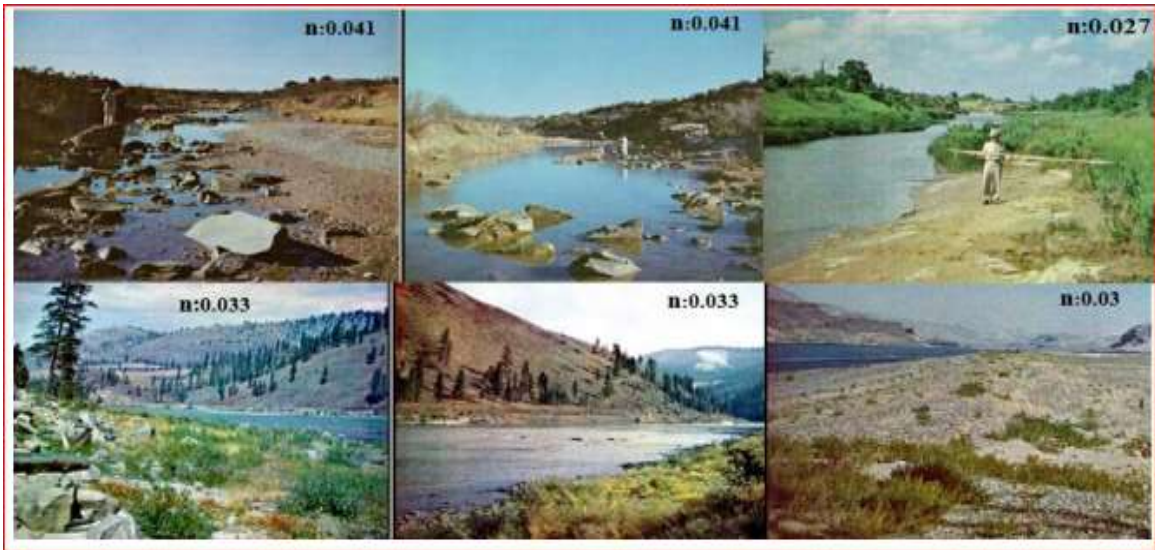


Figure 3-24:-U. S Geological Survey Manning's Roughness estimated values

However; this method was developed considering other country rivers and natural condition that may have a different topographic, soil type, river characteristics, as well as weather condition and many other factors as compare to our country in Ethiopia. For this reason, it should not advisable to apply directly for our Country Rivers and floodplains.

The second method was using annex 10 that recommended by different authors that give typical or average values of n for different channel conditions, a value of n can be obtained by comparing the roughness characteristics of the observed channel using the annex, the one that appears most similar with actual river channel properties would select as shown in Annex 10.



Figure 3-25: -Upper Temie River channel and floodplain profile of the study area
This method is basically a table look-up solution, with the basic “n” value and each of the corrections obtained from a table. The method involves the selection of a base value of n and then correcting the base value based on the following five factors:

- ✓ The degree of regularity of the surfaces of the channel cross section
- ✓ The character of variations in the size and shape of cross section
- ✓ The presence and characteristics of obstructions in the channel
- ✓ The effect of vegetation on flow conditions
- ✓ The degree of channel meandering

The Manning's roughness coefficient value and field survey photos of upper Temie River channel as shown in above. The general procedure for estimating "n" involves first, the selection of a basic value of "n" for a channel and floodplain materials involved, then, through critical consideration of the factors listed above, the selection of a modifying value associated with each factor. The modifying values are added to the basic value to obtain "n" for the channel under consideration.

Step 1: Selection of basic value (n₁). The selection of a basic n value of the study area is assumed that for the character of a bottom and sides of the channel and floodplain are of different materials involved.

Step 2: Correction for channel irregularity (n₂). The modify value n of the study area is assumed that the degree of roughness or irregularity of the channel surfaces of sides and bottom is good dredged channels; moderately eroded or scoured side slopes of canals or drainage channels.

Step 3: Correction for cross-section variation (n₃). The modifying value n of the study area is assumed that the character of variations of size and shape of cross sections is large and small sections alternating frequently or shape changes causing frequent shifting of main flow from side to side these changes causing the greatest turbulence.

Step 4: Correction for obstructions (n₄). The selection of modifying value n for obstructions is based on the presence and characteristics of obstructions such as debris deposits, stumps, exposed roots, boulders, fallen, lodged logs and light floating debris. But in these step care should be taken that conditions considered in other steps are not re-evaluated or double-counted for both of channel and floodplain the obstruction is negligible.

Step 5: Correction for vegetation (n₅) the retard effect of vegetation is probably due primarily to the turbulence induced as the water flows around and between the limbs, stems and foliage, and secondarily to reduction in cross section. As depth and velocity

increase, the force of the flowing water tends to bend the vegetation. Furthermore, the amount and character of foliage; that is, the growing season condition versus dormant season condition is important. Therefore, modify value n of the study area is assumed that the effect of vegetation for channel is low and floodplain is high.

Step 6: Correction for channel meandering (n_6). The modify value n of the Temie River is assumed that the degree of meander is appreciable channel or can be measured using the ratio of the total meander length of the channel in the reach (l_m) to the straight length of the reach (Nelson et al.).

step7: Computation of n for the reach. The actual value of the reach roughness coefficient equals the sum of the values of the basic value n_1 and the modifying values n_2 to n_6 .

Therefore, from Annex 10 and during the field visit, the stream was characterized by fine gravel bed; sever meandering, moderate irregularity, alternating change in shape and size, minor obstruction, and medium vegetation cover the total reach “ n ” values were obtained for main channel of Temie River and floodplain. Finally, were performed the computation sheet calculation of a manning roughness coefficient value of 0.046 for the main channel and 0.03for the lift and right bank of the floodplain.

4 RESULTS AND DISCUSSION

4.1 HEC-HMS Calibration and Validation

The model results as obtained from the final automatic calibration using the peak weighted root mean square error (PWRMSE). The objective function showed that there was a good agreement between the simulated and observed flow. This is confirmed by correlation coefficient, absolute mean error, relative volumetric error and the(Nash & Sutcliffe, 1970) efficiency values catchments.

Model calibration is a systematic process of adjusting model parameter values until model results match with the observed data. The quantitative measure of the match is described by the objective function. In the precipitation-runoff models, this function measures the degree of variation between computed and observed hydrographs. The

calibration process finds the optimal parameter values that minimize the objective function.

For this study, calibration could be performed by shared both manual and automated (optimization) methods. Manual calibration relies on user’s knowledge of basin physical properties and expertise in hydrologic modelling. While in the automated calibration, model parameters are iteratively adjusted until the value of the selected objective function is minimized.

The latest version of HEC-HMS 4.2.1 model includes optimization manager that allows automated model calibration. There are fourteen objective functions available in HEC-HMS 4.2.1 optimization manager(US Army Corps of Engineers, 2000). Among fourteen objective functions, Peak –weighted root mean square error, Nash- Sutcliffe Coefficient, absolute mean error and coefficient of determination were used for this thesis. The optimization output was assessed by means of observing objective function summary value, optimized parameter values, hydrograph comparison, objective function graph, and statistical goodness-of-fit measures.

Table 4-1:- Objective function summary for Calibration

Objective function at basin element” Outlet”				
Measure	Simulated	Observed	Difference	% Difference
Volume(m ³)	11908.16	12058.09	-149.93	-1.24
Peak Flow(M ³ /s)	46.6	46.4	0.2	0.5
Time to Peak	19Jul1986	28Jul1988		
Time of Center of Mass	21Apr1991	17Mar1991,21:38		

From Table 4.1The value of the simulated and the observed peak discharge is 46.6m³/s and 46.4m³/s respectively, and the percent difference is 0.5. This low percent value has indicated good agreement between simulated and observed peak discharge value.

Table 4-2:-Optimized parameter values for Calibration

Optimized Parameter Results for W480, W490 & W710					
Element	Parameter	Unit	Initial value	Optimized Value	Objective Function sensitivity

R10	Muskingum-k	HR	1.50	2.28	0.0
R30	Muskingum-k	HR	2.00	2.03	0.0
R40	Muskingum-k	HR	3.00	3.05	0.0
R60	Muskingum-k	HR	3.50	7.91	0.0
R90	Muskingum-k	HR	4.00	4.09	0.0
R10	Muskingum-x		0.15	0.06	0.0
R30	Muskingum-x		0.20	0.20	0.0
R40	Muskingum-x		0.35	0.33	0.0
R60	Muskingum-x		0.35	0.22	0.0
R90	Muskingum-x		0.36	0.34	0.0
W480	Clark Unit Hydrograph- Time of concentration	HR	2.00	2.00	0.0
W490	Clark Unit Hydrograph- Time of concentration	HR	2.50	2.50	0.0
W710	Clark Unit Hydrograph- Time of concentration	HR	3.00	3.00	0.0
W480	SCS Curve Number- Initial Abstraction	MM	0.50	0.15	0.0
W490	SCS Curve Number- Initial Abstraction	MM	3.00	10.10	0.0
W710	SCS Curve Number- Initial Abstraction	MM	3.50	11.80	0.0

From the above table 4.2 the value of objective function sensitivity is zero. This indicates there is a good agreement between the initial and optimized parameter values.

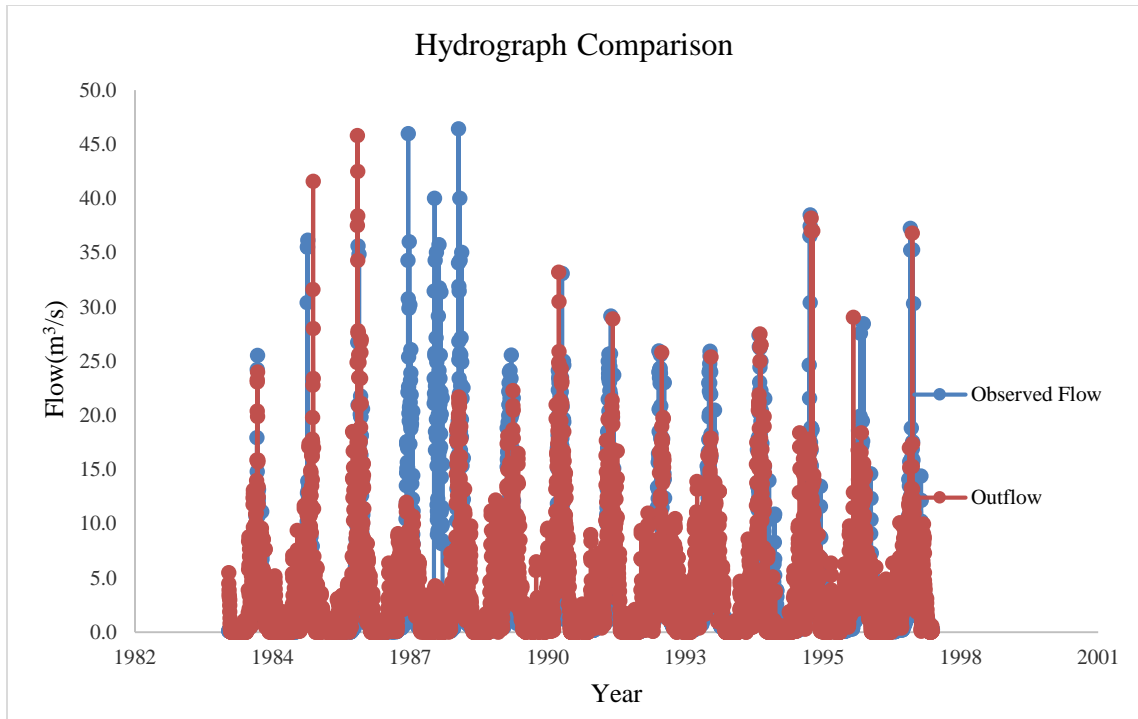


Figure 4-1:-Model Calibration of Simulated and Observed flow

From the above figure 4.1 the magnitude of peak simulated and observed flow from 1984 -1997 year have approximately vertical height. Meaning the value of simulated and observed flow was compared for that specific year. This simple observation clarifies the goodness of fit between the initial and optimized input parameters. Generally, the model has satisfactorily showed a good pattern for 10 years i.e. 1994, 1989, 1990, 1991, 1992, 1993,1994,1995,1996 and 1997. And the calibrated model under estimated for two years i.e. 1987 and 1988. While the model slightly over estimates for two years i.e. 1985 and 1986.

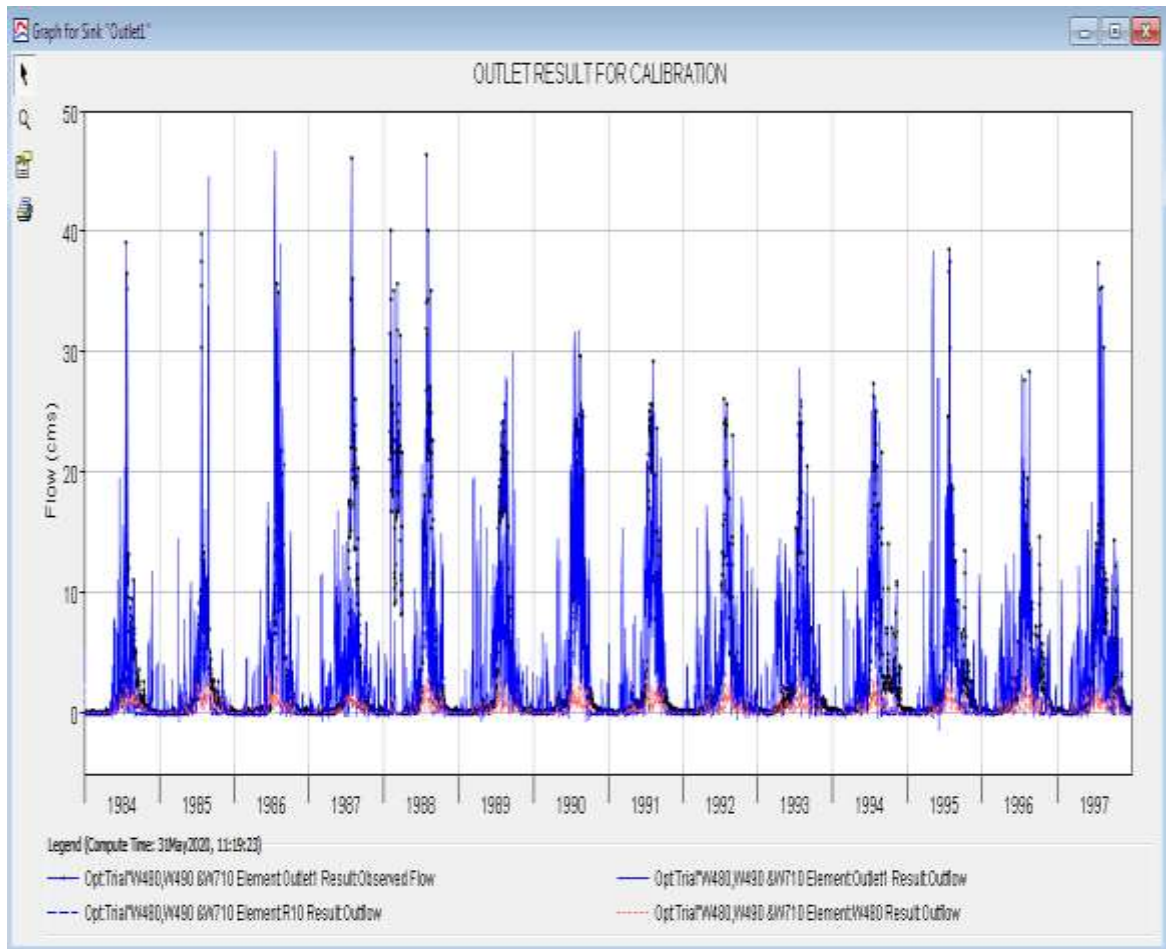


Figure 4-2:- HEC-HMS Calibration Result

Table 4-3:- Calibration and Validation performance of the model

Description	Statistical goodness of fit measures of the model			
	NSE	AME (%)	RVE (%)	PWRMSE (%)
Calibration	0.65	3	13.45	9.84
Validation	0.565	1.7	16.45	3.1

Table 4.3 shown, the second method was statistical goodness-of-fit measures to check the performance of the calibrated model. Here four different statistical measures were evaluated for Gundowion station to assess the performance of the model. The first measure was the Nash-Sutcliffe coefficient of efficiency (NSE) defined as equation 3.48, the second was the Relative Volumetric Error (RVE) defined as equation 3.49, the third was the Mean absolute error (MAE) and the fourth was the peak weighted root mean square error (PWRMSE) defined as equation 3.47.

4.2 HEC-HMS Model Validation Results and Discussion

Model validation is a process of testing model performance to simulate observed data other than those used for the calibration with acceptable precision. During this process, calibrated model parameters were not subject to change, their values were kept constant. The quantitative measure of the match is again the degree of variation between computed and observed hydrographs. For this study the validation of the model output was assessed by flow comparison graph and statistical goodness-of-fit measures.

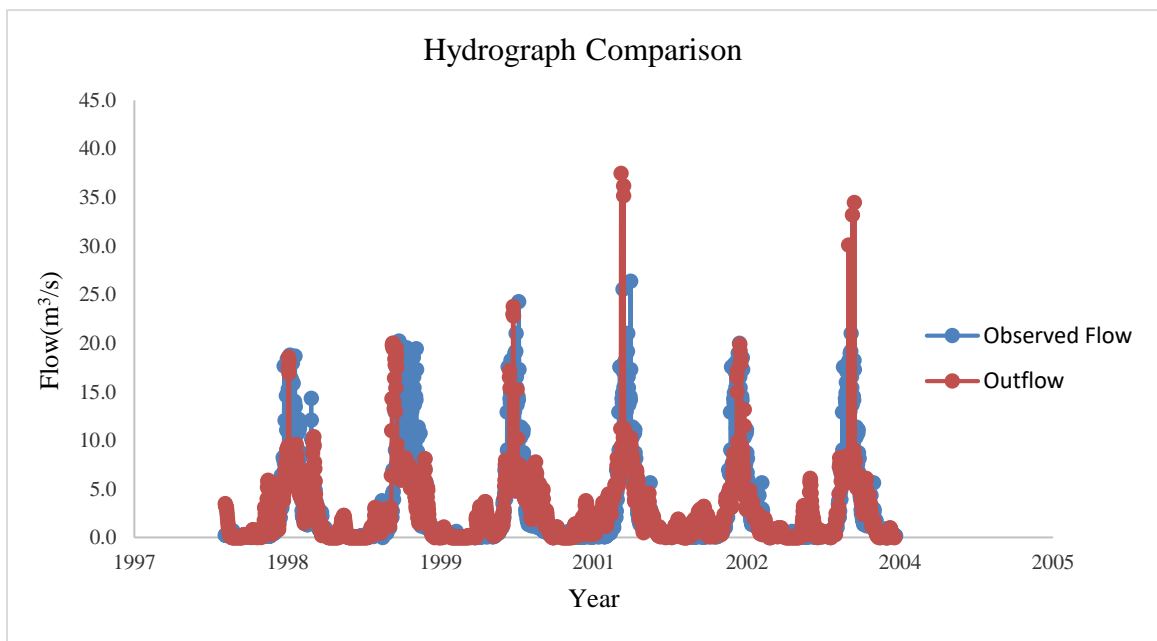


Figure 4-3:-Model Validation of Simulated and Observed flow

Figure 4.3 showed good pattern four years (i.e. 1998, 1999, 2000 and 2002). While the validation model overestimate in 2001 and 2003.the outlet result.

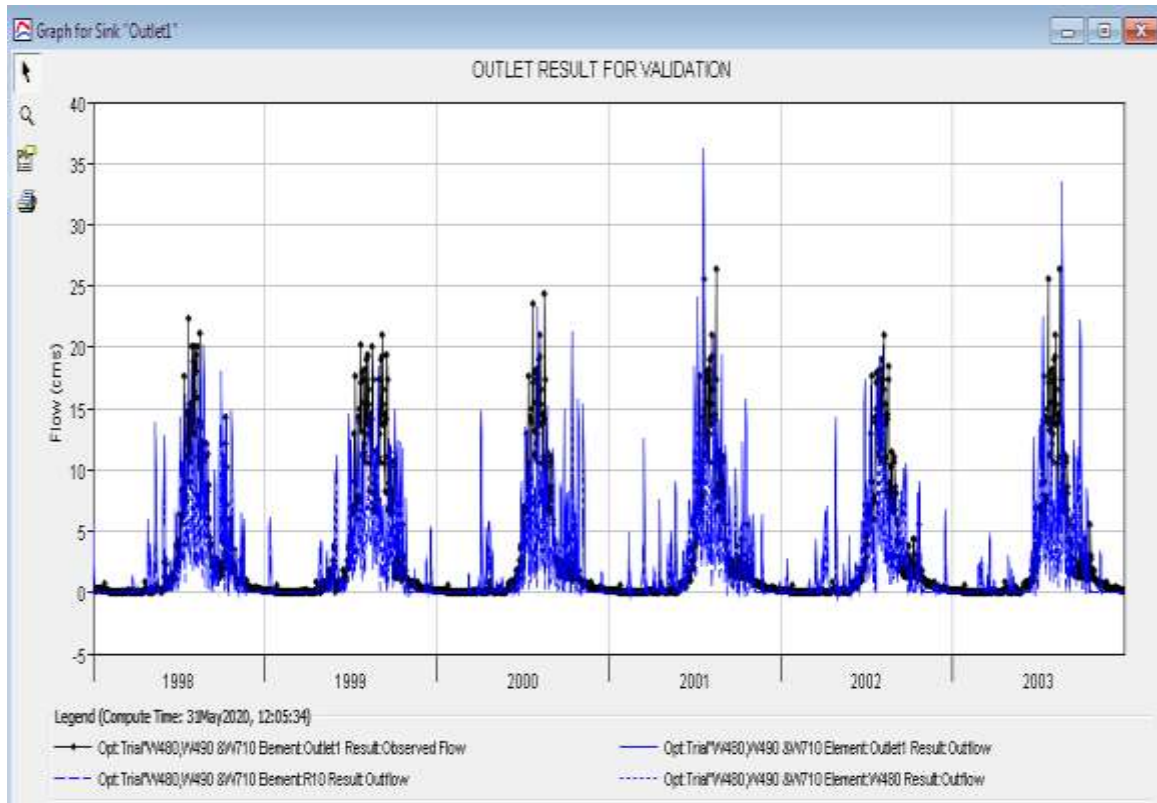


Figure 4-4:-HEC-HMS Validation Result

4.3 PMF Inflow Hydrograph

After calibration and validation of HEC-HMS Model were accomplished, PMF was forecasted by using probability distribution in the HEC-HMS model. The calculated PMF was used as an upstream boundary condition for HEC-RAS model for both sunny day and hydrologic PMF conditions. For 20 and 1000 years return period, the value of the 24 hr PMP was 95.8mm and 134.75mm and obtained PMF value of 50.8/s and 94 m³/s.

Table 4-4: - Peak Discharge output of HEC-HMS from Hyetograph

Return period(yrs.)	ppt(mm)	Peak flood(m ³ /s)
20	95.8	50.8
50	104.5	63.5
100	111.3	70.8
500	128.0	86.2
1000	134.6	94

4.4 Hydraulic Model development

The methodology used for performing hydraulic analysis can be diving into three parts such as;

- ✓ Pre-processing: Developing geometry of river in ArcGIS
- ✓ Processing: Performing hydraulic computation in HEC-RAS
- ✓ Post-processing: Processing RAS results in ArcGIS

4.4.1 Pre-RAS (HEC-GeoRAS) processing

The HEC-GeoRAS toolbar has four menus (RAS Geometry, RAS Mapping ApUtilities, and Help) and seven tools /buttons (Assign River Code/Reach Code, Assign From station/To station, assign line type, Construct XScutline plot cross section and assign levee elevation. The goal of this section is to develop the spatial data required to generate a HEC-RAS import file with a 3-D stream network and 3-D cross sections defined. The RAS Geometry menu containing functions for Pre-processing of GIS data for input to HEC-RAS.the RAS Mapping menu contains functions for post processing of HEC-RAS result to produce flood inundation map. The ApUtilites menu contains functions mainly for data management.

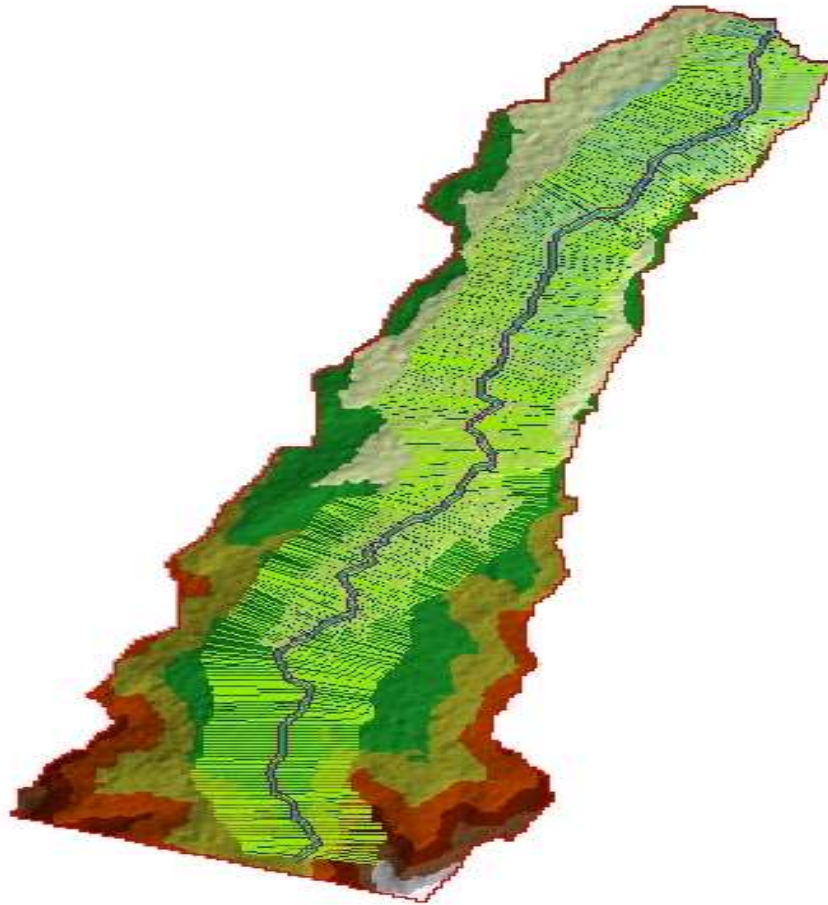


Figure 4-5: - Pre-processing in the study Area

Generating the RAS GIS Import File

Form the above Geo RAS Data to generate the RAS GIS Import File, the 3D stream Centerline and Cross Section Surface Line (3D) shape file created from the RAS Theme. Geometric data from the 3D (Stream Centerline and Cross Section Surface Line) shape files is written to the RAS GIS Export File. The geometric data includes: river, reach, and station identifiers; cross-section Cut lines; cross-section surface lines; main channel bank stations; downstream reach Lengths for the left overbank, main channel; and overbank.

4.4.2 HEC-RAS Results

Geometric Data

HEC-RAS has the ability to import three-dimensional (3D) river schematic cross section data Created in a GIS /Arc View HEC-GeoRAS/ While the HEC-RAS utilizes

two-dimensional data. During the computations, the three-dimensional information is used in the program for display purpose. Surface profiles exported back to the GIS /Arc View HEC-GeoRAS/system for development and display of a flood inundation map.

The following geometric data imported using HEC-RAS: River system schematic and Cross section data:- Cross section surface line, Cross section main channel bank stations, River, Reach and River station identifiers/S reach length for the left overbank, main channel, and right over bank and Cross section cut lines(x and y coordinate of the plan view line that represents the cross section).

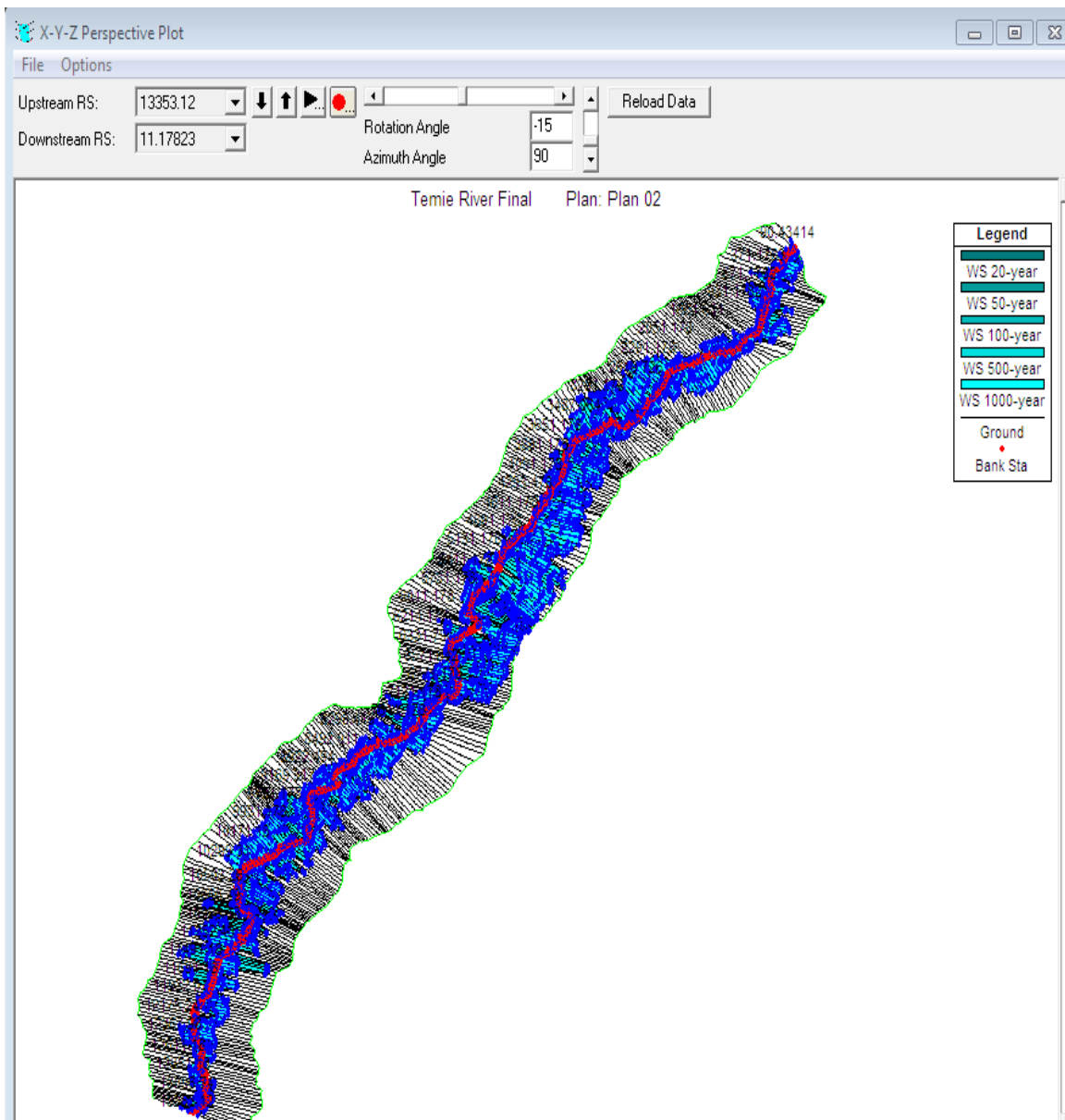


Figure 4-6: - x-y-z View of the Flood Plain in HEC-RAS

4.4.3 Detailed output tables for selected cross sections

The detailed output table shows discharge amount, reach length, flow area, top width, average velocity, hydraulic depth, wetted perimeter, shear, stream power, cumulative volume, cumulative storage area for channel, left and right over banks.

Table 4-5:- Detailed output tables of channel simulation for selected cross sections

Cross Section Output					
File Type Options Help					
River:	TEMIE RIVER	Profile:	20-year		
Reach:	DOWNSTREAM	RS:	12624.16	Plan:	Plan 02
Plan: Plan 02 TEMIE RIVER DOWNSTREAM RS: 12624.16 Profile: 20-year					
E.G. Elev (m)	2554.08	Element	Left OB	Channel	Right OB
Vel Head (m)	0.00	Wt. n-Val.	0.030	0.046	0.030
W.S. Elev (m)	2554.07	Reach Len. (m)	13.05	12.98	12.94
Crit W.S. (m)		Flow Area (m ²)	24.57	129.16	16.89
E.G. Slope (m/m)	0.000068	Area (m ²)	24.57	129.16	16.89
Q Total (m ³ /s)	50.80	Flow (m ³ /s)	8.25	39.34	3.20
Top Width (m)	106.07	Top Width (m)	18.08	58.46	29.53
Vel Total (m/s)	0.30	Avg. Vel. (m/s)	0.34	0.30	0.19
Max Chl Dpth (m)	2.55	Hydr. Depth (m)	1.36	2.21	0.57
Conv. Total (m ³ /s)	6147.6	Conv. (m ³ /s)	998.9	4761.3	387.4
Length Wtd. (m)	12.99	Wetted Per. (m)	18.25	58.49	29.57
Min Ch EI (m)	2551.52	Shear (N/m ²)	0.90	1.48	0.38
Alpha	1.04	Stream Power (N/m s)	57200.65	0.00	0.00
Frctn Loss (m)	0.00	Cum Volume (1000 m ³)	284.78	330.41	606.41
C & E Loss (m)	0.00	Cum SA (1000 m ²)	451.27	462.58	878.62

Cross Section Output					
File Type Options Help					
River:	TEMIE RIVER	Profile:	50-year		
Reach:	DOWNSTREAM	RS:	12624.16	Plan:	Plan 02
Plan: Plan 02 TEMIE RIVER DOWNSTREAM RS: 12624.16 Profile: 50-year					
E.G. Elev (m)	2554.16	Element	Left OB	Channel	Right OB
Vel Head (m)	0.01	Wt. n-Val.	0.030	0.046	0.030
W.S. Elev (m)	2554.15	Reach Len. (m)	13.05	12.98	12.94
Crit W.S. (m)		Flow Area (m ²)	26.10	134.03	19.45
E.G. Slope (m/m)	0.000092	Area (m ²)	26.10	134.03	19.45
Q Total (m ³ /s)	63.50	Flow (m ³ /s)	10.41	48.63	4.46
Top Width (m)	109.17	Top Width (m)	18.59	58.46	32.11
Vel Total (m/s)	0.35	Avg. Vel. (m/s)	0.40	0.36	0.23
Max Chl Dpth (m)	2.63	Hydr. Depth (m)	1.40	2.29	0.61
Conv. Total (m ³ /s)	6612.5	Conv. (m ³ /s)	1084.1	5064.4	463.9
Length Wtd. (m)	12.99	Wetted Per. (m)	18.77	58.49	32.15
Min Ch EI (m)	2551.52	Shear (N/m ²)	1.26	2.07	0.55
Alpha	1.04	Stream Power (N/m s)	57200.65	0.00	0.00
Frctn Loss (m)	0.00	Cum Volume (1000 m ³)	318.74	366.17	674.04
C & E Loss (m)	0.00	Cum SA (1000 m ²)	487.91	489.82	940.59

Cross Section Output

File Type Options Help

River: TEMIE RIVER Profile: 100-year

Reach: DOWNSTREAM RS: 12624.16 Plan: Plan 02

Plan: Plan 02 TEMIE RIVER DOWNSTREAM RS: 12624.16 Profile: 100-year

		Element	Left OB	Channel	Right OB
E.G. Elev (m)	2554.21	Wt. n-Val.	0.030	0.046	0.030
Vel Head (m)	0.01	Reach Len. (m)	13.05	12.98	12.94
W.S. Elev (m)	2554.20	Flow Area (m2)	26.93	136.60	20.90
Crit W.S. (m)		Area (m2)	26.93	136.60	20.90
E.G. Slope (m/m)	0.000106	Flow (m3/s)	11.66	53.90	5.24
Q Total (m3/s)	70.80	Top Width (m)	18.86	58.46	33.48
Top Width (m)	110.80	Avg. Vel. (m/s)	0.43	0.39	0.25
Vel Total (m/s)	0.38	Hydr. Depth (m)	1.43	2.34	0.62
Max Chl Dpth (m)	2.68	Conv. (m3/s)	1130.9	5227.6	508.4
Conv. Total (m3/s)	6867.0	Wetted Per. (m)	19.04	58.49	33.52
Length Wtd. (m)	12.99	Shear (N/m2)	1.47	2.43	0.65
Min Ch EI (m)	2551.52	Stream Power (N/m s)	57200.65	0.00	0.00
Alpha	1.05	Cum Volume (1000 m3)	337.92	385.66	711.16
Frcn Loss (m)	0.00	Cum SA (1000 m2)	509.26	503.85	977.22
C & E Loss (m)	0.00				

Cross Section Output

File Type Options Help

River: TEMIE RIVER Profile: 500-year

Reach: DOWNSTREAM RS: 12624.16 Plan: Plan 02

Plan: Plan 02 TEMIE RIVER DOWNSTREAM RS: 12624.16 Profile: 500-year

		Element	Left OB	Channel	Right OB
E.G. Elev (m)	2554.29	Wt. n-Val.	0.030	0.046	0.030
Vel Head (m)	0.01	Reach Len. (m)	13.05	12.98	12.94
W.S. Elev (m)	2554.28	Flow Area (m2)	28.58	141.65	23.90
Crit W.S. (m)		Area (m2)	28.58	141.65	23.90
E.G. Slope (m/m)	0.000136	Flow (m3/s)	14.31	64.83	7.05
Q Total (m3/s)	86.20	Top Width (m)	19.39	58.46	36.16
Top Width (m)	114.01	Avg. Vel. (m/s)	0.50	0.46	0.30
Vel Total (m/s)	0.44	Hydr. Depth (m)	1.47	2.42	0.66
Max Chl Dpth (m)	2.76	Conv. (m3/s)	1225.9	5553.4	604.3
Conv. Total (m3/s)	7383.6	Wetted Per. (m)	19.57	58.49	36.20
Length Wtd. (m)	12.99	Shear (N/m2)	1.95	3.24	0.88
Min Ch EI (m)	2551.52	Stream Power (N/m s)	57200.65	0.00	0.00
Alpha	1.05	Cum Volume (1000 m3)	376.99	424.34	785.68
Frcn Loss (m)	0.00	Cum SA (1000 m2)	550.80	534.76	1056.00
C & E Loss (m)	0.00				

Cross Section Output					
File Type Options Help					
River:	TEMIE RIVER	Profile:	1000-year		
Reach:	DOWNSTREAM	RS:	12624.16	Plan: Plan 02	
Plan: Plan 02 TEMIE RIVER DOWNSTREAM RS: 12624.16 Profile: 1000-year					
Element		Left OB	Channel	Right OB	
E.G. Elev (m)	2554.34				
Vel Head (m)	0.01				
W.S. Elev (m)	2554.33				
Crit W.S. (m)					
E.G. Slope (m/m)	0.000151				
Q Total (m3/s)	94.00				
Top Width (m)	115.54				
Vel Total (m/s)	0.47				
Max Chl Dpth (m)	2.81				
Conv. Total (m3/s)	7639.9				
Length Wtd. (m)	12.99				
Min Ch EI (m)	2551.52				
Alpha	1.05				
Frctn Loss (m)	0.00				
C & E Loss (m)	0.00				
Wt. n-Val.		0.030	0.046	0.030	
Reach Len. (m)		13.05	12.98	12.94	
Flow Area (m2)		29.38	144.07	25.43	
Area (m2)		29.38	144.07	25.43	
Flow (m3/s)		15.66	70.28	8.05	
Top Width (m)		19.64	58.46	37.44	
Avg. Vel. (m/s)		0.53	0.49	0.32	
Hydr. Depth (m)		1.50	2.46	0.68	
Conv. (m3/s)		1273.1	5712.4	654.4	
Wetted Per. (m)		19.83	58.49	37.48	
Shear (N/m2)		2.20	3.66	1.01	
Stream Power (N/m s)		57200.65	0.00	0.00	
Cum Volume (1000 m3)		395.37	443.17	821.37	
Cum SA (1000 m2)		568.37	547.66	1090.62	

For most cross sections, result flow area, flow, top width, average velocity, hydraulic depth, wetted perimeter, shear, stream power, cumulative volume, and cumulative storage area values in the Left bank are greater than the values in the Right bank. This result indicates that the area on the Left side is more affected by the catastrophic flood. The reason is the area on the Left side has flat slope than the Right side.

4.4.4 Flood Inundation Mapping

Flood mapping is the final step for this model analysis. Using the peak flood for 20 and 1000-years return period using HEC-RAS model, downstream flood inundation extent, depth, and velocity, were delineated and mapped in order to differentiate the flooded areas.

Under HEC-GeoRAS tool using the important hydraulic variables from the HEC-RAS output, such as the peak flood, maximum water surface elevation, and velocity plotted on the created TIN and has given the area of inundation.

Area inundated by River channel flood occurs when the elevation of the water surface of the flood is greater than the elevation of the over bank elevations. After exporting the maximum surface profile obtained from the simulation to HEC-GeoRAS, the exported file format was converted from RAS SDF file to RAS XML file format and Arc-GIS can easily read the file and perform the inundation mapping.

According to the exported inundation map, the flood velocity distribution and flood depth value of from Downstream up to floodplain area of the cross section the

catastrophic flood attacks many properties. The left side of the River which are Gult and Kiranyio are critically endangered areas and the right side less endangered areas kogna to Buha gelm. The following figure shows the velocity, depth, and flood vulnerable areas along the downstream. Flood plain delineation is performed using HEC-RAS Post processing and the result is shown below.

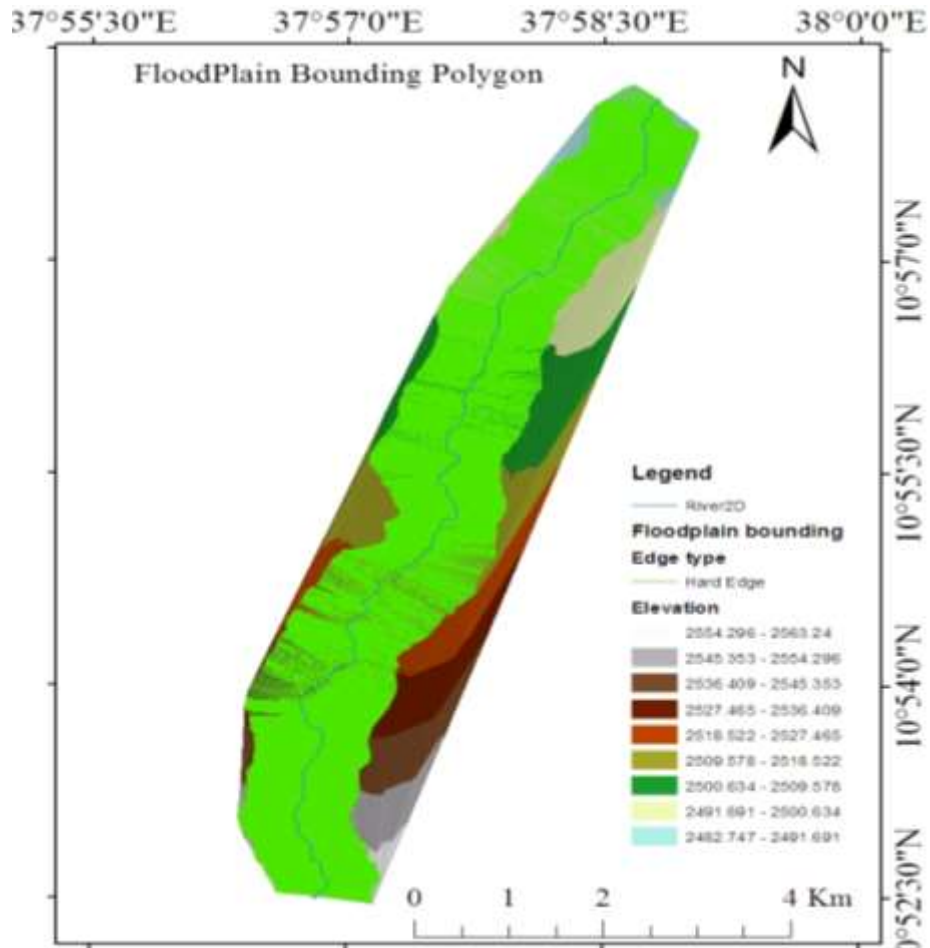


Figure 4-7: - water surface TIN Generated bounding polygon

As seen from the result the inundated areas are the cultivated and also the right and left side of the stream was found to be flood vulnerable areas by the 1000 year flood especially the lower right side and the left side of the cultivated area is highly susceptible by the flood and the right and left side of stream are affected by this flood it varies from place to place and the inundation depth of the 1000 year flood range from 3.04 m -5.54 m depth at the upstream of the watershed and at the downstream of the watershed.

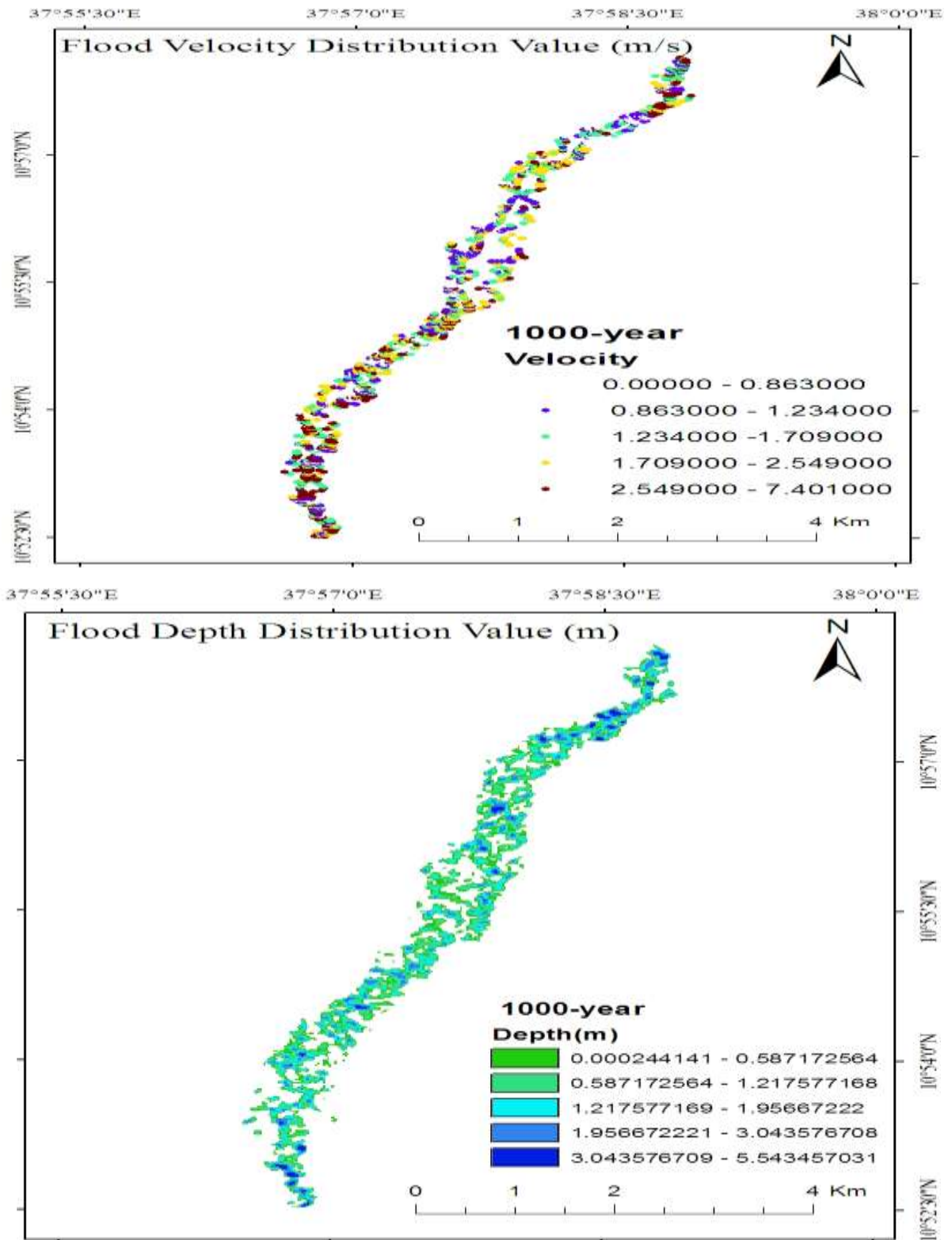


Figure 4-8: - flood velocity and depth distribution map

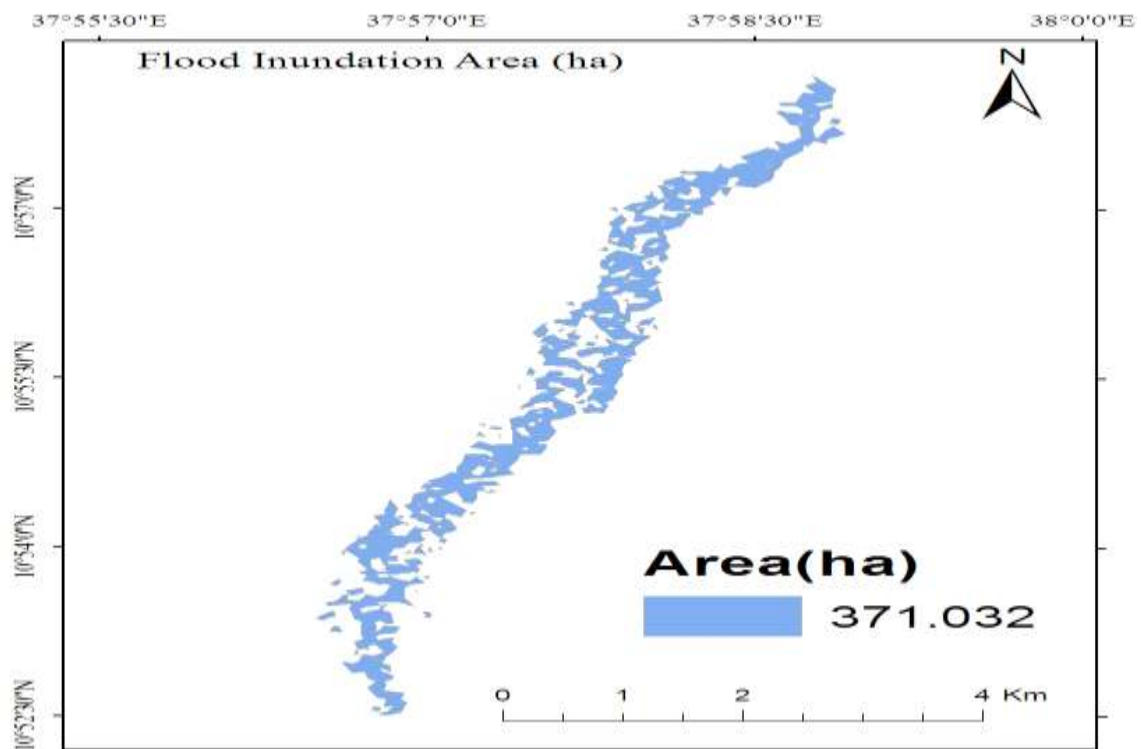
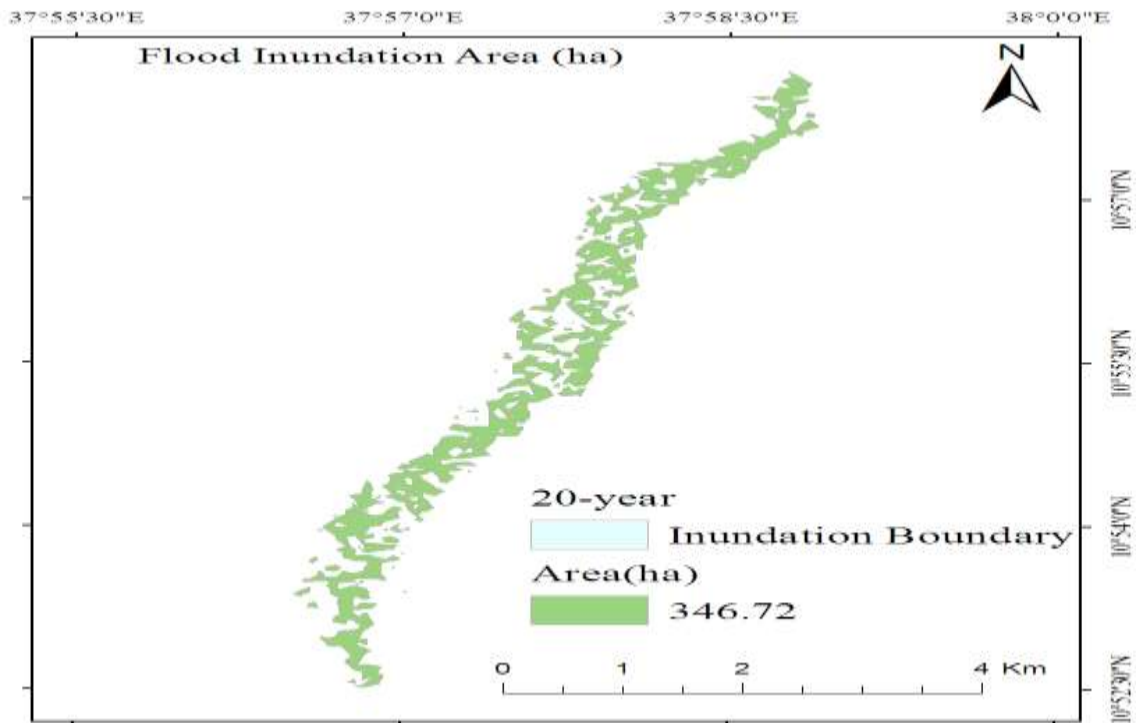


Figure 4-9:-Flood Inundation Map for 20 and 1000YearsReturn Period respectively

As it is clearly shown in figure 4.8 the maximum velocity and depth was estimated to be 7.4m/s and 5.54m which are occurred at around downstream. The value of the flood velocity along the river has not constant decreasing or increasing trend. In some cross section the value becomes increased and in other cross section the value decreased. This is due to slope, obstruction and friction resistance variation of the river and the floodplain at the downstream. For critical stations the value ranges between 2.56 m /s and 7.4 m/s. In the attribute table to the polygon of the flood extent, the inundation area was calculated and used for analysis of the flooding effect on crop yield. The extent of inundation areas for the floods of different return periods floods are indicated in the table 4.6.

Table 4-6:-Flood magnitude and corresponding inundated area

Return Period (Years)	20	50	100	500	1000
Flow(m ³ /S)	50.8	63.5	70.8	86.2	94
Inundated Area (Ha)	346.72	352.23	357.77	362	371.032

Floods that correspond to longer return periods have high flows which can submerge and damage a large amount of cropland and grazing land. Also, this flood can bring in water logging in the area which consequently can result in yield production.

4.4.5 Flood Risk Result

The estimated crop loss due to flooding return periods is indicated

Table 4-7:- Estimated crop land due to Flooding

No.	Crop	Average	% of Coverage	Return Period				
				20yrs	50yrs	100yrs	500yrs	1000yrs
				Flood inundation area				
				346.7	352.2	357.8	363.0	371.0
1	Teff	35	55.0	6674.4	6780.4	6887.1	6987.0	7142.4
2	maize	20	15.0	1040.2	1056.7	1073.3	1088.9	1113.1
3	barley	12	10.0	416.1	422.7	429.3	435.6	445.2
4	wheat	20	15.0	1040.2	1056.7	1073.3	1088.9	1113.1
5	potato	8	5.0	138.7	140.9	143.1	145.2	148.4
Total Crop Loss				9309.4	9457.4	9606.1	9745.5	9962.2

Crop loss = Average Crop grown per hectare*%of crop coverage *Flood Inundated Area for different return period.

Crop Loss= 35*0.55*346.7 = 6674.4 quintal of Teff Loss for 20 years return period

Flood events with long return periods have small probability of occurrences but their magnitude and adverse effect on crop are very high. Flood with short return period occurs frequently and may result in repeated damage to crop. Therefore, this flood lead lost the crop due to on wet season from June to November.

This research mainly focused on the risky areas especially near Temie River that include GultKeraniyo buha geltm and kogna. The location and topography of these areas make them highly vulnerable to flooding.

5 CONCLUSION AND RECOMMENDETION

5.1 Conclusion

The aims of this thesis mainly work on checking the quality of the hydrological data around Temie station, hydrological and hydraulic computation of flood profile in different return periods of the Temie River, flood frequency analysis delineation of flood risk area and effect of flood risk on crop production.

It was found out that the recorded hydrological data of Temie gauging station is good quality, homogenous, and stationary. Flood affected areas were delineated for 20- and 1000-year return periods with peak flood discharge $50.8 \text{ m}^3/\text{s}$ and $94\text{m}^3/\text{s}$ respectively. One Dimensional numerical model HEC-RAS and Arc-GIS for spatial data processing and HEC-GeoRAS for interfacing between HEC-RAS and Arc-GIS were used. The flood hazard map delineation indicated Gult, Keraniyo-Abar, Buha ,Geltim and Kogna adjacent to Hulet Eju Enebsie Woreda to be the most affected areas.

It was also estimated that a total land area of 371.03 hectares could be inundated by the 1000-year return period flood results in a loss of 9962.2quintals of crop. The area affected by the 20-year return period flood was346.7 hectares with an estimated loss of 9309.4 quintals of crop.

A large area of land is inundated by flood magnitude of different return periods that may result in a huge damage to crop, grass land and other infrastructures. But also has positive impact and benefit from flood such as accumulation of fertile soil comes from Upstream of Temie River as result, the farmer they use for agricultural activity to increase the production yield appropriate flood management measure must therefore be identified and practiced.

5.2 Recommendations

In order to reduce the amount of flood hazard, it is recommended that areas inundated by flood should not be used for agricultural activities, settlement infrastructure development and other investment project on the summer season because has high probability occurrence in the study area.

Generally, in the study area the following recommendations are also forwarded.

- ✚ The responsible bodies of the Woreda as well as the region should be incorporating the flood hazard and flood risk assessment studies in their development strategies.
- ✚ Because of limitation of data and resources, the study focused only on the risk of flood on crop yield .it is recommended to carry out additional researches concerning the risk of flooding on other properties.
- ✚ Traditional flood design methods should be supplemented or replaced by risk-oriented methods which are based on compressive risk analysis.
- ✚ Economic oriented criteria will be suggested.
- ✚ Development of flood protection structure and soil conservation measure should be carried out in the Upstream and Downstream part of the site to minimize the magnitude of flood, sediment transport and siltation.
- ✚ Adopt appropriate land use planning practice in flood prone area to minimize the adverse effects.

6 REFERENCES

- Ahmad, Tanveer. (2017). A Study on River Bank Protection Works for the Baleshwar River in Pirojpur District. *Research Gate*.
- Asquith, W. H. (1999). *Areal-Reduction Factors for the Precipitation of the 1-day Design Storm* Texas: US Geological Survey.
- Assefa, Tesfay Hailekiros. (2018). Flood risk assessment in Ethiopia. *Civil and environmental research*, 10(1), 35-40.
- Billi, Paolo, Alemu, Yonas Tadesse, & Ciampalini, Rossano. (2015). Increased frequency of flash floods in Dire Dawa, Ethiopia: Change in rainfall intensity or human impact? *Natural Hazards*, 76(2), 1373-1394.
- Brunner, GW. (2016). HEC-RAS river analysis system, 2D modeling User's manual, version 5.0. *Davis: US Army Corps of Engineers, hydrologic engineering center*.
- Chow, Ven. (1959). T. 1959 Open-Channel Hydraulics. *MCGraw Hiu*.
- Clark, CO. (1945). *Storage and the unit hydrograph*. Paper presented at the Proceedings of the American Society of Civil Engineers.
- Committee, Water Resources Council . Hydrology. (1981). *Guidelines for determining flood flow frequency* (Vol. 17): US Water Resources Council.
- Dahmen, ER, & Hall, MJ. (1990). Screening of Hydrological Data, ILRI Publication No. 49. *International Institute for Land Reclamation and Improvement (ILRI): Netherlands*.
- Darshan Mehta et al., DR. S. M. Y & MRS. SAHITA I. (2017). HEC-RAS FLOW ANALYSIS IN THE RIVER TAPI. *ResearchGate*.
- Davis, HECRAS. (2005). river analysis system," hydraulic reference manual" version 4.1. *US Army corps of Engineers Hydrologic Engineering Center, California*.
- Degefu, Workineh. (1987). *Some aspects of meteorological drought in Ethiopia*: Cambridge University Press Cambridge.
- ENGINEERS–USACE, US ARMY CORPS OF. (2016). HEC-RAS River Analysis System Hydraulic Reference Manual. Version 5.0. *Davis, EUA: Hydrologic Engineering Center, 2010b*.
- Fleming, Matt, & Neary, Vincent. (2004). Continuous hydrologic modeling study with the hydrologic modeling system. *Journal of hydrologic engineering*, 9(3), 175-183.
- Gibson, SA, Pak, JH, & Fleming, MJ. (2010). Modeling watershed and riverine sediment processes with HEC-HMS and HEC-RAS *Watershed Management 2010: Innovations in Watershed Management under Land Use and Climate Change* (pp. 1340-1349).
- Gupta, Vijay K, Mantilla, Ricardo, Troutman, Brent M, Dawdy, David, & Krajewski, Witold F. (2010). Generalizing a nonlinear geophysical flood theory to medium-sized river networks. *Geophysical Research Letters*, 37(11).
- H.McCuen, R. (1998). *Hydrologic Analysis and Design*.
- Hussein Roshun et al., Karim Solaimani, Abdulvahed Khaledi Darvishan & Ghorban Vahabzadeh. (2012). Employing GIS to River Hydraulic Analysis Using HEC-RAS Model (Case Study: Zaremrood River, Mazandaran Province). *ResearchGate*.

- Kumar, Neeraj, Lal, Deepak, Sherring, Arpan, & Issac, RK. (2017). Applicability of HEC-RAS & GFMS tool for 1D water surface elevation/flood modeling of the river: a Case Study of River Yamuna at Allahabad (Sangam), India. *Modeling Earth Systems and Environment*, 3(4), 1463-1475.
- Luna Moni Das, Zahid Husain Qureshi. (2015). Flood Frequency Analysis for Jiya Dhol River of. *International Journal of Sciences: Basic and Applied Research*, pp. ISSN 2307-4531.
- Manjusree, P, Bharathi, S, & Rao, GS. INVESTIGATION OF MULTI FREQUENCIES OF AMSR-2 PASSIVE MICROWAVE DATA FOR FLOOD STUDIES.
- Mardookhpour, A, & Jamasbi, H. (2017). Flood zoning estimation and river management by using HEC-RAS and GIS model. *International Journal of Energy and Water Resources*, 1(1), 13-18.
- Mojaddadi, Hossein, Pradhan, Biswajeet, Nampak, Haleh, Ahmad, Noordin, & Ghazali, Abdul Halim bin. (2017). Ensemble machine-learning-based geospatial approach for flood risk assessment using multi-sensor remote-sensing data and GIS. *Geomatics, Natural Hazards and Risk*, 8(2), 1080-1102.
- Mulugeta, Genene, Durrheim, Ray, Ayonghe, Samuel, Daby, Deolall, Dube, Opha Pauline, Gudyanga, Francis, & Lucio, Filipe. (2007). ICSU ROA's Science plan to address natural and human-induced environmental hazards and disasters in sub-Saharan Africa. *International Council for Science, Pretoria*.
- Nash, J Eamonn, & Sutcliffe, Jonh V. (1970). River flow forecasting through conceptual models part I—A discussion of principles. *Journal of hydrology*, 10(3), 282-290.
- Nelson, E James, Miller, A Woodruff, & Dixon, Eric. (1999). Chino well fire: A hydrologic evaluation of rainfall and runoff from the Mud Canyon watershed. *International Journal of Wildland Fire*, 9(1), 1-8.
- P V Timbadiya et al., Prem Lal Patel & Prakash D. Porey. (2011). Calibration of HEC-RAS Model on Prediction of Flood for Lower Tapi River, India. *Journal of Water Resource and Protection*.
- Patel, Sumit B, Mehta, Darshan J, & Yadav, Sanjay M. (2018). One dimensional hydrodynamic flood modeling for Ambica River, South Gujarat. *J Emerg Technol Innov Res*, 5(4), 595-601.
- Pudasaini, SP, Wang, Y, & Hutter, K. (2005). Modelling debris flows down general channels.
- Rientjes, THM, Perera, BUJ, Haile, AT, Reggiani, P, & Muthuwatta, LP. (2011). Regionalisation for lake level simulation—the case of Lake Tana in the Upper Blue Nile, Ethiopia. *Hydrology and Earth System Sciences*, 15(4), 1167.
- Santhi, C, Arnold, Jeffrey G, Williams, Jimmy R, Dugas, William A, Srinivasan, Raghavan, & Hauck, Larry M. (2001). Validation of the swat model on a large rwer basin with point and nonpoint sources 1. *JAWRA Journal of the American Water Resources Association*, 37(5), 1169-1188.
- Schaffenberg, WA. (2013). Hydrologic Modeling System HEC-HMS, User Manual: Version 4.0. *US Army Corps of Engineers, Hydrologic Engineering Center HEC*, 609.

- Scharffenberg, WA, & Fleming, MJ. (2013). HEC-HMS User's Manual. *Washington, DC*.
- Smith, Keith, & Ward, Roy. (1998). *Floods: physical processes and human impacts*: John Wiley and Sons Ltd.
- Starks, PJ, & Moriasi, DN. (2009). Spatial resolution effect of precipitation data on SWAT calibration and performance: Implications for CEAP. *Transactions of the ASABE*, 52(4), 1171-1180.
- Tate, Eric C, Maidment, David R, Olivera, Francisco, & Anderson, David J. (2002). Creating a terrain model for floodplain mapping. *Journal of Hydrologic Engineering*, 7(2), 100-108.
- Te, Chow Ven, Maidment, David R, & Mays, Larry W. (1988). Applied hydrology. *Water Resources Handbook*.
- Timbadiya, Prafulkumar V, Patel, Prem Lal, & Porey, Prakash D. (2011). Calibration of HEC-RAS model on prediction of flood for lower Tapi River, India. *Journal of Water Resource and Protection*, 3(11), 805.
- US Army Corps of Engineers, UACO. (2000). Hydrologic modeling system HEC-HMS technical reference manual. *Hydrol. Eng. Cent*.
- USACE. (2001a). HEC-HMS Hydrologic Modeling System User's Manual: US Army Corps of Engineers Davis, USA.
- USACE. (2001b). Hydrologic Modeling System HEC-HMS. User's Manual , Version 4.1.: US Army Corps of Engineers, Hydrologic Engineering Center, 178 p.
- USACE., U.S. Army Corps of Engineers. (2017). ENGINEERING AND CONSTRUCTION BULLETIN. USA.
- Woube, Mengistu. (1999). Flooding and sustainable land–water management in the lower Baro–Akobo river basin, Ethiopia. *Applied Geography*, 19(3), 235-251.
- Zelege, Elias. (2015). *Case study: on Bantyeketu River in Addis Ababa*. Addis Ababa University.
- Zemadim (PhD), B. (January, 2010). Hydrology guide book. Bahir Dar: Sustainable Water Harvesting and Institutional Strengthening in Amhara (SWHISA).

7 APPENDICES

Annex 1: - The values of detection deviate kn

Outlier test Kn values							
Sample size n	Kn	Sample size n	Kn	Sample size	kn	Sample size	Kn
10	2.036	21	2.408	32	2.591	43	2.71
11	2.088	22	2.429	33	2.604	44	2.719
12	2.134	23	2.448	34	2.616	45	2.727
13	2.175	24	2.467	35	2.628	46	2.736
14	2.213	25	2.468	36	2.639	47	2.744
15	2.247	26	2.534	37	2.65	48	2.753
16	2.279	27	2.502	38	2.661	49	2.76
17	2.309	28	2.519	39	2.671	50	2.768
18	2.335	29	2.549	40	2.682		
19	2.361	30	2.563	41	2.692		
20	2.385	31	2.577	42	2.7		

Annex 2: Reduced Mean (y_n) and Reduced Standard Deviation (s_n)

N	y_n	S_n
10	0.4952	0.9457
15	0.5128	1.0206
20	0.5236	1.0628
25	0.5309	1.0928
30	0.5362	1.1124
40	0.5436	1.1413
50	0.5485	1.1607
60	0.5521	1.1747
70	0.5548	1.1854
80	0.5569	1.1938
90	0.5586	1.2007
100	0.5600	1.2065
200	0.5672	1.236
500	0.5724	1.2588
∞	0.5772	1.2826

Annex 3: - Probable maximum precipitation in 20 year by normal Distribution

Rank	Xn	P	W	Kt	Xt
1	91.6	0.047619	2.467599	1.665608	86.40192
2	84.4	0.095238	2.168583	1.306596	81.09266
3	83.5	0.142857	1.97277	1.065082	77.52101
4	79.3	0.190476	1.821114	0.873702	74.69078
5	72.8	0.238095	1.694157	0.710042	72.27049
6	68.2	0.285714	1.582885	0.5636	70.10483
7	66.5	0.333333	1.482304	0.428462	68.10633
8	63.3	0.380952	1.389303	0.300849	66.21912
9	62.6	0.428571	1.301766	0.178091	64.40371
10	58.3	0.47619	1.218144	0.058116	62.62945
11	57.5	0.52381	1.137213	-0.06084	60.87024
12	57.4	0.571429	1.057937	-0.18044	59.10163
13	57.2	0.619048	0.97936	-0.30237	57.29835
14	53.7	0.666667	0.900517	-0.4286	55.43168
15	53.6	0.714286	0.820332	-0.56153	53.46574
16	51.7	0.761905	0.737474	-0.7045	51.35142
17	51.0	0.809524	0.650091	-0.86252	49.01458
18	47.3	0.857143	0.555249	-1.0441	46.32933
19	38.9	0.904762	0.4474	-1.26631	43.04314
20	36.6	0.952381	0.312379	-1.57538	38.47242
Average	61.8				
Stdev	14.78855				

Annex 4: -Probable maximum precipitation in 20 year by Log-normal distribution

Rank	Xn	Y=Logxn	P	W	Kt	Xt	Xt=10^Xt
1	91.6	1.961895	0.047619	2.467599	1.665608	1.954478	90.04883
2	84.4	1.926342	0.095238	2.168583	1.306596	1.916612	82.53007
3	83.5	1.921686	0.142857	1.97277	1.065082	1.891139	77.82858
4	79.3	1.899273	0.190476	1.821114	0.873702	1.870954	74.29401
5	72.8	1.862131	0.238095	1.694157	0.710042	1.853692	71.39902
6	68.2	1.833784	0.285714	1.582885	0.5636	1.838247	68.90436
7	66.5	1.822822	0.333333	1.482304	0.428462	1.823993	66.67965
8	63.3	1.801404	0.380952	1.389303	0.300849	1.810534	64.64482
9	62.6	1.796574	0.428571	1.301766	0.178091	1.797586	62.74602
10	58.3	1.765669	0.47619	1.218144	0.058116	1.784932	60.94416
11	57.5	1.759668	0.52381	1.137213	-0.06084	1.772385	59.20867
12	57.4	1.758912	0.571429	1.057937	-0.18044	1.759772	57.51373
13	57.2	1.757396	0.619048	0.97936	-0.30237	1.746911	55.83551
14	53.7	1.729974	0.666667	0.900517	-0.4286	1.733597	54.14986
15	53.6	1.729165	0.714286	0.820332	-0.56153	1.719576	52.42956
16	51.7	1.713491	0.761905	0.737474	-0.7045	1.704497	50.64037
17	51.0	1.70757	0.809524	0.650091	-0.86252	1.68783	48.73382
18	47.3	1.674861	0.857143	0.555249	-1.0441	1.668679	46.63147
19	38.9	1.58995	0.904762	0.4474	-1.26631	1.645242	44.18165
20	36.6	1.563481	0.952381	0.312379	-1.57538	1.612643	40.98674
Average	61.8	1.778802					
Stdev	14.78855	0.105472					

Annex 5: - Probable maximum precipitation in 20 year by Log Pearson Type-III

Rank	Xn	y=logxn	P	W	Z	KT	xt	XT=10^xt
1	91.6	1.96	0.05	2.47	1.67	1.60	1.95	88.77
2	84.4	1.92	0.10	2.17	1.31	1.28	1.91	82.01
3	83.5	1.92	0.14	1.97	1.07	1.06	1.89	77.7
4	79.3	1.89	0.19	1.82	0.87	0.88	1.87	74.4
5	72.8	1.86	0.24	1.69	0.71	0.72	1.85	71.65
6	68.2	1.83	0.29	1.58	0.56	0.58	1.84	69.25
7	66.5	1.82	0.33	1.48	0.43	0.46	1.82	67.09
8	63.3	1.80	0.38	1.39	0.30	0.33	1.81	65.09
9	62.6	1.79	0.43	1.30	0.18	0.21	1.80	63.21
10	58.3	1.76	0.48	1.22	0.06	0.09	1.78	61.41
11	57.5	1.75	0.52	1.14	-0.06	-0.03	1.78	59.67
12	57.4	1.76	0.57	1.06	-0.18	-0.15	1.76	57.95
13	57.2	1.76	0.62	0.98	-0.30	-0.27	1.75	56.24
14	53.7	1.73	0.67	0.90	-0.43	-0.40	1.74	54.50
15	53.6	1.73	0.71	0.82	-0.56	-0.54	1.72	52.72
16	51.7	1.7	0.76	0.74	-0.70	-0.69	1.71	50.85
17	51.0	1.70	0.81	0.65	-0.86	-0.85	1.69	48.85
18	47.3	1.67	0.86	0.56	-1.04	-1.05	1.67	46.61
19	38.9	1.59	0.90	0.45	-1.27	-1.28	1.64	43.99
20	36.6	1.56	0.95	0.31	-1.58	-1.62	1.61	40.53
mean	61.8	1.79						
Stdev	14.79	0.11						
CS	0.38	-0.19						
K		-0.03						

Annex 6 -Probable maximum precipitation in 20 year by Pearson Type III

Rank	Xn	P	W	Z	Kt	Xt
1	91.6	0.047619	2.467599	1.665608	1.769931	86.40192
2	84.4	0.095238	2.168583	1.306596	1.343594	81.09266
3	83.5	0.142857	1.97277	1.065082	1.066672	77.52101
4	79.3	0.190476	1.821114	0.873702	0.852794	74.69078
5	72.8	0.238095	1.694157	0.710042	0.673747	72.27049
6	68.2	0.285714	1.582885	0.5636	0.516517	70.10483
7	66.5	0.333333	1.482304	0.428462	0.3739	68.10633
8	63.3	0.380952	1.389303	0.300849	0.241387	66.21912
9	62.6	0.428571	1.301766	0.178091	0.115882	64.40371
10	58.3	0.47619	1.218144	0.058116	-0.00493	62.62945
11	57.5	0.52381	1.137213	-0.06084	-0.12292	60.87024
12	57.4	0.571429	1.057937	-0.18044	-0.23976	59.10163
13	57.2	0.619048	0.97936	-0.30237	-0.35706	57.29835
14	53.7	0.666667	0.900517	-0.4286	-0.47656	55.43168
15	53.6	0.714286	0.820332	-0.56153	-0.60031	53.46574
16	51.7	0.761905	0.737474	-0.7045	-0.73101	51.35142
17	51.0	0.809524	0.650091	-0.86252	-0.87261	49.01458
18	47.3	0.857143	0.555249	-1.0441	-1.03166	46.32933
19	38.9	0.904762	0.4474	-1.26631	-1.22105	43.04314
20	36.6	0.952381	0.312379	-1.57538	-1.47501	38.47242
Average	61.8					
Stdev	14.78855					
Cs	0.378276					
K	0.063046					

Annex 7: -Probable maximum precipitation in 20 year by Gamble extreme

Rank	Xn	P	Yn	Sn	Kt	Xt
1	91.6	2.970195	0.5236	1.0628	2.302028	95.81365
2	84.4	2.250367	0.5236	1.0628	1.624734	85.79746
3	83.5	1.816961	0.5236	1.0628	1.216937	79.76673
4	79.3	1.49994	0.5236	1.0628	0.918649	75.35548
5	72.8	1.245899	0.5236	1.0628	0.679619	71.82058
6	68.2	1.03093	0.5236	1.0628	0.477353	68.82935
7	66.5	0.842151	0.5236	1.0628	0.299728	66.20254
8	63.3	0.671727	0.5236	1.0628	0.139374	63.83114
9	62.6	0.514437	0.5236	1.0628	-0.00862	61.6425
10	58.3	0.366513	0.5236	1.0628	-0.1478	59.58418
11	57.5	0.225011	0.5236	1.0628	-0.28095	57.61522
12	57.4	0.087422	0.5236	1.0628	-0.4104	55.70071
13	57.2	-0.04862	0.5236	1.0628	-0.53841	53.80772
14	53.7	-0.18563	0.5236	1.0628	-0.66732	51.90132
15	53.6	-0.32663	0.5236	1.0628	-0.79999	49.93924
16	51.7	-0.47588	0.5236	1.0628	-0.94043	47.86246
17	51.0	-0.64034	0.5236	1.0628	-1.09516	45.57416
18	47.3	-0.83403	0.5236	1.0628	-1.27741	42.87895
19	38.9	-1.09719	0.5236	1.0628	-1.52502	39.2172
20	36.6		0.5236	1.0628	-0.49266	54.48426
Average	61.8					
Stdev	14.78855					
CS	0.378276					
K	0.063046					

Annex 8: -Typical Hydrological Soil Group in Ethiopia

Soil Types	Hydrologic Soil Group
Ao Orthic Acrisols	B
Bc Chromic Cambisols	B
Bd Dystric Cambisols	B
Be Eutric Cambisols	B
Bh Humic Cambisols	C
Bk Calcic Cambisols	B
Bv Vertic Cambisols	B
Ck Calcic Chernozems	B
E Rendzinas	D
Hh Haplic Phaeozems	C
HI Luvic Phaeozems	C
ILithosols	D
Jc Calcaric Fluvisols	B
JeEutric Fluvisols	B
Lc Chromic Luvisols	B
LoOrthic Luvisols	B
Lv Vertic Luvisols	C
Nd Dystric Nitosols	B
Ne Eutric Nitosols	B
Od Dystric Histosols	D
Oe Eutric Histosols	D
QcCambic Arenosols	A

Rc	Calcaric Regosols	A
Re	Eutric Regosols	A
Th	Humic Andosols	B
Tm	Mollic Andosols	B
Tv	Vitric Andosols	B
Vc	Chromic Vertisols	D
Vp	Pellic Vertisols	D
Xh	Haplic Xerosols	B
Xk	Caloic Xerosols	B
Xl	Luvic Xerosols	C
Yy	Gypsic Yermosols	B
Zg	Gleyic Solonchaks	D
Zo	Orthic Solonchaks	B

Annex 9: - Temie sub-basins the corresponding soil type and land use

Name Sub-basin	Soil Type	Land use/land cover	Area(km2)
Sub-basin 1	Pellic Vertisols	Cultivation unstocked	4.951297982
		cultivation lightly stocked	2.485864874
		Forest plant	0.417063425
		Grass land	1.255702291
	Lithosols	Cultivation unstocked	2.750721101
		cultivation lightly stocked	1.381036041
		Forest plant	0.231701903
		Grass land	0.697612384
	Eutric Cambisols	Grass land	1.116179814
	Chromic Luvisols	cultivation lightly stocked	1.104828833
	Eutric Nitosols	Cultivation unstocked	1.10028844
	Eutric Nitosols	Cultivation unstocked	1.424536047
		cultivation lightly stocked	0.715207231
		Forest plant	0.119993158
		Grass land	0.361277625
		Afro alpine	0.190698251
Shrub land		0.082787686	
Lithosols	Cultivation unstocked	3.561340118	
	cultivation lightly stocked	1.788018078	

Sub-basin 2	Forest plant	0.299982896
	Grass land	0.903194064
	Afro alpine	0.476745629
	Shrub land	0.206969216
Chromic	Cultivation unstocked	2.849072094
Luvisols	cultivation lightly stocked	1.430414463
	Forest plant	0.239986317
	Grass land	0.722555251
	Afro alpine	0.381396503
	Shrub land	0.165575373

Name Sub-basin	Soil Type	Land use/land cover	Area(km2)
Sub-basin 3	Eutric Nitosols	Cultivation unstocked	1.722886056
		cultivation lightly stocked	0.864997814
		Forest plant	0.14512412
		Grass land	0.436942389
		Afro alpine	0.230637448
		Shrub land	0.100126459
		Lithosols	Cultivation unstocked
	cultivation lightly stocked		2.162494534
	Forest plant		0.362810299
	Grass land		1.092355972
	Afro alpine		0.57659362
	Shrub land		0.250316148
	Chromic Luvisols	Cultivation unstocked	3.445772113
		cultivation lightly stocked	1.729995628
		Forest plant	0.290248239
		Grass land	0.873884778
		Afro alpine	0.461274896
		Shrub land	0.200252919

Annex 10- weighted of curve number

Name	Soil Type	HYSG	Land use/land	Area(km2)	CNII	Area	Weighted CN		
Sub-basin 1	Pellic Vertisols	D	Cultivation un-stocked	4.95129798	79	9.1099	77.9		
			cultivation lightly stocked	2.48586487	77				
			Forest plant	0.41706343	76				
			Grass land	1.25570229	83				
	Lithosols	C	Cultivation un-stocked	2.7507211	78	5.0611			
			cultivation lightly stocked	1.38103604	74				
			Forest plant	0.2317019	74				
			Grass land	0.69761238	80				
				5.06107143					
Cambisols	Eutric	B	Grass land	1.11617981	76	1.1162			
			Chromic Luvisols	D	cultivation lightly stocked		1.10482883	78	1.1048
					Eutric Nitosols		D	Cultivation un-stocked	
Sub-	Nitosols	D	Cultivation un-stocked	1.42453605	81	2.8945	80.01		

basin 2		cultivation	0.71520723	79		
		lightly stocked				
		Forest	0.11999316	77		
		plant				
		Grass land	0.36127763	83		
		Afro-	0.19069825	80		
		alpine				
		Shrub land	0.08278769	80		
			2.8945			
	Lithosols	C	Cultivation	3.56134012	81	7.2363
			un-stocked			
			cultivation	1.78801808	79	
			lightly stocked			
			Forest	0.2999829	77	
			plant			
			Grass land	0.90319406	83	
			Afro-	0.47674563	82	
			alpine			
			Shrub land	0.20696922	80	
						7.23625
	Chromic Luvisols	D	Cultivation	2.84907209	81	5.789
			un-stocked			
			cultivation	1.43041446	79	
			lightly stocked			
			Forest	0.23998632	77	
			plant			
			Grass land	0.72255525	83	
			Afro-	0.3813965	80	

Name	Soil	HYSG	Land	Area(km2)	CNII	ΣA	Weighted CN
Sub-basin	Type		use/land				
			cover				
Sub-basin	Eutric	D	Cultivation	1.7228861	81	3.50071	77.7
3	Nitosols		un-stocked				
			cultivation	0.8649978	79		
			lightly				
			stocked				
			Forest	0.1451241	77		
			plant				
			Grass land	0.4369424	83		
			Afro-	0.2306374	80		
			alpine				
			Shrub land	0.1001265	80		
				3.5007143			
	Lithosols	C	Cultivation	4.3072151	78	8.75179	
			un-stocked				
			cultivation	2.1624945	76		
			lightly				
			stocked				
			Forest	0.3628103	70		
			plant				
			Grass land	1.092356	77		
			Afro-	0.5765936	80		
			alpine				
			Shrub land	0.2503161	74		
				8.7517857			

Chromic	D	Cultivation	3.4457721	81	7.00143
Luvisols		un-stocked			
		cultivation	1.7299956	79	
		lightly			
		stocked			
		Forest	0.2902482	77	
		plant			
		Grass land	0.8738848	83	
		Afro-	0.4612749	80	
		alpine			
		Shrub land	0.2002529	80	
			7.0014286		

Annex 11-Summary Computation sheet for Manning's Roughness Coefficient

Variable	Description alternatives	Recommend value	Actual Value of Channel	Actual value of floodplain
Basic n1	Earth	0.01	n1 = 0.024	n1 = 0.01
	Rock	0.025		
	Fine gravel	0.024		
	Coarse gravel	0.028		
Irregularity n2	Smooth	0	n2 = 0.01	n2 = 0.01
	Minor	0.005		
	Moderate	0.01		
	Severe	0.02		
Cross sections n3	Gradual	0	n3 = 0.01	n3 = 0.000
	Occasional	0.005		
	Alternating	0.010-0.015		
Obstructions n4	Negligible	0	n4 = 0.015	n4 = 0.000
	Minor	0.01-0.015		
	Appreciable	0.02-0.03		
	Severe	0.04-0.06		
Vegetation n5	Low	0.05-0.01	n5 = 0.01	n5 = 0.01
	Medium	0.01-0.02		
	High	0.025-0.05		
	Very high	0.05-0.100		
Meandering n6	Minor	0	n6 = 0.00069	n6 = 0.000
Tot. reach n	Appreciable	0.15*ns	0.046	0.03
	Severe	0.3*ns n		

Annex 12: - Output Table of HEC-RAS

HEC-RAS Plan: Plan 02 River: TEMIE RIVER Reach: DOWNSTREAM												
Reach	River Sta	Profile	Q Total (m3/s)	Min Ch El (m)	W.S. Elev (m)	Crit W.S. (m)	E.G. Elev (m)	E.G. Slope (m/m)	Vel Chnl (m/s)	Flow Area (m2)	Top Width (m)	Froude # Chl
DOWNSTREAM	13353.12	20-year	50.80	2562.37	2563.08	2563.08	2563.23	0.020322	1.53	30.24	104.92	0.83
DOWNSTREAM	13353.12	50-year	63.50	2562.37	2563.13	2563.13	2563.30	0.019320	1.62	35.25	106.86	0.83
DOWNSTREAM	13353.12	100-year	70.80	2562.37	2563.16	2563.16	2563.34	0.018446	1.66	38.26	108.02	0.82
DOWNSTREAM	13353.12	500-year	86.20	2562.37	2563.21	2563.21	2563.41	0.017616	1.75	43.88	110.13	0.81
DOWNSTREAM	13353.12	1000-year	94.00	2562.37	2563.23	2563.23	2563.45	0.017427	1.80	46.48	111.10	0.81
DOWNSTREAM	13320.34	20-year	50.80	2560.43	2561.13	2561.37	2561.89	0.102323	3.88	13.10	31.44	1.92
DOWNSTREAM	13320.34	50-year	63.50	2560.43	2561.21	2561.47	2562.04	0.093697	4.03	15.76	33.38	1.87
DOWNSTREAM	13320.34	100-year	70.80	2560.43	2561.25	2561.52	2562.12	0.091301	4.13	17.15	34.36	1.87
DOWNSTREAM	13320.34	500-year	86.20	2560.43	2561.34	2561.63	2562.26	0.083395	4.24	20.31	36.48	1.82
DOWNSTREAM	13320.34	1000-year	94.00	2560.43	2561.39	2561.68	2562.32	0.079393	4.28	21.96	37.54	1.79
DOWNSTREAM	13289.48	20-year	50.80	2558.90	2561.10	2559.58	2561.11	0.000238	0.48	108.77	72.85	0.12
DOWNSTREAM	13289.48	50-year	63.50	2558.90	2561.25	2559.67	2561.26	0.000283	0.54	119.68	75.90	0.13
DOWNSTREAM	13289.48	100-year	70.80	2558.90	2561.33	2559.73	2561.34	0.000307	0.57	125.60	77.51	0.13
DOWNSTREAM	13289.48	500-year	86.20	2558.90	2561.47	2559.82	2561.49	0.000356	0.64	137.00	80.51	0.15
DOWNSTREAM	13289.48	1000-year	94.00	2558.90	2561.54	2559.87	2561.56	0.000379	0.67	142.56	81.93	0.15
DOWNSTREAM	13248.01	20-year	50.80	2558.21	2561.10		2561.11	0.000140	0.40	128.75	73.36	0.09
DOWNSTREAM	13248.01	50-year	63.50	2558.21	2561.24		2561.25	0.000174	0.46	139.61	75.85	0.10
DOWNSTREAM	13248.01	100-year	70.80	2558.21	2561.32		2561.33	0.000192	0.49	145.44	77.15	0.11
DOWNSTREAM	13248.01	500-year	86.20	2558.21	2561.46		2561.48	0.000230	0.56	156.64	79.60	0.12
DOWNSTREAM	13248.01	1000-year	94.00	2558.21	2561.53		2561.55	0.000248	0.59	162.11	80.77	0.12
DOWNSTREAM	13208.84	20-year	50.80	2559.00	2561.01		2561.08	0.003180	1.22	41.47	41.32	0.39
DOWNSTREAM	13208.84	50-year	63.50	2559.00	2561.13		2561.23	0.003586	1.36	46.86	43.92	0.42
DOWNSTREAM	13208.84	100-year	70.80	2559.00	2561.20		2561.30	0.003794	1.42	49.78	45.27	0.43
DOWNSTREAM	13208.84	500-year	86.20	2559.00	2561.32		2561.44	0.004129	1.56	55.40	47.74	0.46
DOWNSTREAM	13208.84	1000-year	94.00	2559.00	2561.38		2561.51	0.004258	1.62	58.16	48.91	0.47
DOWNSTREAM	13169.8	20-year	50.80	2559.86	2560.68		2560.85	0.013842	1.82	27.85	46.18	0.75
DOWNSTREAM	13169.8	50-year	63.50	2559.86	2560.80		2560.98	0.012413	1.88	33.69	48.99	0.73
DOWNSTREAM	13169.8	100-year	70.80	2559.86	2560.86		2561.05	0.012193	1.94	36.54	50.30	0.73
DOWNSTREAM	13169.8	500-year	86.20	2559.86	2560.94		2561.17	0.013300	2.12	40.64	52.13	0.77
DOWNSTREAM	13169.8	1000-year	94.00	2559.86	2560.97		2561.22	0.013892	2.21	42.52	52.95	0.79
DOWNSTREAM	13131.18	20-year	50.80	2559.00	2560.08	2560.00	2560.26	0.016919	1.87	27.40	56.24	0.81
DOWNSTREAM	13131.18	50-year	63.50	2559.00	2560.12	2560.10	2560.36	0.021493	2.18	29.57	58.95	0.92
DOWNSTREAM	13131.18	100-year	70.80	2559.00	2560.15	2560.15	2560.41	0.022889	2.30	31.32	61.08	0.96
DOWNSTREAM	13131.18	500-year	86.20	2559.00	2560.24	2560.24	2560.52	0.021602	2.38	37.10	67.95	0.95
DOWNSTREAM	13131.18	1000-year	94.00	2559.00	2560.28	2560.28	2560.57	0.021042	2.41	40.00	71.15	0.94
DOWNSTREAM	13096.74	20-year	50.80	2559.00	2559.91		2559.96	0.004101	0.73	53.18	138.47	0.38
DOWNSTREAM	13096.74	50-year	63.50	2559.00	2559.98		2560.04	0.003867	0.79	62.67	142.56	0.38
DOWNSTREAM	13096.74	100-year	70.80	2559.00	2560.01	2559.77	2560.08	0.003747	0.82	67.97	144.79	0.38
DOWNSTREAM	13096.74	500-year	86.20	2559.00	2560.09	2559.84	2560.16	0.003535	0.88	78.78	149.20	0.37
DOWNSTREAM	13096.74	1000-year	94.00	2559.00	2560.12	2559.90	2560.19	0.003446	0.90	84.05	150.89	0.37
DOWNSTREAM	13053.58	20-year	50.80	2558.98	2559.45	2559.45	2559.64	0.017743	1.48	28.88	77.85	0.78
DOWNSTREAM	13053.58	50-year	63.50	2558.98	2559.52	2559.52	2559.72	0.017083	1.58	33.90	80.60	0.78
DOWNSTREAM	13053.58	100-year	70.80	2558.98	2559.55	2559.55	2559.77	0.016754	1.63	36.69	82.09	0.78
DOWNSTREAM	13053.58	500-year	86.20	2558.98	2559.61	2559.61	2559.86	0.016483	1.74	42.08	84.89	0.79
DOWNSTREAM	13053.58	1000-year	94.00	2558.98	2559.65	2559.65	2559.90	0.016207	1.78	44.86	86.29	0.79
DOWNSTREAM	13011.18	20-year	50.80	2557.87	2558.82	2558.50	2558.90	0.003479	1.04	40.81	57.76	0.39
DOWNSTREAM	13011.18	50-year	63.50	2557.87	2558.91	2558.59	2559.02	0.003798	1.14	46.30	60.61	0.41
DOWNSTREAM	13011.18	100-year	70.80	2557.87	2558.96	2558.64	2559.08	0.003955	1.20	49.30	62.10	0.42
DOWNSTREAM	13011.18	500-year	86.20	2557.87	2559.05	2558.73	2559.19	0.004255	1.30	55.24	64.97	0.44
DOWNSTREAM	13011.18	1000-year	94.00	2557.87	2559.09	2558.77	2559.24	0.004426	1.35	57.93	66.23	0.45
DOWNSTREAM	12971.18	20-year	50.80	2557.00	2558.86		2558.87	0.000104	0.27	168.30	166.91	0.07
DOWNSTREAM	12971.18	50-year	63.50	2557.00	2558.97		2558.97	0.000120	0.31	185.74	171.66	0.08
DOWNSTREAM	12971.18	100-year	70.80	2557.00	2559.02		2559.03	0.000128	0.32	195.16	174.18	0.08
DOWNSTREAM	12971.18	500-year	86.20	2557.00	2559.13		2559.14	0.000144	0.36	213.82	179.05	0.09
DOWNSTREAM	12971.18	1000-year	94.00	2557.00	2559.17		2559.18	0.000152	0.38	222.34	181.24	0.09
DOWNSTREAM	12931.5	20-year	50.80	2557.48	2558.85		2558.86	0.000399	0.43	121.08	193.10	0.14
DOWNSTREAM	12931.5	50-year	63.50	2557.48	2558.95		2558.96	0.000390	0.45	141.09	197.80	0.14
DOWNSTREAM	12931.5	100-year	70.80	2557.48	2559.01		2559.02	0.000385	0.47	151.94	200.19	0.14
DOWNSTREAM	12931.5	500-year	86.20	2557.48	2559.11		2559.13	0.000380	0.49	173.08	203.41	0.14
DOWNSTREAM	12931.5	1000-year	94.00	2557.48	2559.16		2559.17	0.000381	0.50	182.68	204.85	0.14

DOWNSTREAM	12891.18	20-year	50.80	2558.00	2558.57	2558.57	2558.79	0.018986	1.86	24.84	56.86	0.85
DOWNSTREAM	12891.18	50-year	63.50	2558.00	2558.64	2558.64	2558.89	0.018295	1.97	29.32	60.37	0.85
DOWNSTREAM	12891.18	100-year	70.80	2558.00	2558.69	2558.69	2558.95	0.017703	2.01	31.97	62.36	0.84
DOWNSTREAM	12891.18	500-year	86.20	2558.00	2558.78	2558.78	2559.05	0.016290	2.07	37.73	67.45	0.82
DOWNSTREAM	12891.18	1000-year	94.00	2558.00	2558.82	2558.82	2559.10	0.015412	2.08	40.95	72.41	0.81
DOWNSTREAM	12851.18	20-year	50.80	2554.32	2555.08	2555.49	2556.76	0.255555	5.75	8.84	23.31	2.98
DOWNSTREAM	12851.18	50-year	63.50	2554.32	2555.16	2555.60	2556.94	0.238228	5.92	10.73	25.69	2.92
DOWNSTREAM	12851.18	100-year	70.80	2554.32	2555.19	2555.66	2557.04	0.232180	6.02	11.75	26.88	2.91
DOWNSTREAM	12851.18	500-year	86.20	2554.32	2555.27	2555.77	2557.26	0.224864	6.25	13.79	29.12	2.90
DOWNSTREAM	12851.18	1000-year	94.00	2554.32	2555.30	2555.82	2557.37	0.223420	6.37	14.75	30.12	2.91
DOWNSTREAM	12809.33	20-year	50.80	2553.85	2554.87	2554.03	2554.89	0.000350	0.30	81.25	79.09	0.12
DOWNSTREAM	12809.33	50-year	63.50	2553.85	2554.99	2554.11	2555.02	0.000400	0.35	90.91	82.24	0.13
DOWNSTREAM	12809.33	100-year	70.80	2553.85	2555.05	2554.15	2555.08	0.000425	0.37	96.12	83.88	0.14
DOWNSTREAM	12809.33	500-year	86.20	2553.85	2555.17	2554.24	2555.21	0.000475	0.42	106.50	87.07	0.15
DOWNSTREAM	12809.33	1000-year	94.00	2553.85	2555.23	2554.28	2555.27	0.000497	0.44	111.50	88.56	0.15
DOWNSTREAM	12773.11	20-year	50.80	2552.40	2554.87		2554.88	0.000224	0.41	123.30	86.27	0.11
DOWNSTREAM	12773.11	50-year	63.50	2552.40	2554.99		2555.00	0.000282	0.47	133.86	90.26	0.12
DOWNSTREAM	12773.11	100-year	70.80	2552.40	2555.05		2555.07	0.000313	0.51	139.58	91.88	0.13
DOWNSTREAM	12773.11	500-year	86.20	2552.40	2555.17		2555.19	0.000374	0.57	150.93	95.01	0.14
DOWNSTREAM	12773.11	1000-year	94.00	2552.40	2555.23		2555.25	0.000403	0.60	156.40	96.48	0.15
DOWNSTREAM	12691.18	20-year	50.80	2554.00	2554.57	2554.57	2554.80	0.027362	2.10	24.18	54.11	1.00
DOWNSTREAM	12691.18	50-year	63.50	2554.00	2554.65	2554.65	2554.90	0.026338	2.22	28.63	57.39	1.00
DOWNSTREAM	12691.18	100-year	70.80	2554.00	2554.69	2554.69	2554.96	0.026044	2.28	31.02	59.07	1.01
DOWNSTREAM	12691.18	500-year	86.20	2554.00	2554.77	2554.77	2555.07	0.025208	2.39	36.05	62.46	1.00
DOWNSTREAM	12691.18	1000-year	94.00	2554.00	2554.81	2554.81	2555.12	0.024987	2.45	38.44	64.01	1.01
DOWNSTREAM	12651.18	20-year	50.80	2552.79	2554.05	2553.50	2554.09	0.001802	0.87	58.93	70.80	0.29
DOWNSTREAM	12651.18	50-year	63.50	2552.79	2554.13	2553.58	2554.18	0.002116	1.00	64.49	72.40	0.32
DOWNSTREAM	12651.18	100-year	70.80	2552.79	2554.17	2553.62	2554.23	0.002278	1.06	67.51	73.25	0.33
DOWNSTREAM	12651.18	500-year	86.20	2552.79	2554.25	2553.71	2554.32	0.002591	1.19	73.46	74.90	0.36
DOWNSTREAM	12651.18	1000-year	94.00	2552.79	2554.29	2553.74	2554.37	0.002730	1.25	76.35	75.69	0.37
DOWNSTREAM	12624.16	20-year	50.80	2551.52	2554.07		2554.08	0.000068	0.30	170.61	106.07	0.07
DOWNSTREAM	12624.16	50-year	63.50	2551.52	2554.15		2554.16	0.000092	0.36	179.58	109.17	0.08
DOWNSTREAM	12624.16	100-year	70.80	2551.52	2554.20		2554.21	0.000106	0.39	184.43	110.80	0.08
DOWNSTREAM	12624.16	500-year	86.20	2551.52	2554.28		2554.29	0.000136	0.46	194.13	114.01	0.09
DOWNSTREAM	12624.16	1000-year	94.00	2551.52	2554.33		2554.34	0.000151	0.49	198.88	115.54	0.10
DOWNSTREAM	12611.18	20-year	50.80	2551.09	2554.07		2554.07	0.000021	0.19	273.69	156.30	0.04
DOWNSTREAM	12611.18	50-year	63.50	2551.09	2554.16		2554.16	0.000028	0.23	286.87	158.71	0.04
DOWNSTREAM	12611.18	100-year	70.80	2551.09	2554.20		2554.20	0.000032	0.25	293.99	159.84	0.05
DOWNSTREAM	12611.18	500-year	86.20	2551.09	2554.29		2554.29	0.000042	0.29	308.02	162.06	0.05
DOWNSTREAM	12611.18	1000-year	94.00	2551.09	2554.33		2554.33	0.000047	0.31	314.80	163.12	0.06
DOWNSTREAM	12571.18	20-year	50.80	2550.42	2554.07		2554.07	0.000018	0.17	277.61	160.18	0.03
DOWNSTREAM	12571.18	50-year	63.50	2550.42	2554.15		2554.16	0.000024	0.21	291.26	167.42	0.04
DOWNSTREAM	12571.18	100-year	70.80	2550.42	2554.20		2554.20	0.000028	0.23	298.78	171.28	0.04
DOWNSTREAM	12571.18	500-year	86.20	2550.42	2554.29		2554.29	0.000037	0.27	314.04	178.86	0.05
DOWNSTREAM	12571.18	1000-year	94.00	2550.42	2554.33		2554.33	0.000042	0.28	321.52	182.46	0.05
DOWNSTREAM	12536.43	20-year	50.80	2552.18	2554.06		2554.07	0.000292	0.43	113.90	101.27	0.12
DOWNSTREAM	12536.43	50-year	63.50	2552.18	2554.14		2554.15	0.000367	0.51	122.08	104.75	0.14
DOWNSTREAM	12536.43	100-year	70.80	2552.18	2554.18		2554.20	0.000409	0.55	126.55	106.60	0.15
DOWNSTREAM	12536.43	500-year	86.20	2552.18	2554.26		2554.29	0.000492	0.62	135.49	110.21	0.16
DOWNSTREAM	12536.43	1000-year	94.00	2552.18	2554.30		2554.33	0.000533	0.66	139.79	111.91	0.17
DOWNSTREAM	12492.07	20-year	50.80	2552.83	2554.01		2554.04	0.001976	0.81	63.06	90.26	0.29
DOWNSTREAM	12492.07	50-year	63.50	2552.83	2554.08		2554.12	0.002305	0.92	69.12	92.24	0.32
DOWNSTREAM	12492.07	100-year	70.80	2552.83	2554.11		2554.16	0.002483	0.98	72.32	93.28	0.34
DOWNSTREAM	12492.07	500-year	86.20	2552.83	2554.18		2554.24	0.002826	1.10	78.64	95.28	0.36
DOWNSTREAM	12492.07	1000-year	94.00	2552.83	2554.21		2554.28	0.002981	1.16	81.69	96.23	0.38
DOWNSTREAM	12457.75	20-year	50.80	2551.95	2554.02		2554.02	0.000144	0.36	146.11	114.95	0.09
DOWNSTREAM	12457.75	50-year	63.50	2551.95	2554.08		2554.09	0.000193	0.43	153.98	117.04	0.11
DOWNSTREAM	12457.75	100-year	70.80	2551.95	2554.12		2554.13	0.000221	0.47	158.18	118.13	0.11
DOWNSTREAM	12457.75	500-year	86.20	2551.95	2554.19		2554.20	0.000281	0.54	166.91	151.75	0.13
DOWNSTREAM	12457.75	1000-year	94.00	2551.95	2554.22		2554.24	0.000311	0.57	171.97	154.29	0.14

DOWNSTREAM	12412.7	20-year	50.80	2550.85	2554.02		2554.02	0.000013	0.14	372.36	226.11	0.03
DOWNSTREAM	12412.7	50-year	63.50	2550.85	2554.09		2554.09	0.000017	0.17	388.09	231.36	0.03
DOWNSTREAM	12412.7	100-year	70.80	2550.85	2554.12		2554.12	0.000020	0.19	396.54	234.14	0.04
DOWNSTREAM	12412.7	500-year	86.20	2550.85	2554.19		2554.20	0.000027	0.22	413.22	247.02	0.04
DOWNSTREAM	12412.7	1000-year	94.00	2550.85	2554.23		2554.23	0.000030	0.24	421.90	265.94	0.05
DOWNSTREAM	12367.98	20-year	50.80	2550.24	2554.02		2554.02	0.000007	0.12	476.46	294.03	0.02
DOWNSTREAM	12367.98	50-year	63.50	2550.24	2554.09		2554.09	0.000009	0.14	496.97	303.75	0.03
DOWNSTREAM	12367.98	100-year	70.80	2550.24	2554.12		2554.12	0.000011	0.16	508.43	331.86	0.03
DOWNSTREAM	12367.98	500-year	86.20	2550.24	2554.19		2554.19	0.000015	0.19	531.94	336.50	0.03
DOWNSTREAM	12367.98	1000-year	94.00	2550.24	2554.23		2554.23	0.000017	0.20	543.28	338.05	0.03
DOWNSTREAM	12331.15	20-year	50.80	2551.93	2554.01		2554.02	0.000104	0.26	197.85	245.86	0.07
DOWNSTREAM	12331.15	50-year	63.50	2551.93	2554.08		2554.09	0.000126	0.29	214.72	249.03	0.08
DOWNSTREAM	12331.15	100-year	70.80	2551.93	2554.12		2554.12	0.000139	0.31	223.50	250.64	0.09
DOWNSTREAM	12331.15	500-year	86.20	2551.93	2554.19		2554.19	0.000163	0.35	240.93	255.37	0.09
DOWNSTREAM	12331.15	1000-year	94.00	2551.93	2554.22		2554.23	0.000174	0.37	249.35	258.88	0.10
DOWNSTREAM	12291.18	20-year	50.80	2552.75	2553.84	2553.84	2553.99	0.012619	1.78	31.98	111.72	0.72
DOWNSTREAM	12291.18	50-year	63.50	2552.75	2553.90	2553.90	2554.05	0.012465	1.86	38.93	117.36	0.72
DOWNSTREAM	12291.18	100-year	70.80	2552.75	2553.93	2553.93	2554.09	0.012700	1.92	42.15	119.87	0.73
DOWNSTREAM	12291.18	500-year	86.20	2552.75	2553.98	2553.98	2554.15	0.013057	2.01	48.48	124.68	0.75
DOWNSTREAM	12291.18	1000-year	94.00	2552.75	2554.00	2554.00	2554.19	0.013533	2.08	51.02	126.56	0.77
DOWNSTREAM	12251.18	20-year	50.80	2550.89	2551.29	2551.59	2552.62	0.181564	3.96	10.53	38.63	2.39
DOWNSTREAM	12251.18	50-year	63.50	2550.89	2551.35	2551.65	2552.73	0.161163	4.02	12.92	42.29	2.30
DOWNSTREAM	12251.18	100-year	70.80	2550.89	2551.39	2551.69	2552.75	0.147480	4.01	14.45	44.45	2.22
DOWNSTREAM	12251.18	500-year	86.20	2550.89	2551.45	2551.75	2552.82	0.132584	4.08	17.45	65.65	2.14
DOWNSTREAM	12251.18	1000-year	94.00	2550.89	2551.47	2551.78	2552.83	0.130919	4.19	18.92	67.88	2.14
DOWNSTREAM	12211.18	20-year	50.80	2550.19	2550.53	2550.58	2550.81	0.015616	0.83	22.58	58.91	0.65
DOWNSTREAM	12211.18	50-year	63.50	2550.19	2550.59	2550.66	2550.92	0.016219	0.95	26.22	62.59	0.68
DOWNSTREAM	12211.18	100-year	70.80	2550.19	2550.62	2550.70	2550.97	0.016443	1.00	28.26	64.56	0.69
DOWNSTREAM	12211.18	500-year	86.20	2550.19	2550.69	2550.78	2551.08	0.016573	1.11	32.60	68.57	0.71
DOWNSTREAM	12211.18	1000-year	94.00	2550.19	2550.72	2550.82	2551.13	0.016150	1.14	35.11	70.78	0.71
DOWNSTREAM	12175.24	20-year	50.80	2550.21	2549.79	2549.89	2550.15	0.021561		19.26	48.68	0.00
DOWNSTREAM	12175.24	50-year	63.50	2550.21	2549.87	2550.06	2550.25	0.020862		23.06	53.25	0.00
DOWNSTREAM	12175.24	100-year	70.80	2550.21	2549.91	2550.08	2550.31	0.020649		25.11	55.58	0.00
DOWNSTREAM	12175.24	500-year	86.20	2550.21	2549.98	2550.13	2550.42	0.020465		29.21	60.96	0.00
DOWNSTREAM	12175.24	1000-year	94.00	2550.21	2550.05	2550.16	2550.41	0.024333		34.93	101.93	0.00
DOWNSTREAM	12131.18	20-year	50.80	2549.95	2548.83	2548.83	2549.06	0.011933		24.05	54.41	0.00
DOWNSTREAM	12131.18	50-year	63.50	2549.95	2548.77	2548.92	2549.25	0.028218		20.59	50.34	0.00
DOWNSTREAM	12131.18	100-year	70.80	2549.95	2548.80	2548.96	2549.31	0.028242		22.33	52.43	0.00
DOWNSTREAM	12131.18	500-year	86.20	2549.95	2548.87	2549.03	2549.43	0.028009		25.97	56.54	0.00
DOWNSTREAM	12131.18	1000-year	94.00	2549.95	2548.94	2549.07	2549.44	0.022651		29.99	60.69	0.00
DOWNSTREAM	12091.18	20-year	50.80	2549.00	2548.62	2547.48	2548.63	0.000206		90.51	70.97	0.00
DOWNSTREAM	12091.18	50-year	63.50	2549.00	2548.69	2547.57	2548.72	0.000272		95.96	72.52	0.00
DOWNSTREAM	12091.18	100-year	70.80	2549.00	2548.73	2547.61	2548.76	0.000312		98.78	73.31	0.00
DOWNSTREAM	12091.18	500-year	86.20	2549.00	2548.81	2547.70	2548.84	0.000397		104.27	74.83	0.00
DOWNSTREAM	12091.18	1000-year	94.00	2549.00	2548.84	2547.74	2548.88	0.000440		106.87	75.54	0.00
DOWNSTREAM	12051.18	20-year	50.80	2549.65	2548.62		2548.63	0.000024		200.98	104.73	0.00
DOWNSTREAM	12051.18	50-year	63.50	2549.65	2548.70		2548.71	0.000034		209.24	106.13	0.00
DOWNSTREAM	12051.18	100-year	70.80	2549.65	2548.74		2548.75	0.000039		213.55	106.86	0.00
DOWNSTREAM	12051.18	500-year	86.20	2549.65	2548.82		2548.83	0.000052		221.90	108.25	0.00
DOWNSTREAM	12051.18	1000-year	94.00	2549.65	2548.86		2548.87	0.000059		225.81	108.90	0.00
DOWNSTREAM	12012.58	20-year	50.80	2548.71	2548.62		2548.63	0.000014		255.00	123.00	0.00
DOWNSTREAM	12012.58	50-year	63.50	2548.71	2548.70		2548.71	0.000019		264.70	124.66	0.00
DOWNSTREAM	12012.58	100-year	70.80	2548.71	2548.74		2548.75	0.000022	0.01	269.85	130.92	0.02
DOWNSTREAM	12012.58	500-year	86.20	2548.71	2548.82		2548.83	0.000030	0.02	280.65	146.78	0.02
DOWNSTREAM	12012.58	1000-year	94.00	2548.71	2548.86		2548.86	0.000034	0.02	286.08	153.65	0.03
DOWNSTREAM	11971.18	20-year	50.80	2547.16	2548.62		2548.63	0.000061	0.18	199.79	179.97	0.05
DOWNSTREAM	11971.18	50-year	63.50	2547.16	2548.70		2548.70	0.000079	0.21	213.99	185.39	0.06
DOWNSTREAM	11971.18	100-year	70.80	2547.16	2548.74		2548.74	0.000088	0.23	221.42	187.65	0.07
DOWNSTREAM	11971.18	500-year	86.20	2547.16	2548.82		2548.82	0.000109	0.26	236.00	191.98	0.08
DOWNSTREAM	11971.18	1000-year	94.00	2547.16	2548.85		2548.86	0.000120	0.28	242.89	193.94	0.08

DOWNSTREAM	11932.07	20-year	50.80	2547.08	2548.61		2548.62	0.000274	0.33	127.95	160.30	0.11
DOWNSTREAM	11932.07	50-year	63.50	2547.08	2548.69		2548.70	0.000328	0.38	140.28	167.21	0.12
DOWNSTREAM	11932.07	100-year	70.80	2547.08	2548.72		2548.74	0.000359	0.41	146.77	170.73	0.13
DOWNSTREAM	11932.07	500-year	86.20	2547.08	2548.80		2548.81	0.000419	0.47	159.62	177.51	0.14
DOWNSTREAM	11932.07	1000-year	94.00	2547.08	2548.83		2548.85	0.000447	0.49	165.80	180.67	0.15
DOWNSTREAM	11892	20-year	50.80	2548.00	2548.42	2548.42	2548.57	0.011652	0.83	31.66	106.16	0.58
DOWNSTREAM	11892	50-year	63.50	2548.00	2548.47	2548.47	2548.64	0.011770	0.90	37.57	115.62	0.59
DOWNSTREAM	11892	100-year	70.80	2548.00	2548.51	2548.51	2548.68	0.011438	0.93	41.38	121.32	0.59
DOWNSTREAM	11892	500-year	86.20	2548.00	2548.56	2548.56	2548.75	0.011243	0.99	48.60	131.47	0.60
DOWNSTREAM	11892	1000-year	94.00	2548.00	2548.59	2548.59	2548.78	0.011370	1.02	51.78	135.69	0.60
DOWNSTREAM	11855.96	20-year	50.80	2547.17	2547.84	2547.85	2548.04	0.019657	1.58	27.26	76.54	0.83
DOWNSTREAM	11855.96	50-year	63.50	2547.17	2547.90	2547.92	2548.12	0.019471	1.70	32.13	82.91	0.84
DOWNSTREAM	11855.96	100-year	70.80	2547.17	2547.93	2547.95	2548.16	0.019114	1.74	35.00	86.45	0.84
DOWNSTREAM	11855.96	500-year	86.20	2547.17	2548.00	2548.05	2548.24	0.018326	1.83	41.03	93.43	0.83
DOWNSTREAM	11855.96	1000-year	94.00	2547.17	2548.03	2548.07	2548.26	0.019514	1.93	44.22	128.23	0.87
DOWNSTREAM	11811.18	20-year	50.80	2545.78	2546.20	2546.32	2546.59	0.062355	2.73	18.33	56.82	1.46
DOWNSTREAM	11811.18	50-year	63.50	2545.78	2546.25	2546.39	2546.70	0.060241	2.88	21.55	59.71	1.46
DOWNSTREAM	11811.18	100-year	70.80	2545.78	2546.28	2546.43	2546.76	0.059872	2.96	23.22	61.00	1.47
DOWNSTREAM	11811.18	500-year	86.20	2545.78	2546.34	2546.51	2546.88	0.059232	3.13	26.59	63.51	1.48
DOWNSTREAM	11811.18	1000-year	94.00	2545.78	2546.38	2546.54	2546.91	0.052230	3.07	29.41	65.54	1.41
DOWNSTREAM	11771.18	20-year	50.80	2545.00	2546.15	2545.69	2546.19	0.002050	0.91	56.86	83.10	0.31
DOWNSTREAM	11771.18	50-year	63.50	2545.00	2546.22	2545.77	2546.27	0.002319	1.03	63.24	86.20	0.33
DOWNSTREAM	11771.18	100-year	70.80	2545.00	2546.26	2545.81	2546.32	0.002476	1.09	66.50	87.75	0.35
DOWNSTREAM	11771.18	500-year	86.20	2545.00	2546.35	2545.89	2546.42	0.002599	1.18	74.55	91.45	0.36
DOWNSTREAM	11771.18	1000-year	94.00	2545.00	2546.37	2545.93	2546.45	0.002818	1.25	76.88	92.49	0.38
DOWNSTREAM	11731.18	20-year	50.80	2545.83	2546.02		2546.09	0.002707	0.25	46.21	130.37	0.25
DOWNSTREAM	11731.18	50-year	63.50	2545.83	2546.08		2546.17	0.002952	0.36	55.15	141.51	0.28
DOWNSTREAM	11731.18	100-year	70.80	2545.83	2546.12		2546.21	0.003053	0.42	60.13	147.36	0.29
DOWNSTREAM	11731.18	500-year	86.20	2545.83	2546.22		2546.30	0.003723	0.61	78.51	195.39	0.35
DOWNSTREAM	11731.18	1000-year	94.00	2545.83	2546.25		2546.32	0.003802	0.65	82.85	198.77	0.36
DOWNSTREAM	11691.18	20-year	50.80	2545.74	2545.71	2545.71	2545.88	0.012766		27.85	82.78	0.00
DOWNSTREAM	11691.18	50-year	63.50	2545.74	2545.78	2545.78	2545.95	0.011141	0.28	35.71	121.47	0.43
DOWNSTREAM	11691.18	100-year	70.80	2545.74	2545.82	2545.82	2545.99	0.010822	0.39	39.86	127.62	0.47
DOWNSTREAM	11691.18	500-year	86.20	2545.74	2545.89	2545.89	2546.06	0.009639	0.41	50.31	167.93	0.45
DOWNSTREAM	11691.18	1000-year	94.00	2545.74	2545.92	2545.92	2546.09	0.009100	0.50	55.96	174.02	0.46
DOWNSTREAM	11651.18	20-year	50.80	2543.57	2544.29	2544.45	2544.80	0.081145	3.14	16.16	44.65	1.67
DOWNSTREAM	11651.18	50-year	63.50	2543.57	2544.34	2544.53	2544.94	0.087478	3.42	18.57	47.85	1.75
DOWNSTREAM	11651.18	100-year	70.80	2543.57	2544.38	2544.58	2545.00	0.085501	3.48	20.32	50.04	1.75
DOWNSTREAM	11651.18	500-year	86.20	2543.57	2544.44	2544.66	2545.14	0.085674	3.72	23.20	53.51	1.78
DOWNSTREAM	11651.18	1000-year	94.00	2543.57	2544.46	2544.70	2545.20	0.084779	3.81	24.72	55.22	1.78
DOWNSTREAM	11611.18	20-year	50.80	2543.00	2543.71	2543.60	2543.85	0.012131	1.59	30.93	62.23	0.69
DOWNSTREAM	11611.18	50-year	63.50	2543.00	2543.79	2543.68	2543.95	0.012026	1.68	36.14	65.60	0.70
DOWNSTREAM	11611.18	100-year	70.80	2543.00	2543.83	2543.72	2544.01	0.011905	1.72	39.09	67.45	0.70
DOWNSTREAM	11611.18	500-year	86.20	2543.00	2543.92	2543.80	2544.11	0.011766	1.81	44.98	71.01	0.70
DOWNSTREAM	11611.18	1000-year	94.00	2543.00	2543.96	2543.83	2544.16	0.011686	1.85	47.89	72.70	0.71
DOWNSTREAM	11571.18	20-year	50.80	2542.15	2543.70		2543.73	0.000841	0.53	69.14	79.82	0.19
DOWNSTREAM	11571.18	50-year	63.50	2542.15	2543.77		2543.81	0.001062	0.62	75.06	83.15	0.22
DOWNSTREAM	11571.18	100-year	70.80	2542.15	2543.81		2543.86	0.001182	0.66	78.34	84.94	0.23
DOWNSTREAM	11571.18	500-year	86.20	2542.15	2543.88		2543.95	0.001424	0.75	84.86	88.41	0.26
DOWNSTREAM	11571.18	1000-year	94.00	2542.15	2543.92		2543.99	0.001538	0.79	88.08	90.06	0.27
DOWNSTREAM	11531.18	20-year	50.80	2541.66	2543.71		2543.71	0.000100	0.28	157.89	128.03	0.07
DOWNSTREAM	11531.18	50-year	63.50	2541.66	2543.78		2543.79	0.000131	0.33	167.85	131.18	0.09
DOWNSTREAM	11531.18	100-year	70.80	2541.66	2543.82		2543.83	0.000148	0.36	173.19	132.83	0.09
DOWNSTREAM	11531.18	500-year	86.20	2541.66	2543.90		2543.92	0.000184	0.42	183.96	136.11	0.10
DOWNSTREAM	11531.18	1000-year	94.00	2541.66	2543.94		2543.96	0.000202	0.44	189.17	137.67	0.11
DOWNSTREAM	11491.18	20-year	50.80	2541.83	2543.71		2543.71	0.000054	0.16	219.48	217.02	0.05
DOWNSTREAM	11491.18	50-year	63.50	2541.83	2543.78		2543.79	0.000069	0.19	236.36	224.66	0.06
DOWNSTREAM	11491.18	100-year	70.80	2541.83	2543.82		2543.83	0.000078	0.21	245.54	228.83	0.06
DOWNSTREAM	11491.18	500-year	86.20	2541.83	2543.90		2543.91	0.000095	0.24	264.27	237.10	0.07
DOWNSTREAM	11491.18	1000-year	94.00	2541.83	2543.94		2543.95	0.000103	0.26	273.45	241.05	0.07
